OPTICAL AND DC ELECTRICAL PROPERTIES OF PLASMA POLYMERIZED QUINOLINE THIN FILMS

By

Dalia Parven

Roll No: 0409143005

Session: April, 2009

Department of Physics

BANGLADESH UNIVERSITY OF ENGINEERING AND TECHNOLOGY (BUET)

DHAKA – 1000

October, 2015

OPTICAL AND DC ELECTRICAL PROPERTIES OF PLASMA POLYMERIZED QUINOLINE THIN FILMS

A thesis submitted to the Department of Physics, Bangladesh University of Engineering and Technology in partial fulfillment of the requirement for the degree of MASTER OF PHILOSOPHY (M.Phil.) IN PHYSICS

By

Dalia Parven

Roll No: 0409143005

Session: April, 2009

Department of Physics

BANGLADESH UNIVERSITY OF ENGINEERING AND TECHNOLOGY (BUET)
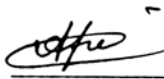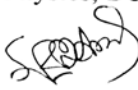
DHAKA – 1000

October, 2015

BANGLADESH UNIVERSITY OF ENGINEERING & TECHNOLOGY (BUET), DHAKA
DEPARTMENT OF PHYSICS

CERTIFICATION OF THESIS

The thesis titled **"OPTICAL AND DC ELECTRICAL PROPERTIES OF PLASMA POLYMERIZED QUINOLINE THIN FILMS"** submitted by **Dalia Parven**, Roll No-0409143005F, Registration No-0409143005F, Session: April-2009, has been accepted as satisfactory in partial fulfillment of the requirement for the degree of **Master of Philosophy** (M. Phil.) in Physics on 27 October, **2015**.

BOARD OF EXAMINERS

1. _____
   Dr. Md. Abu Hashan Bhuiyan   Chairman
   Professor,   (Supervisor)
   Department of Physics, BUET, Dhaka

2. _____
   Dr. Afia Begum   Member
   Professor & Head   (Ex-Officio)
   Department of Physics, BUET, Dhaka

3. _____
   Dr. A.K.M. Akther Hossain   Member
   Professor
   Department of Physics, BUET, Dhaka

4. _____
   Dr. Md. Forhad Mina   Member
   Professor
   Department of Physics, BUET, Dhaka

5. _____
   Dr. Mohammad Mizanur Rahman   Member
   Associate Professor   (External)
   Department of Physics
   University of Dhaka, Dhaka

BUET

CANDIDATE'S DECLARATION

It is hereby declared that this thesis or any part of it has not been submitted elsewhere for the award of any degree or diploma.

Dalia Parven

_____

(Dalia Parven)

Roll No- 0409143005

Session- April, 2009

Dedicated

To

My Family and Respected Teachers

Prof. Dr. Md. Abu Hashan Bhuiyan

Prof. Md. Abdul Quddus

CONTENTS

CHAPTER-5   RESULTS AND DISCUSSION   81-100

CHAPTER-6   CONCLUSIONS

101-103

List of Figures

CHAPTER-1

CHAPTER-2

CHAPTER-3

CHAPTER-4

CHAPTER-5

List of Tables

CHAPTER-5

Glossary

ABS	Absorbance
AC, ac	Alternative Current
Al	Aluminium
BN	Benzonitrile
CBD	Chemical Bath Deposition
cc	Capacitively Coupled
CRT	Cathode-ray Tube
d	Sample Thickness
DC, dc	Direct Current
DEA	2, 6 Diethylaniline
DSC	Differential Scanning Calorimetry
DTA	Differential Thermal Analysis
$E_{g(d)}$	Direct transition energy gap
$E_{g(i)}$	Indirect transition energy gap
FL	Fermi Level
FTIR	Fourier Transform Infrared
I	Current
I	Intensity of Radiation
IR	Infrared
k	Boltzmann Constant
k	Extinction Co-efficient
MHz	Mega Hertz
PECVD	Plasma Enhanced Chemical Vapor Deposition
PPBN	Plasma Polymerized Benzonitrile
PPDEA	Plasma Polymerized 2, 6 Diethylaniline
PPDP	Plasma Polymerized Diphenyl

PPm-X	Plasma Polymerized m-Xylene
PPPA	Plasma Polymerized Polylaniline
PVD	Physical Vapor Deposition
rf	Radio Frequency
SCLC	Space Charge Limited Conduction
SEM	Scanning Electron Microscopy
T_g	Glass Transition Temperature
T_m	Melting Point
TGA	Thermo gravimetric Analysis
TSDC	Thermally Stimulated Depolarization Current
UV-vis	Ultraviolet-Visible
V	Voltage
XPS	X-ray Photoelectron Spectroscopy
α	Absorption Coefficient
β_{exp}	Experimental β Co-efficient
β_S	Schottky Co-efficient
β_{PF}	Pool-Frenkel Co-efficient
ϕ	Columbic barrier height of the electrode polymer interface
ϕ_c	Ionization potential of the PF centers
λ	Wavelength
ΔE	Activation Energy
σ	Electrical Conductivity
σ_{ac}	ac Electrical Conductivity
ε	Dielectric Constant
ε_0	Permittivity of Free Space
μ	Mobility of Charge Carrier
θ	Trapping Factor

Acknowledgements

Abstract

Plasma polymerized quinoline (PPQ) thin films were deposited onto glass substrate at room temperature by a capacitively coupled plasma polymerization system. The aims of the study are to explore the dc conduction mechanism, optical characteristics and structure-property relation of PPQ thin film. The thickness of the films was measured by Multiple Beam Interferometric method.

The SEM investigation shows smooth, uniform, flawless and fracture free surface of the PPQ thin films. The differential thermal analysis (DTA) shows that a peak which reaches a maximum at around 673 K may be due to the removal of water content and the breaking bonds in the PPQ. The thermogravimetric analysis(TGA) shows the mass loss starts from 312 K. Major degradation occurs above 673 K. So it is seen from TGA, PPQ is observed to be stable up to about 600 K. The Fourier transform infrared spectroscopy (FTIR) observations show that the sharpness of the absorption bands decreases significantly in the PPQ thin films compared to that of Q because of hydrogen loss. Also there are shift of bands in the FTIR spectrum of PPQ. It is found that the chemical nature of the PPQ thin films deposited by plasma polymerization technique is departed to some extent from that of the monomer Q.

From UV-vis spectroscopy it is found that indirect energy gap varies from 2.20 to 2.00 eV and direct energy gap varies from 3.50 to 3.30 eV with film thickness. The current density-voltage characteristics of PPQ thin films of different thicknesses have been studied at different temperatures. In the low voltage region, the conduction current obeys Ohm's law and that in the higher voltage region the conduction mechanism in the PPQ thin films is Schottky/PF. For applied voltage 10 V (Ohmic), the activation energies are observed to be around 0.15 ± 0.07 eV at the low temperature region and that at the higher temperature region is 0.75 ± 0.02 eV. While for applied voltage 30 V (Non-ohmic), the activation energies are observed to be around 0.18 ± 0.02 eV at the low temperature region and 0.86 ± 0.07 eV at the higher temperature region.

Chapter-1

Introduction

1.1 Introduction

Studies on thin films have been increasing for the last several decades because of their application in science and technology. Characteristics of thin films are being investigated by many scientists, researchers and students engaged in the field of material science. Most of the electronic, optoelectronic semiconductor devices and optical coatings are mainly produced from thin film construction. The use of thin films as solar cell to solve the problem of energy crisis is now known to all. Besides that the potential use of thin films in magnetic memory devices (such as RAM, ROM etc.), optical filters, different active and passive micro-miniaturized components and devices, sensors and detectors, light emitting diode, etc. have attracted scientists to do further studies on thin films. Recently special attention has been focused on organic polymers for their potential application in scientific and industrial appliances as advanced materials. Thin polymer films can be formed in two ways. One is wet processing, such as the Langmuir-Blodgett film method, spin-coating, dip-coating and chemical vapor deposition (CVD). Although excellent results have been achieved this way, there are a number of problems that can arise such as pinholes, inclusion of solvents in different polymer layers, contaminants, etc. An alternative approach, which can avoid such difficulties, is plasma polymerization. Plasma polymerization is gaining recognition as an important technique for direct thin film deposition, which are difficult to obtain by the conventional polymerization methods. This type of vapor deposition under vacuum provides a clean environment. It is solvent free and is well suited to sequential depositions. It is possible to deposit thin films from any monomer onto variety of substrate materials. Furthermore, it is a solvent-free, fast and versatile process [1, 2, 6].

The films obtained by plasma polymerization are generally homogeneous, adherent and pinhole free. Plasma polymerized thin films may have molecular structures different from that of the conventional polymers. The plasma polymer films have cross-linked structure and have good chemical and physical stability [1, 2].

In the cases of a free radical mechanism, two types of reaction may be postulated: i) plasma induced polymerization and ii) plasma state polymerization. Plasma induced polymerization is the conventional free-radical induced polymerization of molecules to the containing unsaturated carbon-carbon bonds, while plasma state polymerization depends on the presence, in a plasma, of electrons and other species energetic enough to break any bond.

Applications of plasma polymerized thin films in various fields have increased over the time. In the past few decades the study of the structural, electronic, electrical and optical properties of organic polymers received special attention of the scientist as potential materials. Among those plasma-polymerized thin films have received a lot of interest due to their wide-ranging applications in chemical, physical and biological sensors, microelectronic devices, nonlinear optical and molecular devices, coating for chemical fibers films, surface hardening of tools, spaceship components, etc [1, 2-4].

It can thus be noticed that plasma polymerization emerges an important technique in thin film processing in wet and vacuum conditions in a clean environment. In this work, plasma polymerization technique has been chosen to synthesize thin films of quinoline and to study their structural, optical and electrical properties.

1.2 Review of Previous Research Work

The recent development of various devices from thin films of organic-inorganic compounds produced by plasma polymerization has drawn attention of the researchers to elucidate various characteristics of those materials.

The structural behavior of plasma polymerized thin films is different than that of the conventionally prepared polymer thin films. This change in the structure of monomer after plasma polymerization affects the other characteristics. So there are a lot of investigations on these materials during the last several decades.

Bradley and Hammes [7], Gregor [8] and Hirai and Nakada [9] studied the chemical and electrical properties of plasma polymerized organic thin films. The concept of plasma polymerization has been based on the application of polymers developed under plasma conditions. Plasma polymerization process is nothing but the well known plasma enhanced chemical vapor deposition (PECVD) process. Plasma polymerization is based on the molecular processes by the size of molecules increases.

Majumder and Bhuiyan [10] investigated the chemical structure of the monomer vinylene carbonate (VC) and plasma polymerized vinylene carbonate (PPVC) by Fourier transformed infrared (FTIR) spectroscopy found that there was some chemical change in the VC structure.

The electrical study revealed that there were ohmic conduction in the low voltage region and non-ohmic conduction in the high voltage region. The most probable conduction mechanism in PPVC thin films was of Schottky type (Fig.1.1).
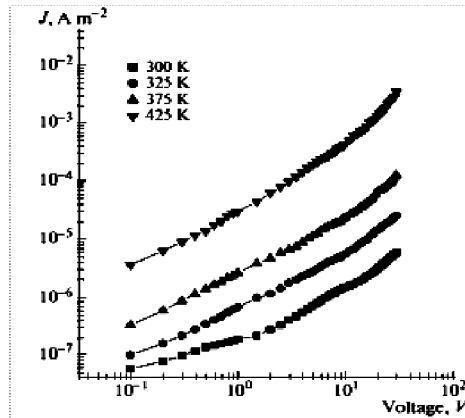
Fig.1.1 Plots of current density against applied voltage at different temperatures for a PPVC thin fiim.

Akther and Bhuiyan [11, 12] deposited plasma polymerized N, N, 3, tetramethylaniline (PPTMA) thin film onto glass substrates at room temperature by a capacitively coupled plasma polymerization system. They reported from the IR spectroscopy, and UV-vis spectroscopy (Fig.1.2) that this film contains more conjugation as compared to the monomer. From UV-vis spectroscopy it is found that indirect energy gap varies from 1.49 to 1.86 eV with film thickness. Electrical and optical measurements suggested that the top of valance band and the bottom of the conduction band may have gap states and the middle of the energy gap may be equal to the high temperature activation energy.
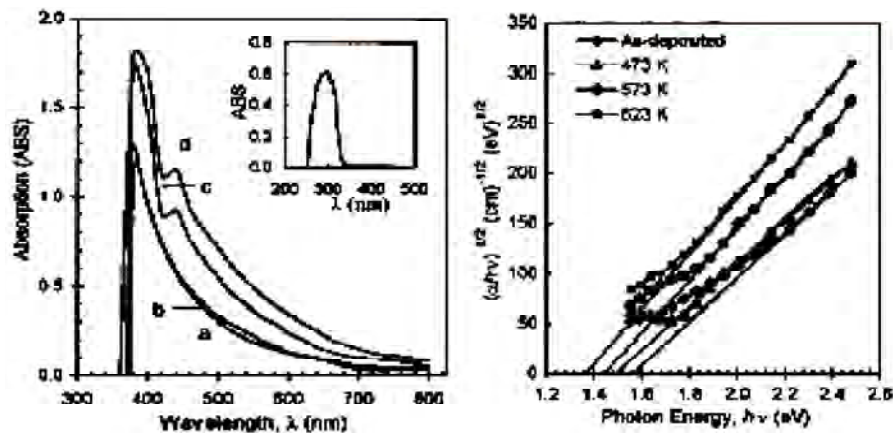
Fig.1.2 (a) Plots of ABS vs. λ for PPTMA thin films of different thicknesses and (b) photon energy, hν vs $(\alpha h\nu)^{1/2}$ for a PPTMA thin film at different heat treatment temperatures.

Matin and Bhuiyan [13] investigated by FTIR spectroscopic analysis of 2, 6, diethylaniline monomer and plasma polymerized 2, 6 diethylaniline (PPDEA) thin films and found that structural rearrangement/ cross-linking have occurred in the chemical structure of formed thin films due to plasma polymerization process. However, the aromatic ring structure and the ethyl group of the starting monomer are retained in PPDEA thin film. The optical band gaps (E_g) of PPDEA thin films of different thickness were found to be about 3.60 and 2.23 to 2.38 eV for direct and indirect transition respectively. The change in E_g values with thickness is, due to increased structural modification in PPDEA with plasma duration. The Urbach energy, steepness parameter and extinction coefficient are also assessed for PPDEA thin films of different thickness from UV-vis spectroscopic data (Fig.1.3).
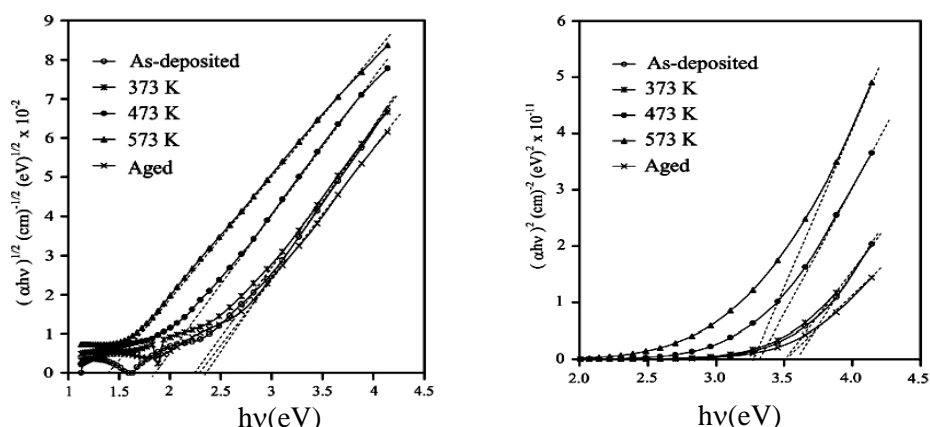
Fig.1.3 (a) Plots of $(\alpha h\nu)^2$ vs $h\nu$ and (b) $(\alpha h\nu)^{1/2}$ vs $h\nu$ for a PPDEA thin film at different heat treatment temperatures.

Chowdhury and Bhuiyan [14] investigated the optical properties and chemical structure of plasma polymerized diphenyl (PPDP) thin films. The IR spectroscopic analysis revealed that the structure of PPDP thin films are not structurally the same as that of the monomer and cycliztion / aggregation by conjugation occurs in the PPDP structure on heat treatment. Optical properties were evaluated from ultraviolet vis (UV-Vis) spectroscopic measurements of as-deposited, heat treated and aged (as-deposited and heat treated) PPDP thin films. From optical absorption data band gaps, allowed direct and indirect transition energy gaps were determined. The E_g was not affected appreciably by heat treatment whereas it is modified on ageing (Fig.1.4).
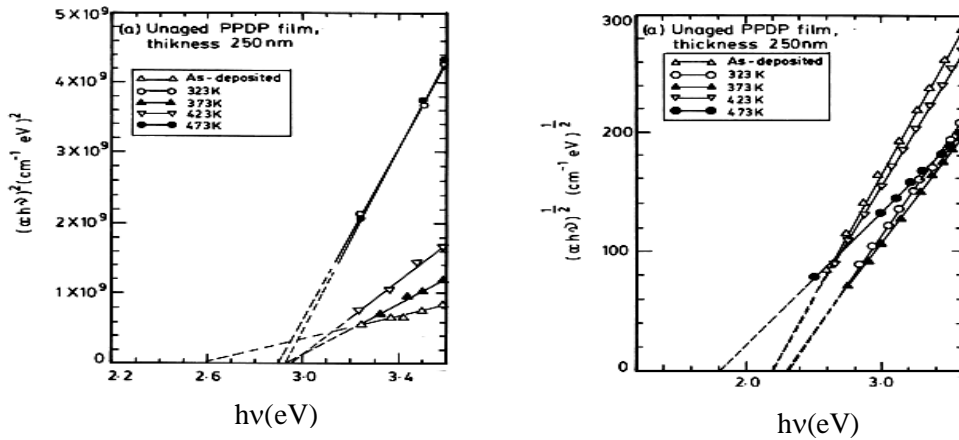
Fig.1.4 (a) Plots of $(\alpha h\nu)^2$ vs hν and (b) $(\alpha h\nu)^{1/2}$ vs hν for a PPDP thin film at different heat treatment temperatures.

Shah Jalal et al. [15] deposited plasma polymerized m-Xylene thin films using a capacitively coupled glow discharge reactor. They found that Pool-Frenkel conduction mechanism was most probable in these films.

Plasma polymerized 1, 1, 3, 3-tetramethoxy-propane (PPTMP) thin films of different thicknesses were prepared by Afroze and Bhuiyan [16] through glow discharge using a capacitively coupled reactor. They found smooth, uniform and pinhole free films with aliphatic conjugation C=C and C=O bonds. There was formation of C-O-C bond owing to rearrangement of oxygen due to heat treatment of PPTMP thin films. The allowed direct transition (E_{gd}) and indirect transition (E_{qi}) energy gaps were found to be about 2.92 to 3.16 eV and 0.80 to 1.53 eV respectively, for as deposited PTMP samples of different thicknesses heat treated at 673 K for 1 hour are 0.55 and 0.65 eV (Fig.1.5).
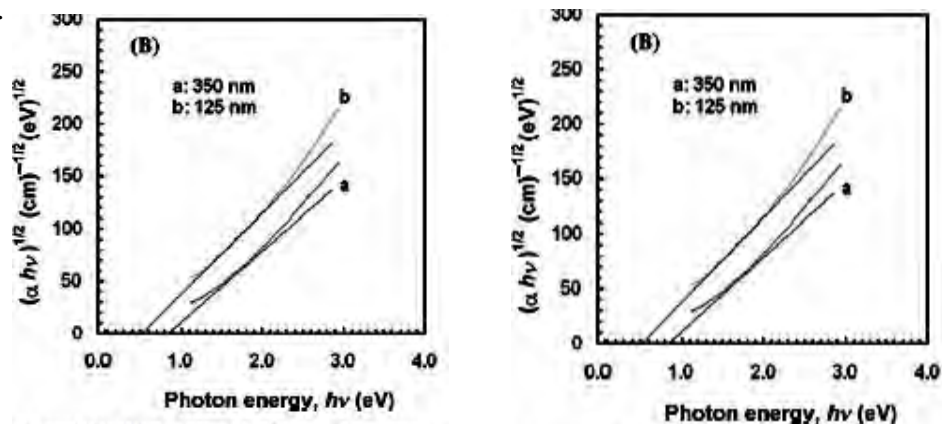
Fig.1.5 (a) Plot of $(\alpha h\nu)^2$ vs hν and (b) $(\alpha h\nu)^{1/2}$ vs hν for PPTMP thin films of different thicknesses.

Xiao Hu et al. [17] prepared plasma polymerized 4-cyanopyridine (PPCPD) thin films of desired thickness through plasma polymerization under different glow discharge conditions. The effect of the discharge power on this thin film was investigated by FITR and UV- measurements. A high retention of atomic ring structure of the staring monomer in the deposited plasma films was obtained when a low discharge power was used. A red shift in the maximum absorption wavelength for the films was observed as compared with the monomer absorption spectrum. low discharge power.

Kamal and Bhuiyan [18] studied the direct current conduction mechanism in plasma polymerized pyrrole-N, N, 3, 5 tetramethylaniline (PPPy-PPTMA) bilayer thin films. FTIR analyses showed that the PPPy-PPTMA bilayer thin films contained the structural characteristics of both the PPPy and PPTMA. The current density-voltage (J-V) characteristics of PPPy-PPTMA bilayer thin films of different deposition time-ratios indicated an increase in electrical conductivity as the proportion of PPTMA was increased in the bilayer films (Fig1.6). It is also observed that the conductivity of the bilayer thin film is reduced compared with its component thin films. It is seen that in the lower voltage region the current conduction obeys Ohm's law, while the charge transport phenomenon appears to be the space charge limited conduction in the higher voltage region. The mobility of the charges, the free charge carrier density, and the permittivity of the PPPy, PPTMA and PPPy - PPTMA bilayer thin films have been calculated.
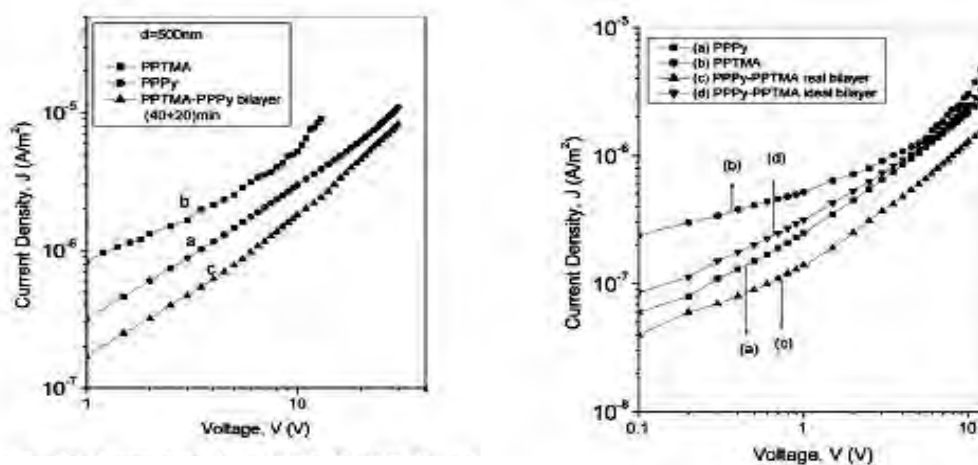
Fig.1.6 Plots of current density against applied voltage for PPPy, PPTMA and PPPy-PPTMA thin films.

From the UV–vis absorption spectra (PPPy), (PPTMA), and (PPPy-PPTMA) bilayer thin films on to glass substrates, allowed direct transition (E_{qd}) and allowed indirect transition (E_{qi}) energy gaps were determined (Fig1.7). The E_{qd} for PPPy, PPTMA, and PPPy-PPTMA bilayer films are found to be 3.30, 2.85, and 3.65 eV respectively. On the other hand, the E_{qi} for the same series are 2.25, 1.80, and 2.35 eV, respectively. From these results, it is seen that the energy gaps of the PPPy PPTMA bilayer films have been increased compared with the PPPy and PPTMA thin films [19].
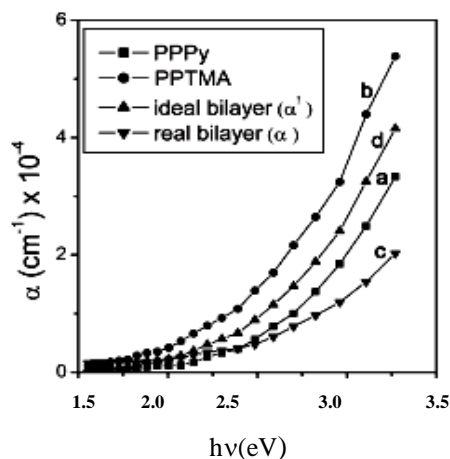
Fig.1.7 Plots of α vs hν for PPPy, PPPTMA and PPPy- PPTMA bilayer thin films.

Sajeev et al. [20] reported of pristine and iodine doped polyaniline thin films prepared by ac and rf plasma polymerization techniques compared the optical and electrical properties. It has been found that the optical band gap of the polyaniline thin films prepared by plasma polymerization techniques differ considerably and the band gap was further reduced by in situ doping by iodine. The measurement on these films shows higher value of electrical conductivity in the case of rf plasma polymerized thin films when compared to ac plasma polymerized thin films. Also it is found that the iodine doping enhanced conductivity of the thin films considerably. The result are compared, correlated and explained with respect to the different structure adopted under two preparation techniques (Fig.1.8).
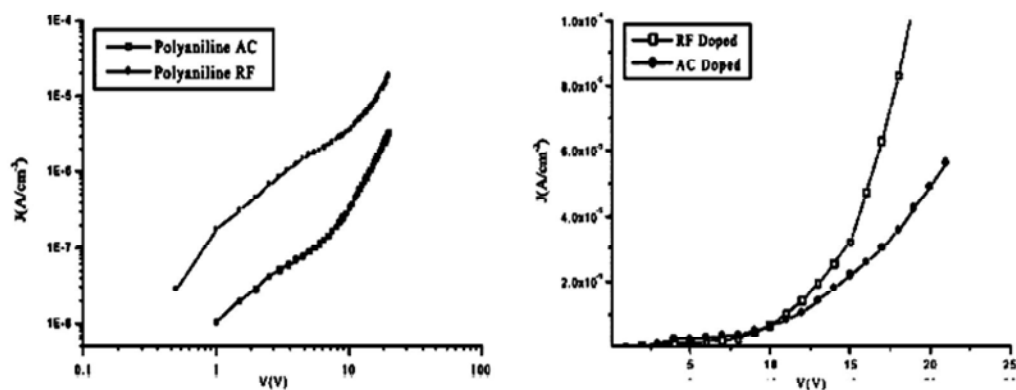
Fig.1.8 Plots of current density against applied voltage for Polyaline thin film depositied by ac and r.f plasma polymerization methods.

Silverstein and Fisher [21] investigated structural, electrical, optical properties of plasma polymerized thiophene (PPTH) and found that the PPTH films differed from the monomer structure and the band gap for the PPTH films was similar to that for conventional PTH. Undoped films exhibited nonlinear I-V behavior, typical of Schottky metal- semi conductor barrier with break down at reverse bias. Iodine doping yielded Ohmic I-V behavior.

El-Naahas et al. [22] investigated the physical characteristics of 4-tricyanovinyl-N, N-diethylaniline. The differential scanning calorimetrioy (DSC) showed the stability of this compound up to 423 K. The temperature dependence of the electrical conductivity was found typical for semiconducting compounds. The J-V characteristics revealed that the conduction current obeys Ohm's law while the charge transport phenomenon appears to be space-charge limited in the higher voltage region.

Zhao et al. [23] characterized the plasma polymerized 1-Cyanoisoquinoline thin films. From IR, XRD and SEM studies it was found that a high retention of aromatic ring structure of the starting monomer was found in the films. As the films were homogeneous it was used for dielectric measurements and showed a low dielectric constant which was obtained for this film for the first time.

Cho and Boo [24] deposited nitrogen-doped thiophene plasma polymer (N-ThioPP) thin films by rf method. The FITR spectra showed that the N-ThioPP films are completely fragmented and

polymerized from thiophene. NH_x species was increased by increasing the N_2 low rate. Also, decreasing the contact angle shows the surface energy of the N-ThioPP thin film with increasing N^2 low rate. Additionally, decreasing the contact angle indicates the indirect cause of the increasing N amounts in the N-ThioPP thin film. N bonded with thiophene molecules during the PECVD process. UV- is spectra of all samples show 80% of transmittance in the infrared region. However, transmittance in the visible region was dramatically changed by increasing the N amounts. Thus, the E_g of N-ThioPP was increased by increasing the N amounts.

Cho et al. [25] polymer-like organic thin films were deposited at room temperature and different rf powers by PECVD method using ethylcyclohexane as precursor. The corrosion protective abilities were examined by potentiodynamic curves measurements in 3.5 wt.% NaCl solution. The experimental results show an increased of corrosion protective abilities of ethylcyclohexane were provided an increased corrosion performance with increasing rf power. The SEM data showed that the polymer films with smooth surface and sharp interface could be grown under different rf powers.

Kim et al. [26] synthesized three kinds of chromophores were synthesized incorporating aromatic quinoline unit as a conjugated bridge in order to prepare more thermally stable nonlinear optical (NLO) chromophores than general stilbene unit. The NLO poly (methylmethacrylate) (PMMA) copolymer, olyimides, and polyester were successfully synthesized by these corresponding quinoline-based monomers. Their physical and optical properties were investigated by thermo gravimetry, ultraviolet-visible spectroscopy, second harmonic generation (SHG) and electro-optic (EO) measurements. All the polymers exhibited better thermal stability, however their NLO activity was a little lower than that of general stilbene-based NLO polymers. Among three kinds of polymers, the PMMA copolymer with quinoline chromophores had the largest HG coefficient d33 value of 27 pm/V (at 1.064 μm) and EO coefficient r33 value of 6.8 pm/V (at 1.3 μm).

Jae-Sung Lim et al. [27] organic polymer dielectric thin films of styrene and vinyl acetate were prepared by the plasma   polymerization deposition technique and applied for the fabrication of an organic thin film   transistor device. The structural properties of the plasma polymerized thin films were characterized by FTIR, XRD, and contact angle measurements. Investigation of the electrical properties of the plasma polymerized thin films was carried out by capacitance-voltage

and current-voltage measurements. The organic thin film transistor device with gate dielectric of the plasma polymerized thin film revealed a low operation voltage of 10 V and a low threshold voltage of -3 V. It was confirmed that plasma polymerized thin films of styrene and vinyl acetate could be applied to functional organic thin film transistor devices as a gate dielectric.

Ahmed et al. [28] fabricated plasma polymerized c-terpinene (pp-GT) thin films are using rf plasma polymerization. MIM structures are fabricated and using the capacitive structures dielectric properties of the material is studied. The current density – voltage (J-V) characteristics of pp–GT thin films are investigated as a function of rf deposition power at room temperature to determine the resistivity and dc conduction mechanism of the films (Fig. 1.9). At higher applied voltage region, Schottky conduction is the dominant dc conduction mechanism. The capacitance and the loss tangent are found to be frequency dependent. The conductivity of the pp2GT thin films is found to decrease from 1.39×10^{-2} S/cm (10 W) to 1.02×10^{-2} S/cm (75 W) and attributed to the change in the chemical composition and structure of the polymer. The breakdown field for pp–GT thin films increases from 1.48 MV/cm (10 W) to 2 MV/cm (75 W). A single broad response for temperature dependent J-V.
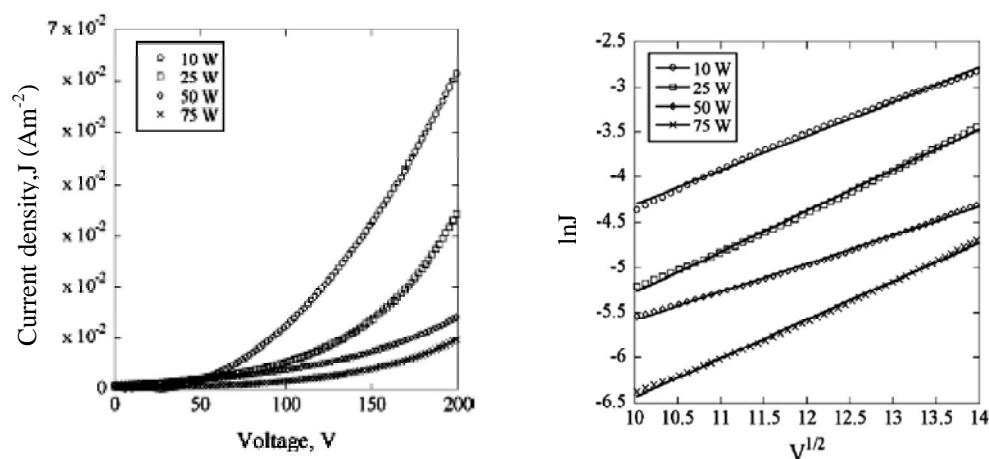
Fig.1.9 (a) Plots of current density against applied voltage and (b) variation of lnJ with square root of applied voltage at different plasma powers for polymerized c - terpinene thin film.

Islam Shama et al. [29] synthesized Poly (*o*-toluidine) (POT) polymer by chemical method and rf plasma polymerization at a rf power input of 15 W on ultrasonically cleaned glass and silicon water substrates. The dc-conductivity was measured at 410 K, which was found to increase by

two orders of magnitude for thin film as compared to pellet samples. It has been observed that the activation energy increases for rf plasma-polymerized POT. The results indicate (Fig1.10) that the structures of plasma-polymerized POT are rather different from polymers synthesized by conventional chemical methods, due to a higher degree of cross-linking and branching reactions in plasma polymerization. This makes them suitable for various electro active devices. A higher and more stable conductivity can be obtained with rf plasma polymerized POT which is much smoother and more uniform.
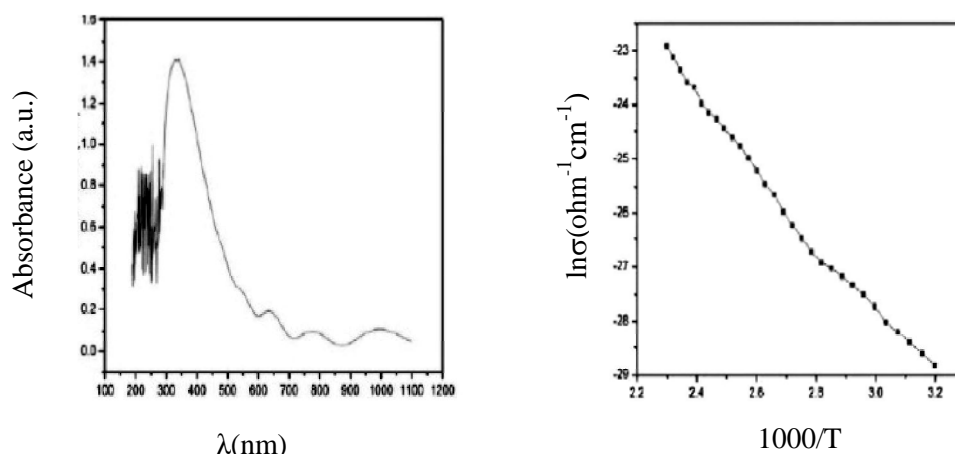
Fig.1.10 (a) Plots of ABS vs λ and (b) $\ln\sigma$ (ohm^{-1}cm^{-1}) vs 1000/T for a poly (o-toluidine).

Tamanna and Bhuiyan [30] the review of the research publications declares to synthesize organic thin films by plasma polymerization technique and to characterize these for suitability of using is different electronic, optoelectronic device, sensors, etc. The Fourier transform infrared spectroscopic investigation indicates the presence of the –CH2– group in as-deposited PPDEAEMA and heat treated PPDEAMEA. The absorption coefficient, allowed direct transition, E_{qd}, and allowed indirect transition, E_{qi}, energy gaps were determined from the ultraviolet–visible absorbance spectra (Fig1.11). E_{qd} and E_{qi} decrease with an increase in thickness and are found to be about 3.25 eV –3.45 eV and 1.65–1.90 eV, respectively, for as deposited PPDEAEMA thin films of different thicknesses.
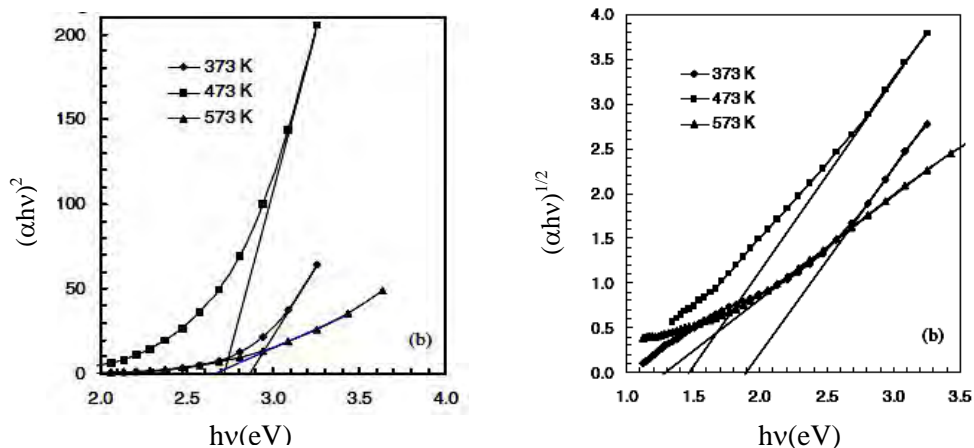
Fig.1.11 (a) Plots of $(\alpha h\nu)^2$ vs hν and (b) $(\alpha h\nu)^{1/2}$ vs hν for a PPDEAEMA thin film at different heat treatment temperatures.

Islam Shama et al. [31] prepared thin films of poly(*o*-toluidine) (POT) by rf plasma polymerization at radio frequency (rf) power input 15 W, making suitable modifications in a rf-sputtering set-up. The deposition rate is found to be 3.33 nm/min. The films are characterized by dc conductivity, UV-Vis, FTIR. The dc conductivity of the POT thin films has been analyzed in the temperature range 312-435 K and is found to increase with temperature. The Arrhenious plot of dc conductivity shows straight line behavior (Fig1.12). The optical band gap has been estimated to be 1.66 eV from UV-vis absorption spectrum.
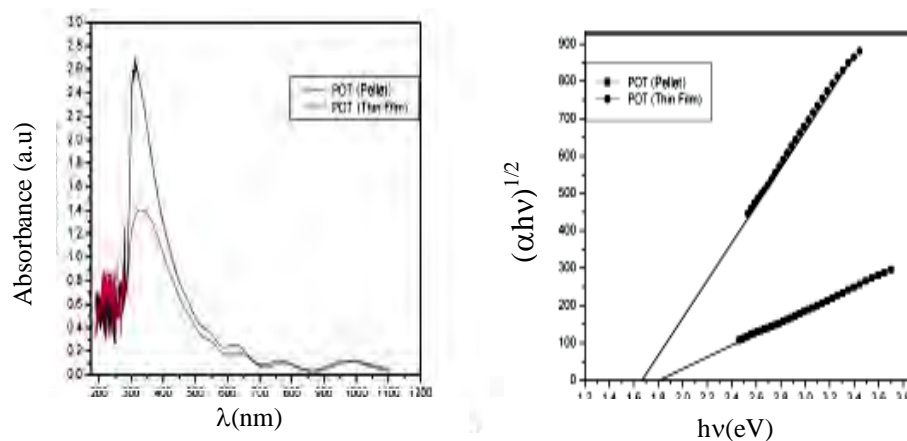
Fig.1.12 (a) Plots of ABS vs λ and (b) $(\alpha h\nu)^{1/2}$ vs hν for POT thin films .

Zhao Xiong et al. [32] prepared a novel plasma polyquinoline derivative thin film, plasma-polymerized 3 –cyanoquinoline (PP3QCN). Fourier transform infrared spectroscopy (FTIR), UV-visible (UV-Vis) absorption spectroscopy, X-ray photoelectron spectroscopy (XPS), and atomic force microscopy (AFM) characterization revealed that the plasma polymerization conditions affected the chemical structure, surface composition, morphology, and dielectric property of the plasma deposited films (Fig1.13). A smooth and homogenous PP3QCN film with a large conjugated system and a high retention of the aromatic ring structure of the monomer was obtained at a low discharge power of 10 W. At 25 W, more severe monomer molecular fragmentation was apparent during the plasma polymerization and thus the conjugation length of the PP3QCN films decreased because of the formation of a non-conjugated polymer.
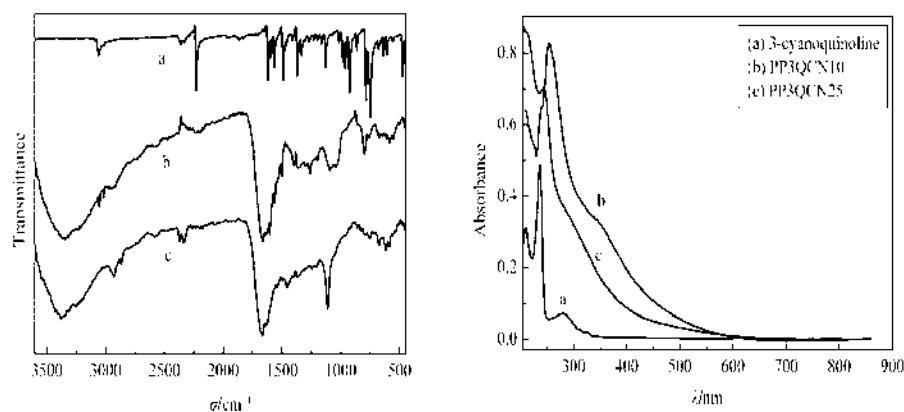
Fig.1.13 (a) Transmittance vs σ/cm^{-1} and (b) Absorbance vs λ (nm) for PP3QCN thin films.

1.3 Objectives of the Present Study

The objectives of this works are to prepare thin film of Quinoline by plasma polymerization technique, an attractive technique over conventional methods and characterizing those using different physical techniques. The chemical structure, absorption coefficient, optical energy gaps, direct, and indirect transitions, etc, of the plasma polymerized quinoline (PPQ) will be investigated. The charge transport mechanism in the PPQ thin films would be determined. Finally, the structure property relation of the thin films will be analyzed with a view to find its suitability in efficient devices.

Scanning electron microscopic (SEM) and an Energy Dispersive X-ray (EDX) analysis would be done to investigate the surface morphology and compositional analysis of PPQ thin films. The

chemical structure of the quinoline monomer and PPQ thin film would be investigated by FTIR spectroscopy and the chemical changes occurred in PPQ thin film would be compared with quinoline structure.

DTA and TGA would be employed for thermal analysis.

The UV-vis absorption spectroscopic analysis would be done to determine the absorption coefficient, direct and indirect transition energy gaps in PPQ thin films.

The variation of current with voltage at different temperatures of PPQ thin films of different thicknesses would be measured to specify the charge transport mechanism in PPQ. The temperature dependence of current would also be investigated to understand the thermally activated conduction process in PPQ.

1.4 Thesis Layout

This research work has been organized into six chapters in this thesis.

Chapter 1 presents the introduction, review of some earlier and recent research work of interest and objectives of this thesis work.

Chapter 2 gives a brief discussion on polymers, plasma and polymerization, different polymerization process, different types of glow discharge and Glow discharge reactors, some characteristic difference of plasma polymers from the conventional polymers etc.

Chapter 3 discussion of scanning electron microscopy (SEM), energy dispersive X-ray analysis (EDX), consists of the different theories of FTIR spectroscopy, UV-vis spectroscopy, DTA – TGA and DC electrical conduction mechanism.

Chapter 4 includes description of materials and also contains the experimental procedures different measurements.

Chapter 5 covers results and discussion of thermal Analysis, UV-vis absorption spectroscopic analysis on PPQ thin films, FTIR analysis PPQ and J-V characteristics and temperature dependence of current density of PPQ thin films.

Chapter 6 offers the conclusions and suggestions for further research work.

Reference

[1]. Yasuda H., 'Plasma Polymerization', Academic Press, Inc, New York (1985).

[2]. Riccardo d' Agostino (Ed.), 'Plasma Deposition, Treatment and Etching of Polymers' Academic Press, Boston (1990).

[3]. Chermisinoff N P, 'Handbook of Polymer Science and Technology', Marcel Dekker Inc., New York, 4, (1989).

[4]. Biderman H, Osada Y, 'Plasma Chemistry of Polymers', in: H Biderman (Ed.), Polymer Physics, Springer Verlag, Berlin, 57-109, (1990).

[5]. Suhur, H., Bell A. T., 'In technique and application of plasma chemistry': Hollahan', (Ed.), John Wiley & Sons, New York, (1974).

[6]. Bell. A. T., l A. T., Shen (Eds) 'Plasma Polymerization' Amer. Chem. Soc., Washington, D. C. (1979).

[7]. Bradely A, Hammers J. P., 'Electrical properties of thin organic films', J. Electrochem. Soc.,110(1), 15-22, (1963).

[8]. Gregor L. V., 'Electrical conductivity of polydivinylbenzene films', Thin Solid Films, 2, 235-246, (1968).

[9]. Hirai T., Nakada O., 'Formation of thin polyacrylonitrile films and their electrical properties'. Jpn. J. Appl. Phys., Jpn. J. Appl. Phys., 7(2), 112-121, (1968).

[10]. Majumder, S., Bhuiyan A. H., 'DC conduction mechanism in plasma polymerized vinylene carbonate thin films prepared by glow discharge technique', Polym. Sci., 53, 85-91, (2011).

[11]. Akther H., Bhuiyan A. H., 'Electrical and optical properties of plasma polymerized N, N, 3, 5,-tetramethylaniline thin films', New J. Phys., 7,173, (2005).

[12]. Akther H., Bhuiyan A. H., 'Infrared and ultra violet-visible spectroscopic investigation of plasma polymerized N, N, 3, 5,-tetramethylaniline thin films'. Thin Solid Films, 474, 14-18, (2005).

[13]. Matin R., Bhuiyan A. H., 'Infrared and ultraviolet-visible spectroscopic analyses of plasma polymerized 2, 6 diethylaniline thin films', Thin Solid Films, 534, 100-106, (2013).

[14]. Chowdhury F. U. Z., Bhuiyan A. H., 'An investigation of the optical properties of plasma polymerized diphenyl thin films,' Thin Solid Films, 360 , 69±74, (2000).

[15]. Shah Jalal A. B. M., Bhuiyan A. H.,Ahmed S., Ibrahim M., 'On the conduction mechanism in plasma polymerized m-xylene thin films', Thin Solid Films, 295, 125-130, (1997).

[16]. Tamanna A., Bhuiyan A. H., 'Infrared and ultraviolet-visible spectroscopic studies of plasma polymerized 1, 1, 3, 3-tetramethoxypropane thin films,' Thin Solid Films, 519, 1825-1830, (2011).

[17]. Zhao, Wang X., Xiao M., J. 'Deposition of plasma conjugated polynitrile thin films and their optical properties,' Eur. Polym. J., 42, 2161-2167, (2006).

[18]. Kamal M. M., Bhuiya A.H., 'Direct current electrical characterization of plasma polymerized pyrrole-N,N,3,5 tetramethylaniline bilayer thin films,' J. of Appl. Polym. Sci., 125, 1033–1040, (2012).

[19]. Kamal M. M., Bhuiyan A.H., ' Optical characterization of plasma-polymerized pyrrole-N, N, 3, 5-tetramethylaniline bilayer thin films,' J. Appl. Polym. Sci., 121, 2361–2368, (2011).

[20]. Sajeev U. S., Mathai, C. J., Saravanan S., Ashokan R, Venkatachlm S., Anantharaman M. R., 'On the optical and electrical properties of rf a.c plasma polymerized aniline thin films.,' Bull. Mater. Sci., 29, No. 2(2006).

[21]. Silverstein M. S., Visoly-Fisher 'Plasma polymerized thiophene: molecular structure and electrical properties,' Polym. 43, 11-20, (2002).

[22]. E-Nahass M. M., Abd-El-Rahman K. F., Darwish A. A. A., Electrical conductivity of 4-trycyanovinyl-N, N-diethylaniline', Physica, B403, 291-223, (2008).

[23]. Zhao X. Y., Wang M.Wang Z., 'Deposition of plasma polymerized 1-cynoisoquinoline thin films and their dielectric properties', Plasma Process Polym., 4, 840-846, (2007).

[24]. Cho S., Boo J., 'A study on the characteristics of plasma polymer thin film with controlled nitrogen flow rate', Nanoscale Res. Lett., 7, 62(1-4) (2012).

[25]. Cho S. H., Park Z. T., Kim J. H., 'Physical optical properties of plasma polymerized thin films depositied by PECVD method,' Surf. Coa. Technol., 174-175, 1111-1115, (2003).

[26]. Kim., Jin., Lee., Nakjoong Kim, Park.,'Synthesis and characterization of nonlinear optical polymers having quinoline-based chromophores', Electronic Materials and Devices Research Center, Korea Institute of Sci. and Technol., 130-650, (2002).

[27]. Jae-Sung Lim, Paik-Kyun Shin, Boong-Joo Lee, 'Organic thin film transistors with gate dielectrics of plasma polymerized styrene and vinyl acetate thin films', Trans Electr Electr. Mater, 16, 95-98, (2015) .

[28]. Ahmad Jakaria, Bazaka Kateryma, Vasilev krasimir, Jacob Mohan V., 'Electrical conduction in plasma polymerized thin films of γ-terpinene', J. Appl. Sci., 132, 42318, (2015).

[29]. Islam Shama, Lakshmi G. B. V. S., Zulfequar M, Husain M, Siddiqui M. A., 'Comparative studies of chemically synthesized and rf plasma-polymerized poly(o-toluidine)', J. phys. , 84, 653-665, (2015).

[30].Tammana A., Bhuiyan A. H., ' Effect of aging on the optical properties of plasma polymerized1,1,3,3tetramethoxypropane thin films', Inc. Adv Polym. Tech., 32, 21347, (2013).

[31]. Islam Shama, Lakshmi G. B. V. S., Zulfequar M, Husain M, Siddiqui M. A., 'RF plasma polymerization and electrical, optical and structural properties of thin films of poly (*o*-toluidine)', Ind. Pure Appl. Phys, 52, 486-490, (2014).

[32]. Zhao Xiong-Yan. 'Synthesis and characterization of a polyquinoline derivative thin film with a low dielectric constant.' Acta Phys. -Chim. Sin., 26(4),1164-1170, (2010).

Chapter-2

Polymer and Plasma Polymerization

2.1 Introduction

Polymers form a very important class of materials without which the life seems very difficult. They are all around us in everyday use; in rubber, in plastic, in resins, and in adhesives and adhesives tapes. The word polymer is derived from Greek words, poly = many and mers = parts or units of high molecular mass each molecule of which consist of a very large number of single structural units joined together in a regular manner. In other words polymers are giant molecules of high molecular weight, called macromolecules, which are build up by linking together of large number of small molecules, called monomers. The reaction by which the monomers combine to form polymer is known as polymerization [1]. The polymerization is a chemical reaction in which two or more substances combine together with or without evolution of anything like heat or any other solvents to form a molecule of high molecular weight.

Monomers

Polymerization
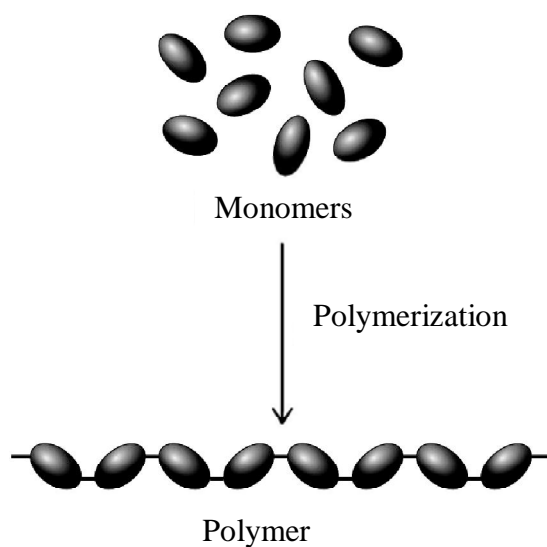
Polymer

Fig.2.1 Monomer and Polymer.

The product is called polymer and the starting material is called polymer and the starting materials is called monomer.

The transformation of ethene to polythene and interaction of hexamethylene diamine and adipic acid leading to the formation of Nylon 6, 6 are examples of two different types of polymerization reactions.

The systematic study of polymer science started only about a century back with the pioneering work of Herman Staudinger. Staudinger has given a new definition of polymer. He in1919 first published this concept that high molecular mass compounds were composed of long covalently bonded molecules.

2.1.1 Classification of polymer [1]

Polymer can have different chemical structure, physical properties, mechanical behavior, thermal characteristics, etc., and on the basis of these properties polymer can be classified in different ways, which are summarized in Table 2.1. Important and broad classifications of polymers are described below. There are several ways of classification of polymers based on some special considerations.

Table 2.1 Classification of polymer.
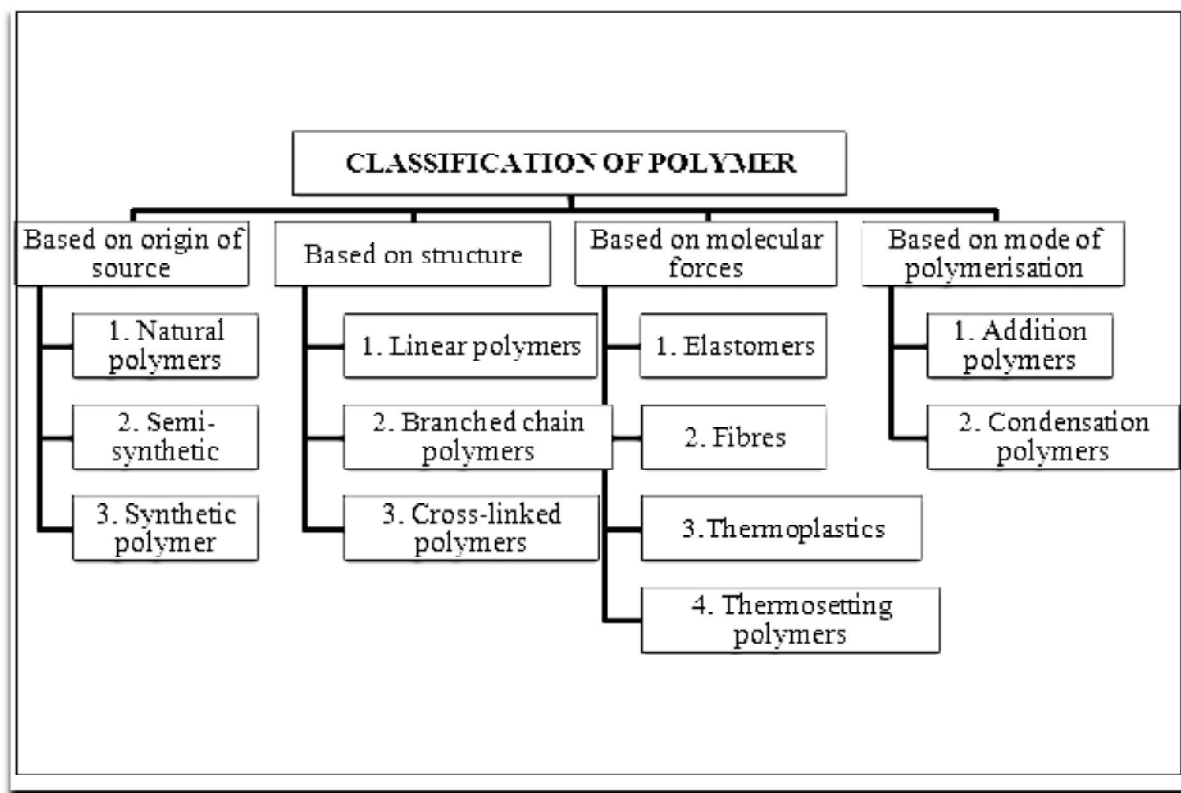
Classification Based on Source: This type of classification, there are three sub categories

[i] *Natural Polymers*: These polymers are found in plants and animals. Examples are proteins, cellulose, starch, resins and rubber.

[ii] *Semi-synthetic Polymers*: Cellulose derivatives as cellulose acetate (rayon) and cellulose nitrate, etc. are the usual examples of this sub category.

[iii] *Synthetic Polymers*: A variety of synthetic polymers as plastic (polythene), synthetic fibers (nylon 6,6) and synthetic rubbers (Buna - S) are examples of man-made polymers.

Classification Based on Structure of Polymers:

[i] *Linear Polymers*: These polymers consist of long and straight chains. The examples are high density polythene, polyvinyl chloride, etc.

[ii] *Branched Polymers*: These polymers contain linear chains having some branches, *e.g.*, low density polythene.

[iii] *Cross-linked Polymers*: These are usually formed from bi-functional and tri-functional monomers and contain strong covalent bonds between various linear polymer chains, e.g. vulcanized rubber, urea-formaldehyde resins, etc.

[i] Linear polymers   [ii] Branched polymers   [iii] Crossed-linked polymers

Fig.2.2 Network structure of [i] Linear polymers, [ii] Branched polymers, [iii] Crossed-linked polymers.

Homopolymer: A polymer resulting from the polymerization of a single monomer; a polymer consisting substantially of a single type of repeating unit.

A-A-A-A-…. Homopolymers

Copolymer: When two different types of monomers are joined in the same polymer chain, the polymer is called a copolymer. Let's imagine now two monomers, which we'll call *A* and *B*. *A* and *B* can be made into a copolymer in many different ways.

(i) When the two monomers are arranged in an alternating fashion, the polymer is called an alternating copolymer.

(ii) In a **random copolymer**, the two monomers may follow in any order.

(iii) In a **block copolymer**, all of one type of monomers are grouped together, and all of the other are grouped together. A block copolymer can be thought of as two homopolymers joined together at the ends:

(iv) **Branched copolymers** with one kind of monomers in their main chain and another kind of monomers in their side chains are called graft copolymers.

Block Copolymer   Graft Copolymer   Random Copolymer
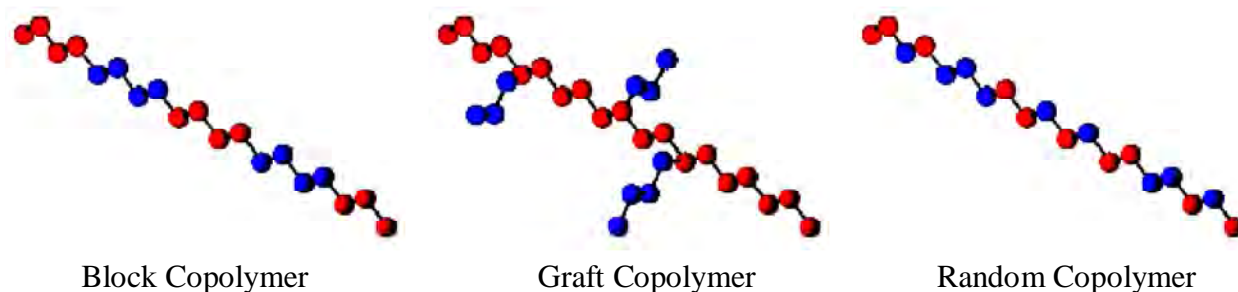
Fig.2.3 Network structure of Block Copolymer, Graft Copolymer, Random Copolymer.

Copolymerization: A **heteropolymer** or **copolymer** is a polymer derived from two (or more) monomeric species, as opposed to a homopolymer where only one monomer is used. Copolymerization refers to methods used to chemically synthesize a copolymer. Commercially relevant copolymers include ABS plastic, SBR, Nitrile rubber, styrene-acrylonitrile, styreneisoprene- styrene.

Tacticity: The orientation of monomeric units in a macromolecule can take an orderly or disorderly fashion with respect to the chain.

If all the side groups lie on the same side of the chain (cis arrangement), it is called an **'isotactic'** polymer, *e.g.*, natural rubber.

If the monomers have entered the chain in a random fashion, it is called an **'atactic'** polymer, *e.g.*, polypropylene.

If the arrangement of side groups is in alternating fashion (trans arrangement), it is called a **'syndiotactic'** polymer, *e.g.*, Guttapercha.

Classification Based on Mode of Polymerization**:**

Polymers can also be classified on the basis of mode of polymerization into two sub groups; (a) **Addition Polymers** and (b) **Condensation Polymers**.

Addition Polymers: The addition polymers are formed by the repeated addition of monomer molecules possessing double or triple bonds, *e.g.*, the formation of polythene from ethene and poly propene from propene. However, the addition polymers formed by the polymerization of a single monomeric species are known as homopolymer, *e.g.*, polythene.

Condensation Polymers: The condensation polymers are formed by repeated condensation reaction between two different bi-functional or tri-functional monomeric units. In these polymerization reactions, the elimination of small molecules such as water, alcohol, hydrogen chloride, etc. take place.

Classification Based on Molecular Forces

Mechanical properties of polymers like tensile strength, toughness, elasticity depends upon intermolecular forces like van-der waals forces and Hydrogen bonding. On the basis of these forces they are classified as

a. Elastomers: These are rubbery like solids with elastic properties. In these elastomeric polymers, the polymer chains are held together by the weakest intermolecular forces. These weak binding forces permit the polymer to be stretched. A few 'crosslinks' are introduced in between the chains, which help the polymer to retract to its original position after the force is released as in vulcanized rubber.

b. Fibers: Fibers are the thread forming solids which possess high tensile strength and high modulus. These characteristics can be attributed to the stronger molecular forces like hydrogen bonding. These strong forces also lead to close of chains and thus impart crystalline nature. Used in textile industries.

c. Thermoplastic polymers: These are the polymers having intermolecular forces between elastomers and fibers. They are those polymers which can be softened on heating and hardened on cooling room temperature. They may be linear or branched chain polymers. These polymers can be recycled many times.

d. Thermosetting polymers: This polymer is hard and infusible on heating. These are not soft on heating under pressure and they are not remolded. These polymers are cross linked or heavily branched molecules. We cannot reuse or recycle these polymers**.**

2.1.2 Crystalline and amorphous of polymer

Although it may at first seem surprising, Polymers can form crystal structures (all we need is a repeating unit, which can be based on molecular chains rather than individual atoms). Some parts of structure align during cooling to form crystalline regions (chains align alongside each other). Around crystallites get amorphous regions. Most real polymers contain both amorphous and crystalline regions, called semi-crystalline.

The morphology of most polymers is semi-crystalline. That is, they form mixtures of small crystals and amorphous material and melt over a range of temperature instead of at a single melting point. The crystalline material shows a high degree of order formed by folding and

stacking of the polymer chains. The amorphous or glass-like structure shows no long range order, and the chains are tangled as illustrated below.

Crystalline   Amorphous
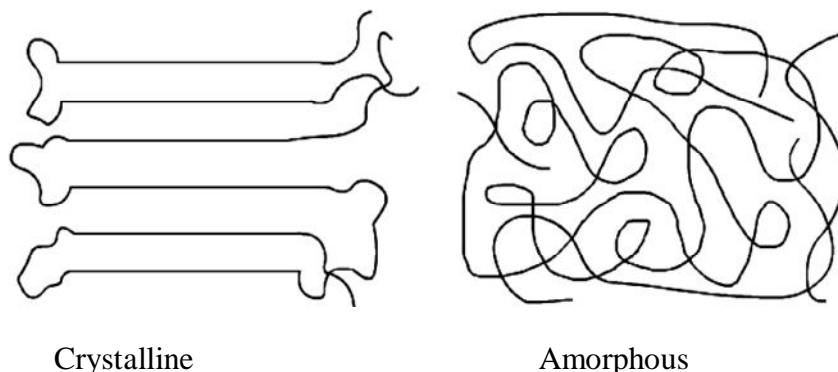
Fig.2.4 Crystalline and amorphous states of polymer.

There are some polymers that are completely amorphous, but most are a combination with the tangled and disordered regions surrounding the crystalline areas. Such a combination is shown in the following diagram.

Fig.2.5 Disordered region in amorphous polymer.

An amorphous solid is formed when the chains have little orientation throughout the bulk polymer. The *glass transition temperature* is the point at which the polymer hardens into an amorphous solid. This term is used because the amorphous solid has properties similar to glass.

In the crystallization process, it has been observed that relatively short chains organize themselves into crystalline structures more readily than longer molecules. Therefore, the degree of polymerization (DP) is an important factor in determining the crystallinity of a polymer. Polymers with a high DP have difficulty organizing into layers because they tend to become tangled.

The cooling rate also influences the amount of crystallinity. Slow cooling provides time for greater amounts of crystallization to occur. Fast rates, on the other hand, such as rapid quenches, yield highly amorphous materials. Low molecular weight polymers (short chains) are generally weaker in strength. Although they are crystalline, only weak Van der Waals forces hold the lattice together. This allows the crystalline layers to slip past one another causing a break in the material. High DP (amorphous) polymers, however, have greater strength because the molecules become tangled between layers.

Also influencing the polymer morphology is the size and shape of the monomers' substituent groups. If the monomers are large and irregular, it is difficult for the polymer chains to arrange themselves in an ordered manner, resulting in a more amorphous solid. Likewise, smaller monomers, and monomers that have a very regular structure (e.g. rod-like) will form more crystalline polymers.

Cross-Linking in polymer

In addition to the bonds which hold monomers together in a polymer chain, many polymers form bonds between neighboring chains. These bonds can be formed directly between the neighboring chains, or two chains may bond to a third common molecule. Though not as strong or rigid as the bonds within the chain, these cross-links have an important effect on the polymer. Polymers with a high enough degree of cross-linking have "memory." When the polymer is stretched, the cross-links prevent the individual chains from sliding past each other. The chains may straighten out, but once the stress is removed they return to their original position and the object returns to its original shape. One example of cross-linking is vulcanisation. In vulcanisation, a series of cross-links are introduced into an elastomer to give it strength. This technique is commonly used to strengthen rubber [1].

2.1.3 States of polymer

To characterize polymers usual description of three states (Solid, Liquid and Gaseous) of matter is not sufficient. The concept of phase state is also not enough for these specifications either. The polymer structure is liquid in physical state, but it is in fact in the solid state of aggregation and there is no three-dimensional long-range order. Polymers can exist in three different states: a) the viscofluid state b) the rubbery state and c) the glassy state.

a) The viscofluid state

The viscofluid state of polymer is characterized by the intensive thermal motion of individual units, large fragments of the polymeric chain and the movement of the macromolecule as a whole. This state is typical of most liquids. The most important specific feature of polymers existing in this state is the ability to flow under the influence of the applied stress (fluidity).

b) The rubbery state

The rubbery (high elastic) state is the characteristic of polymer only. In the rubbery state individual units, atomic groups and segments undergo intensive thermal motion. Polymers in these states possess remarkable mechanical properties. The folded flexible long chains straighten out under the influence of the applied stress and return to their original shape after the stress is removed as a result of thermal motion.

c) The glassy state

When the temperature is lowered a liquid can crystalline or pass to the glassy state, which sets in when highly viscous liquids are overcooled. The transition to the glassy state is possible for both low-molecular mass substances and polymers. In this state polymers are no longer capable of undergoing segmental motion. The glassy state is characterized by the vibration motion, small units in the main chain and also atomic groups.

2.1.4 Different Polymerization Processes

Polymerization may generally be defined as intermolecular reaction between bifunctional or polyfunctional compounds avoiding formation of ring or cyclic structures and in a manner that make the process functionally capable of proceeding to infinity. Functional groups or atoms are: reactive hydrogen (-H), hydroxy(-OH), carboxyl group(-COOH), amino group(-NH2), halogen atoms(-Cl,-Br) and C=C double bond etc. The process of polymerization may be divided into two ways (i) Chemical process and (ii) Physical process.

2.1.4.1 Chemical process or conventional polymerization process

A variety of methods are employed for producing polymer films and the three most important groups are step growth, addition, and free radical polymerization [2, 3].

 i) Step growth polymerization

In step-growth polymerization, a linear chain of monomer residues is obtained by the stepwise intermolecular condensation or addition of the reactive groups in bifunctional monomers. These

reactions are analogous to simple reactions involving monofunctional units as typified by a polyesterification reaction,

HO-R-OH + HOOC-R-COOH <=> HO-R-OCO-R-COOH + H2O Two major groups,
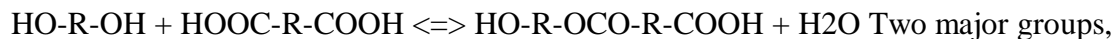
 ii) Addition polymerization or chain-growth polymerization

Addition or chain-growth polymerization is a process by which unsaturated monomers are converted to polymers of high molecular weight, exhibiting the characteristics of a typical chain reaction.

Addition or chain-growth polymerization is usually done in gas phase in liquid bulk monomer or under melt condition, or by solution suspension or emulsion techniques.

iii) Free radical polymerization

A free radical is an atomic or molecular species whose normal bonding system has been modified such that an unpaired electron remains associated with the new structure. The radical is capable of reacting with an olefinic monomer to generate a chain carrier which can retain its activity long enough to propagate a macromolecular chain under the appropriate conditions. The most important aspects of free radical polymerization are:

The rate of polymerization is proportional to the square root of the initiator concentration or the square root of the rate of the initiation. The degree of polymerization is inversely proportional to the square root of the initiator concentration or the square root of the rate of the initiation. Accordingly, faster polymer formation leads to a shorter chain length of the resulting polymers.

Except these methods, thin polymer films can be prepared in the two ways: one includes wet process like Langmuir-Blodgett (LB), spreading, dipping or solvent casting methods and the other is dry processing, such as physical vapor deposition(PVD) and chemical vapor deposition(CVD).

2.1.4.2 Physical process

The important physical processes of thin film formation are that a)Vacuum evaporation and b) Plasma polymerization.

a) Vacuum evaporation [4]: The vacuum evaporation is a kind of technique for the preparation of thin films, which includes sublimation and a condensation process. The condensation process where the film formation occurs is related with a balance among the adsorption of sublimated molecules at the substrate surface, the surface-diffusion of the adsorbed molecules, and the secession of the adsorbed molecules from the substrate surface. The important characteristic

features of this technique are that the transport of vapors from the source to the substrate takes place by physical means. In this process, a vacuum chamber evacuated to about 10-5 Torr or below, contains a vapor source for example a resistive foil source and a substrate. The material to be evaporated is in thermal contact with foil source. When the vapor source is heated by passing an electric current, the vapor pressure of the evaporate becomes substantial and liberated atoms are sent out into the vacuum chamber and stick to the substrate where a thin film consequently formed.

As the name implies vacuum evaporation technique consists of vaporization of the solid material by heating it to sufficiently high temperature and condensing it onto a cooler substrate to form a film. The deposition of thin films by vacuum evaporation consists of several distinguishable steps.

Transition of a condensed phase, which may be solid or liquid into the gaseous state. Vapor traversing the space between the evaporation source and the substrate at reduced gas pressure, Condensation of the vapor upon arrival on the substrates.

The liquid vapor transformation is called evaporation and solid to vapor transformation is called sublimation. Thus by evaporation method films of high quantity are produced with a minimum of interfering conditions. In practice they are applicable to all substances and to a great range of thicknesses.

b) Plasma polymerization

A little detail about plasma and plasma polymerization is documented in the following sections.

2.2 Plasma and Plasma Polymerization

2.2.1 Plasma

Plasma is often called the "Fourth State of Matter,". A plasma is a distinct state of matter containing a significant number of electrically charged particles, a number sufficient to affect its electrical properties

Plasma is used to describe the state of ionized gas. Plasmas are ionized gases. An ionized gas consists mainly of positively charged molecules or atoms and negatively charged electrons. The state of plasma can be created by variety of means. A gaseous complex that may be composed of electrons, ions of either polarity, gas atoms and molecules in the ground or any higher state of any form of excitation as well as of light quanta is referred to as plasma. The ionization degree can vary from 100% (fully ionized gases) to very low values (partially ionized gases). When the

temperatures greater than 10,000 K all molecules and atoms tend to become ionized. Plasma is considered as being a state of materials, and the state is more highly activated than in the solid liquid, or gas state. Besides the astroplasmas there are two main groups of laboratory plasmas, i.e. the high-temperature or fusion plasma and the so-called low temperature plasma or gas discharge [4, 6]. Generally subdivision can be made between plasmas, which are in thermal equilibrium, and those, which are not in thermal equilibrium. Thermal equilibrium implies that the temperature of all species (electrons, ions, and neutral species) is the same. Often the term 'Local thermal equilibrium (LTE) is used, which implies that the temperatures of all plasma species are the same in localized areas in the plasma. On the other hand, interstellar plasma matter is typically not in thermal equilibrium also called 'non-LTE'. The gas discharge plasmas can also be classified into LTE and non-LTE plasmas. This subdivision is typically related to the pressure in the plasma. Indeed a high gas pressure implies many collisions in the plasma, leading to a efficient energy exchange between the plasma species and hence equal temperatures. A low gas pressure, on the other hand, results in only a few collisions in the plasma species due to inefficient energy transfer. In recent years, the field of gas discharge plasma applications has rapidly expanded [8-10]. The wide variety of chemical non-equilibrium conditions is possible since the parameters such as the chemical input, the pressure, the electromagnetic field structure, the discharge configuration, the temporal behavior can easily be modified. Because of this multi-dimensional parameter space of the plasma conditions, there exists a large variety of gas discharge plasmas employed in a large range of applications. Four types of plasma i.e., the glow discharge (GD), capacitively coupled (CC), inductively coupled plasma (ICP), and the microwave-inductively plasma (MIP) are more widely used in technological fields.

2.2.2 Plasma polymerization

Plasma polymerization is defined as the formation of polymeric materials under the influence of plasma conditions. The deposition of solid coatings under plasma conditions has been well studied since the 1960s, with a very wide range of materials now accessible. The solid materials deposited under plasma conditions are generally referred to as plasma polymers, but they are unique and distinct from traditional polymers in that they lack the repeat structure that typically defines a polymer chain. Plasma polymerization takes place in a low pressure and low temperature plasma that is produced by a glow discharge through an organic gas or vapor [10]. Plasma polymerization depends on monomer flow rate, system pressure and discharge power

among other variable parameters such as the geometry of the system, the reactivity of the starting monomer, the frequency of the excitation signal and the temperature of the substrate. Various plasma polymer deposition methods such as dc, af-magnetron and RF are discussed by Yasuda et al [11]. The overall power input in plasma polymerization is used for two things: for creating the plasma and for fragmentation of monomer. Plasma is a direct consequence of the ionization of the gases present in the reactor and fragmentation leading to polymerization is secondary process. Plasma polymerization is a process in which organic materials are reacted in an ionizing gas environment to form cross-linked polymer films. An ultra thin film can be formed by this process where thin films deposit directly on surfaces as comprising the vacuum deposition of covalently bonded materials. In this process, the growth of low-molecular-weight molecules (Polymer) occurs with the assistance of the plasma energy, which involves activated electrons, ions and radicals. The mechanisms of plasma polymerization and that of free radical polymerization have some similarity but the fundamental processes are vastly different. The materials obtained by plasma polymerization are significantly different from conventional polymers and also different from most inorganic materials. Hence plasma polymerization should be considered as a method of forming new types of materials rather than a method of preparing conventional polymers. This polymerization process covers a wide interdisciplinary area of physics, chemistry, science of interfaces and materials science and so on [12-17]. Thus plasma polymerization is a versatile technique for the deposition of films with functional properties suitable for a wide range of modern applications.

In many cases, polymers formed by plasma polymerization show distinguished chemical composition, chemical and physical properties from those formed by conventional polymerization, even the same monomer is used for the two polymerizations. To appreciate the uniqueness of plasma polymerization, it is useful to compare the steps necessary to obtain a good coating by a conventional coating process and by plasma polymerization. Coating a certain substrate with a conventional polymer, at least several steps are required (1) synthesis of a monomer, (2) polymerization of the monomer to form a polymer, (3) preparation of coating solution, (4) cleaning, (5) application of the coating, (6) drying of the coating and (7) curing of the coating. Polymers formed by plasma polymerization aimed at such a coating are in most cases branched and cross-linked [19-20]. Such polymers are also depend on (1) synthesis of a

monomer, (2) Creation of plasma medium, (3) polymerization of the monomer to form a polymer, (4) cleaning, (5) application of the polymer film, and (7) curing of the film.
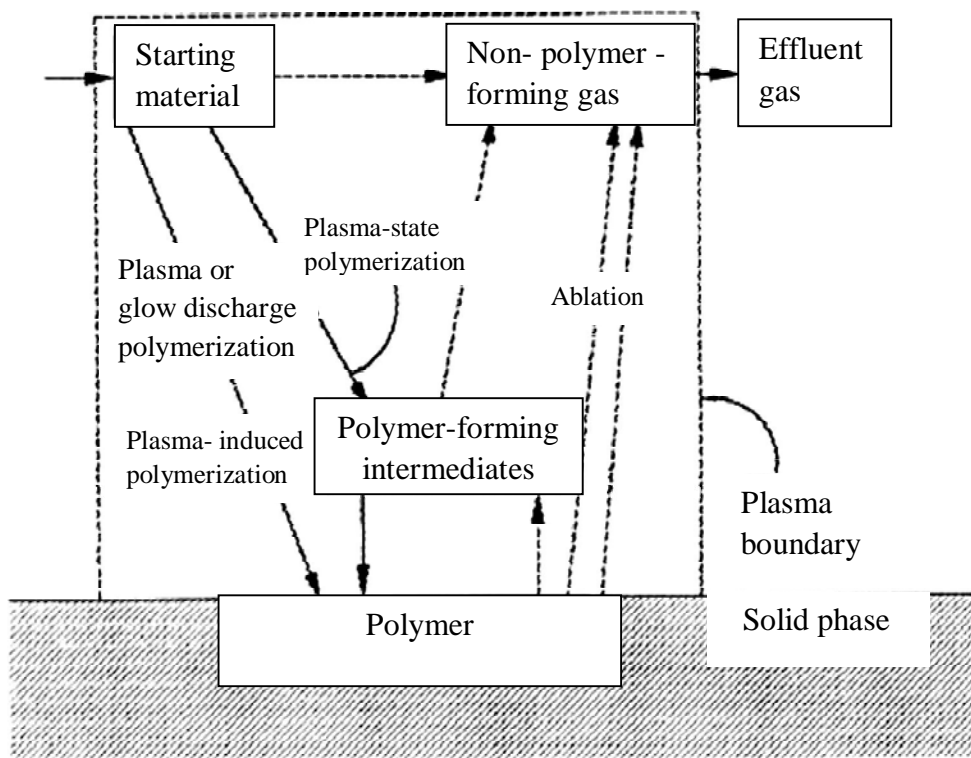
Fig.2.6 Competitive ablation and polymerization scheme of glow discharge polymerization.

Among the many types of electric discharge, glow discharge is by far the most frequently used in plasma polymerization. Some other models were proposed based on ion or electron bombardment. The role of ion bombardment and pointed to a competition between etching and deposition processes in plasma polymerization was given by Yasuda [21] in Fig.2.6.

2.2.3 Glow discharge

A glow discharge is a kind of plasma. It is an ionized gas consisting of equal concentrations of positive and negative charges and a large number of neutral species i.e. a plasma. In the simplest case, it is formed by applying a potential difference (of a few 100 V to a few kV) between two electrodes that are inserted in a cell (or that form the walls of the cell). The cell is filled with a gas (an inert gas or a reactive gas) at a pressure ranging from a few m Torr to atmospheric pressure. Due to the potential difference, electrons that are emitted from the cathode, give rise to collisions with the gas atoms or molecules (excitation, ionization, dissociation). The excitation

collisions give rise to excited species, which can decay to lower levels by the emission of light. This process is responsible for the characteristic name of the "glow discharge". The ionization collisions create ion-electron pairs. The ions are accelerated toward the cathode, where they release secondary electrons. These electrons are accelerated away from the cathode and can give rise to more ionization collisions. In its simplest way, the combination of secondary electron emission at the cathode and ionization in the gas, gives rise to self-sustained plasma. The character of the gas discharge critically depends on the frequency or modulation of the current.
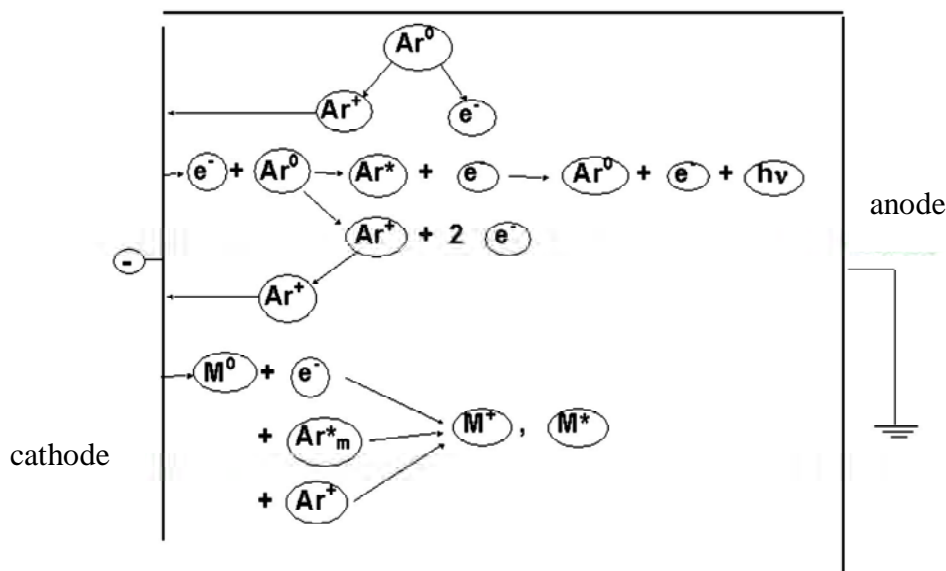
Fig.2.7 Schematic representation of the basic processes in a glow discharge.

a) Direct current glow discharge

For a DC glow discharge, the mechanism involves the bombardment of the cathode with positive ions, resulting in the generation of the secondary electrons which in turn accelerated from the cathode until they have gained enough energy to ionize a molecule (atom) by in elastic collision. A DC glow discharge is observed to have four distinguishable lighter and darker zones which are shown in Fig.2.8.
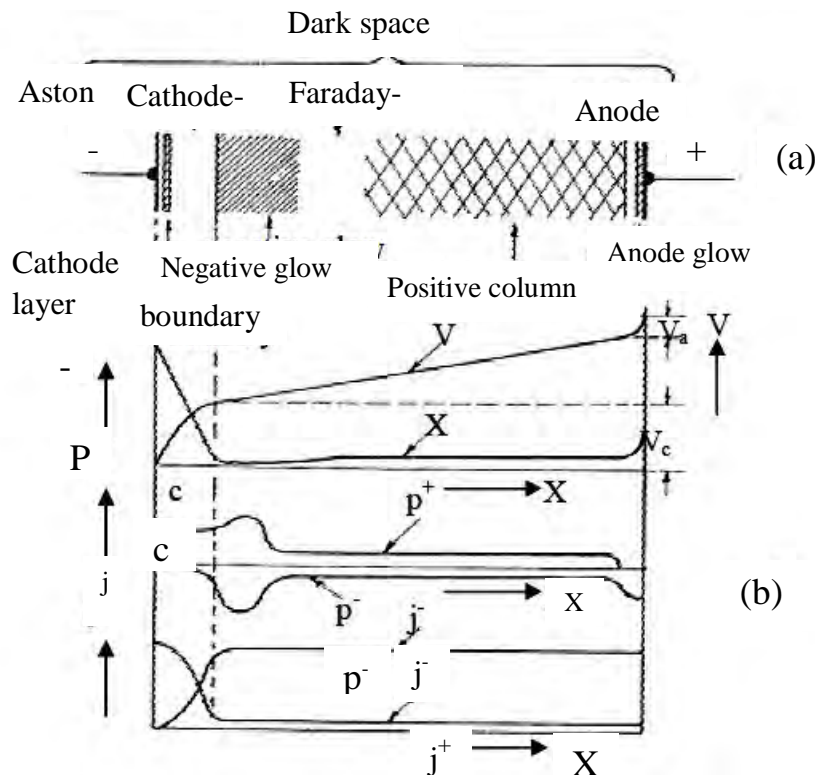
Fig.2.8 Normal glow discharge; (a) the shaded areas are luminous, (b) distribution of potential among luminous zones.

Plasma polymerization take place in a low pressure (or low temperature) plasma that is provided by a glow discharge operated in an organic gas or vapor (monomer) at low pressure between two electrodes. When a sufficient high potential difference is applied between two electrodes placed in a gas, the latter will break down into positive ions and electrons, giving rise to a gas discharge. The mechanism of the gas breakdown can be explained as follows, a few electrons are emitted from the electrodes due to the omnipresent cosmic radiation.

However, when a potential difference is applied the electrons are accelerated by the electric field in front of the cathode and collide with the gas atoms. The most important collisions are the inelastic collisions leading to excitation and ionization. The excitation collisions create new electrons and ions. The ions are accelerated by the electric field toward the cathode, where they release new electrons by ion-induced secondary electron emission. The electrons give rise to new ionization collisions, creating new ions and electrons. These processes of electron emission at the cathode and ionization in the plasma make the glow discharge self-sustaining plasma. Another important process in the glow discharge is the phenomenon of sputtering, which occurs at

sufficiently high voltage. When the ions and fast atoms from the plasma bombard the cathode, they not only release secondary electrons, but also atoms of the cathode materials, which are called sputtering. Glow discharge is characterized by the appearance of several luminous zones and by a constant potential difference between the electrodes independent of current.

b) Alternating current glow discharge

The mechanism of glow discharge generation will basically depend on the frequency of the alternation. At low frequencies (60 Hz), the effect is simply to form dc glow discharges of alternating polarity. However the frequency is higher than 60Hz the motion of ions can no longer follow the periodic changes in field polarity. But above 500 kHz the electrode never maintains its polarity long enough to sweep all electrons or ions, originating at the opposite electrode, out of the inter-electrode volume. In this case the regeneration of electrons and ions that are lost to the walls and the electrodes takes place within the body of the plasma. The mechanism by which electrons pick up sufficient energy to cause bond dissociation or ionization involves random collisions of electrons with gas molecules, the electron picking up an increment of energy with each collision. A free electron in a vacuum under the action of an alternating electric field oscillates with its velocity 90 out of phase with the field, which obtains no energy, on the average, from the applied field. The electron can gain energy from the field only as a consequence of elastic collisions with the gas atoms, as the electric field converts the electron's resulting random motion back to ordered oscillatory motion. Because of its interaction with the oscillating electric field, the electron gains energy on each collision until it acquires enough energy to be able to make an inelastic collision with a gas atom. In that case the process of these inelastic collisions is termed volume ionization. Thus the transfer of energy from the electric field to electrons at high frequencies is generally accepted as that operative in microwave discharges. It has also been put forward as that applicable to the widely used rf of 13.56 MHz [22, 23].

2.2.4 Glow discharge reactors [5]

Glow discharge reactor is the important part of plasma polymerization system. Because reactor geometry influences the extent of charge particle bombardment on the growing films which affects the potential distribution in the system. Different kinds of reactors including capacitively

coupled and inductively coupled RF reactors, microwave, dual-mode etc. can be used for plasma polymerization processes.

The most widely used reactor configurations for plasma polymerization can be broadly divided in to four classes:

i.Internal electrode reactors

ii.External electrode reactors

iii.Electrode less reactor.

Numerous arrangements can be envisaged for coupling an electric field to a reactor and for combining the location of this coupling with this sited of monomer(s) introduction and pump out. Some of the more common geometries reported in the literature will be illustrated

.

Reactors with internal electrodes have different names, e.g. flat bed parallel plates, planar, diode etc. Their main features are power supply, coupling system, vacuum chamber, rf driver electrode, grounded electrode, and eventually one or most substrate holders. Among the internal electrode arrangements a bell-jar-type reactor with parallel plate metal electrodes is mot frequently used by using ac(1-50 kHz) and rf fields for plasma excitation.

For DC and low frequency glow discharge, internal electrons are required. A common setup is to place circular of square electrodes in a bell. Pump out is usually at the base of the bell jar; monomer introduction may be at the base, over the electrodes, or through the center of an electrode. The electrodes may be oriented horizontally or vertically. If the electrode diameter is relatively large and they are placed relatively close together, a large zone of uniform electric field is created. For this reason, this geometry is favored for industrial applications (even for RF plasmas) because of the spatial uniformity of the properties of the resultant plasma polymer.

As pointed out above, at sufficiently high frequencies, the electrodes may be placed outside the reactor vessel ("electrodeless glow discharge"). Such electrodes may be curved to match a cylindrical vessel and create an electric field perpendicular to the cylindrical axis. Alternatively, two cylindrical electrodes may be wrapped around the cylinder to create an electric field roughly parallel to it. Finally, a coil may be wrapped around the cylinder with an electric field between

the ends of the coil exciting the glow discharge. The latter arrangement is called inductive coupling.

On the contrary, the design and arrangement of the cathode require special attention, a metallic shield surrounding the electrode highly improves the glow confinement inside inter electrodic space; electrode material and area greatly affect the extend of sputtering on the target. In the current research, capacitively coupled reactor (glow discharge plasma) system was used for the formation of thin films.
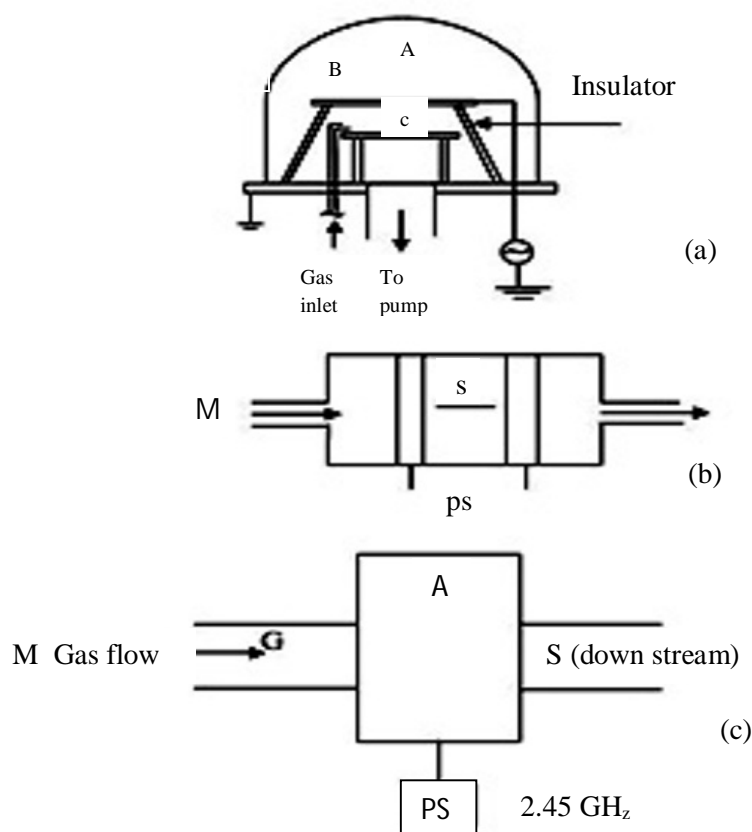
Fig.2.9 Different types of reactor configuration used for plasma polymerization (a) schematic of a bell jar reactor, (b) parallel plate internal electrode reactor, (c) electrode less microwave reactor.

2.2.5 Overall reactions and growth mechanism in plasma polymerization

In plasma monomer molecules gain high energy from electrons , ions, and radicals and are fragmented into activated small fragments, in some cases into atoms, activated fragments are recombined sometimes accompanying rearrangement, and the molecules grow to large-molecular-weight ones in a gas phase or at the surface of substrates. There are petition of

activation, fragmentation, and recombination leads to polymer formation. The chemical structure of polymers formed by plasma polymerization, if the same monomer was used, is never predicted from the structure of the monomer, because the fragmentation and rearrangement of the monomers occur in the plasma. An electron with a high kinetic energy, interacting with atoms, has an approximately equal probability of producing either excitation or ionization (excitation is slightly more probable in the case of interaction with a molecule). The electron passing closely by an atom produces in it an electric field due to coulombic force. This field causes a pulse acting on the 'atom' components. This perturbation of the atom can be theoretically understood as equivalent to the Fourier components of the pulse. The electron interaction with molecules, take place in the same way, as described for atoms. The only difference is that the excitation can result in molecular dissociation.

At first, generation of free radicals and atoms are occurred by collisions of electrons and ions with monomer molecules, or by dissociation of monomers absorbed on the surface of the sample. Secondly, propagation of the formation of polymeric chain which can take place both in the gas phase (by adding radical atoms to other radicals or molecules) and on the deposited polymer film (by interaction of the surface free radicals with either gas phase or absorbed monomers). Finally, termination can also take place in the gas phase or at the polymer surface, by similar process as in the propagation step, but ending either with the final product or with a closed polymer chain. The individual steps and reaction that occurs in plasma polymerization generally depends on the system. This type of polymerization can be represented by the following statements.

Initiation or Reinitiation

$M_i \rightarrow M_i^*$

$M_k \rightarrow M_k^*$
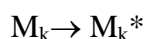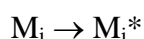
Propagation and Termination

$M_i^* + M_k^* \rightarrow M_i\text{-}M_k$

$M_i^* + M_k \rightarrow M_i\text{-}M_k$
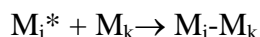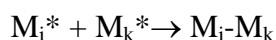
In which i and k are the numbers of repeating units (i.e., i=k=1 for the starting material), and M* represents a reactive species, which can be ion of either charge, an excited molecule, or a free radical produced by M but not necessarily retaining the molecular structure of the

starting material. In plasma state polymerization the polymer is formed by the repeated stepwise reaction.

Yasuda suggested that the growth mechanism of plasma polymerization would vary likely be the rapid step growth reaction,[M_m* + M_n* → M_{m+n}] x N , Where M* is the mono functional reactive species such as a free radical R, N is the number of repetitions of similar reactions and m ad n represents different reactive species. In case of mono functional reactive species, a single elementary step is indeed a termination process and does not contribute without additional elementary step.

For a difunctional reactive species, such as a diradical, the polymerization can be represented by, N *M* → *(M_n)*.

It shows that as polymerized polymers contain a measurable quantity of free radicals. The overall polymerization n mechanism based on the rapid step growth principle is shown in the Fig.2.10.
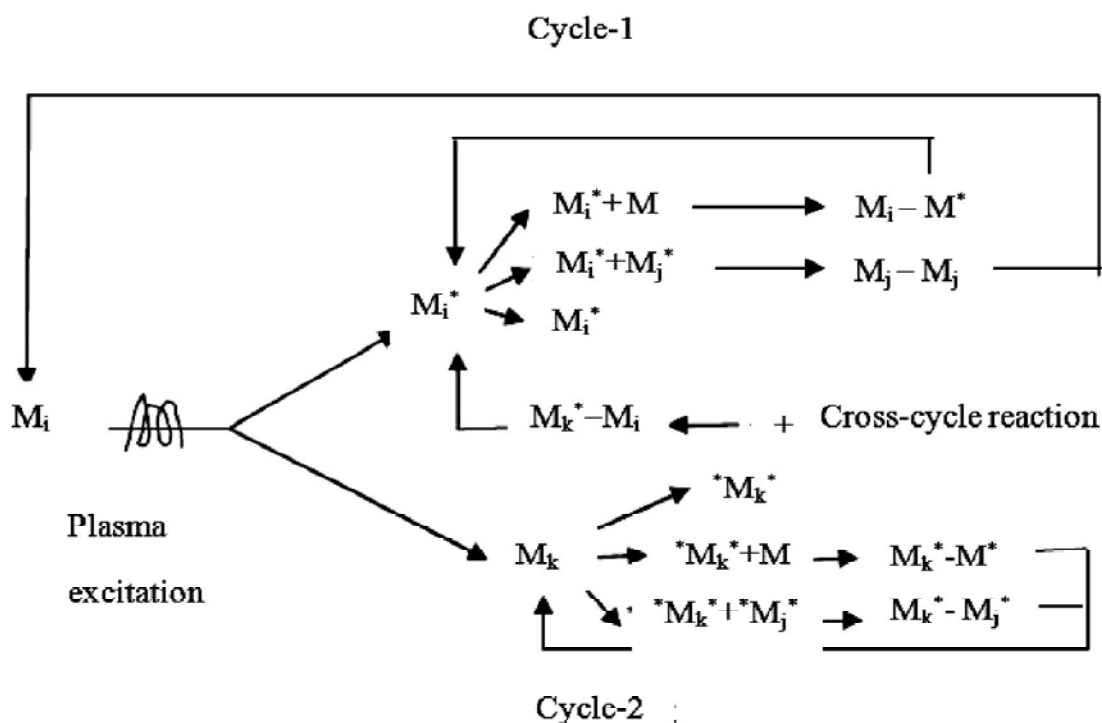
Fig. 2.10 Rapid Step-Growth Polymerization (RSGP) Mechanism

Where M_x refers to a neutral species, M* is the mono functional activated species and *M* is the difunctional, The subscripts i, j, k indicate the difference in the size of species

involved. Cycle - I is via the repeated activation of the reaction products from mono functional activated species, and cycle II is that of difunctional. The species participating in the rapid step growth polymerization can be mono- or multifunctional (radical, cation, cation-radical, diradical, etc.) [2, 21, 23].

Reference

[1] Fried. Joel R , 'Polymer Science and Technology', (Third Edition) (2014).

[2]. Hollahan R, Bell A. T. (Ed), 'Plasma Polymerization', Am. Chem. Soc., Washington, D. C., (1979).

[3]. Morosoff N., 'An Interoduction to Plasma Polymerization', in 'Application of Plasma Polymers', in Plasma Deposition, Treatment, and Etching of Polymers, R. Agostino, Ed., Academic Press, San Diego, CA, (1990).

[4]. Bogaerts A., Neyts E., 'Gas discharge plasma and their applications', Spectrochimica Acta Part B 57, 609-658, (2002).

[5]. Rogoff G. L., Ed., 'Plasma', IEEE Transactions on Plasma Science, 19, 989, Dec. (1991).

[6]. H. Biederman, Y. Osada, 'Plasma Chemistry of Polymers', Spinger Verlag Berlin Heidellberg, Germany, (1990).

[7]. Lieberman M.A, Lichtenberg A.J, 'Principles of plasma discharges and materials processing', Wiley, New York, (1994).

[8]. Grill A., 'Cold plasma in materials fabrication: From fundamentals to applications', IEEE Press, New York, (1994).

[9]. Bogaerts A., Wilken L., Hoffmann V., Gijbels R., Wetzig K., 'Comparison of modeling calculations with experimental results for rf glow discharge optical emission spectroscopy', Spectrochimi. Acta Part B57, 109-19, (2002).

[10].Andy Brooks, Siobhan Woollard, Gareth Hennighan, and Tim von Werne, 'Plasma polymerization:Aversatile and attractive process for conformal coating', Originally published in the Proceedings of SMTA International, Orlando, Florida, 14-18, (2012).

[11]. Lin Y, Yasuda H., 'Effect of plasma polymer deposition methods on copper corrosion protection,' J. Appl. Polym. Sci., 60, 543 (1996).

[12]. Biederman H., Salvinaska ., 'Plasma polymer films and their Future prospects', Surf. and Coat. Technol. 125(1-3), 371 - 376, (2000).

[13]. Chowdhury F. U. Z. , Bhuiyan A. H., 'An investigation of the optical properties of plasma polymerized diphenyl thin films', Thin Solid Films, 360, 69-74, (2000).

[14]. Xiaoyi Gong, Liming Dai, Albert Mau W.H., Griesser Hans J.,'Plasma polymerized polyaniline films: synthesis and characterization', J. Polym. Sci.: Part A: Polym. Chem. 36, 633-643, (1998).

[15]. Kiesow A. , Heilmann, 'Deposition and properties of plasma polymer films made from thiophenes', Thin Solid Films, 343-344, 338-341, (1999).

[16]. Han M. G. , IM S. S. 'Dielectric spectroscopy of conductive polyaniline salt films', J. Appl. Polym. Sci, 82, 2760 - 2769, (2001).

[17]. Shah Jalal A.B.M., Ahmed S., Bhiyan A.H., and Ibrahim M., 'On the conduction mechanism in plasma polymerized m-xylene thin films', Thin Solid Films, 295, 125-130, (1997).

[18]. Inagaki N., 'Plasma Surface Modification and Plasma Polymerization', Wiley New York, (1996).

[19]. Rat ner D., Chilkoti A.,'Plasma Deposition and Treatment for Biomaterial Application', Academic Press, New York, (1990).

[20]. Shi F.F., 'Developments in plasma polymerized organic thin films with novel mechanical, electrical and optical properties,' J.M.S-Rev, Macromol Chem. Phys. , C36, 795-826, (1996).

[21]. Yasuda H.,'Plasma Polymerization', Academic Press, Inc., Tokyo, (1985).

[22]. d'Agostino R., 'Plasma Deposition, Treatment Etching of Polymers', Harcourt Brace Jovanovich, Publishers, NY, (1990).

[23]. Biederman H, Osada Y, 'Plasma Chemistry of Polymers,' Polym. Phys., 95, (1990).

Chapter-3

Theoretical Background

3.1 Introduction

This chapter includes the background theories concerning different studies, Viz, Scanning electron microscopy (SEM), FTIR spectroscopy, DTA/TGA, UV-vis spectroscopy and dc electrical conduction mechanism in insulating materials.

3.2 Scanning Electron Microscopy and Energy Dispersive X-ray Analysis

The scanning electron microscope (SEM) uses a focused beam of high-energy electrons to generate a variety of signals at the surface of solid specimens. It is the mostly important technique to obtain surface morphological information of plasma polymerized thin films. In most applications, data are collected over a selected area of the surface of the sample, and a 2-dimensional image is generated that displays spatial variations in these properties.
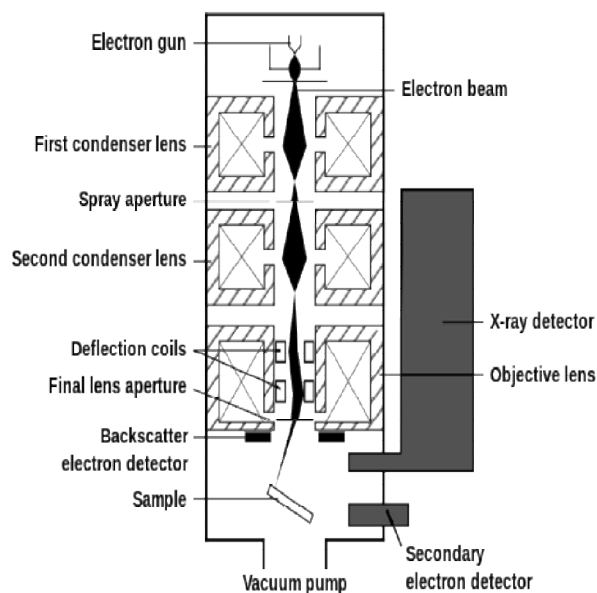
Fig.3.1 Schematic diagram of an SEM.

The surface morphology of the plasma polymerized films can be studied by SEM. This technique has also been used to determine the granular size of powder particles to evidence the presence of powder particles in thin films, to see the uniformity and defects of the films produced in plasma and to determine the location of fracture in adhesion studies by means of the lap-shear test.

EDX Analysis stands for Energy Dispersive X-ray analysis. It is a technique used for identifying the elemental composition of the specimen. It is attached to the SEM, and cannot operate on its

own without the latter. The EDX spectrum is just a plot of how frequently an X-ray is received for each energy level. An EDX spectrum normally displays peaks corresponding to the energy levels for which the most X-rays had been received. Each of these peaks is unique to an atom, and therefore corresponds to a single element. The higher the peak intensity in a spectrum, the more concentrated the element is in the specimen.

3.3 Infrared Spectroscopy

3.3.1 Introduction

Elementary particles in materials are in constant movement, much like a system of springs (chemical bonds) connecting balls (atoms, ions) oscillating around their equilibrium positions. In the case of dissolved or gaseous molecules, rotation around two or three axes also carries energy. All normal fundamental modes carry a certain, quantized amount of energy. Appropriate energies may induce transitions between ground and excited vibrational states. These transitions carry important information about the material.

3.3.2 Infrared absorption

Infrared (IR) is the name given to the range in the electromagnetic spectrum between visible light and microwave radiation. The term "infrared" covers the range of the electromagnetic spectrum between 0.78 and 1000 µm. In the context of IR spectroscopy, wavelength is measured in "wavenumbers", which have the units cm^{-1}. Wavenumber (cm^{-1}) = $\frac{1}{Wavelength(cm-1)}$. It is useful to divide the infrared region into three sections: near, mid and far infrared.

Region	Wavelength range (µm)	Wavenumber range (cm^{-1})
Near	0.78 - 2.5	12800 – 4000
Middle	2.5 – 50	4000 – 200
Far	50 -1000	200 – 10

The most useful IR region lies between 4000 - 670cm^{-1}.

Molecular rotations

Rotational transitions are of little use to the spectroscopic. Rotational levels are quantized, and absorption of IR by gases yields line spectra. However, in liquids or solids, these lines broaden into a continuum due to molecular collisions and other interactions.

Molecular vibrations

The positions of atoms in a molecule are not fixed; they are subject to a number of different vibrations. Vibrations fall into the two main categories of stretching and bending.

Stretching: Change in inter-atomic distance along bond axis

Stretching vibrations

Symmetric   Asymmetric
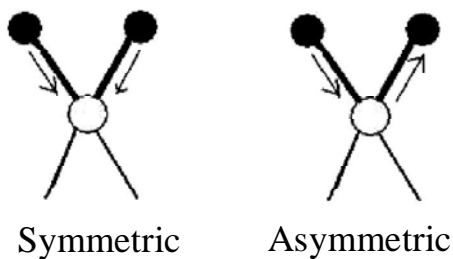
Bending: Change in angle between two bonds. There are four types of bend: i) Rocking ii) Scissoring iii) Wagging iv) Twisting.

Bending vibrations

+ - aove the plane   - - below the plane

Scissoning   Rocking   Wagging   Twisting

In- plane bending   Out of plane bending
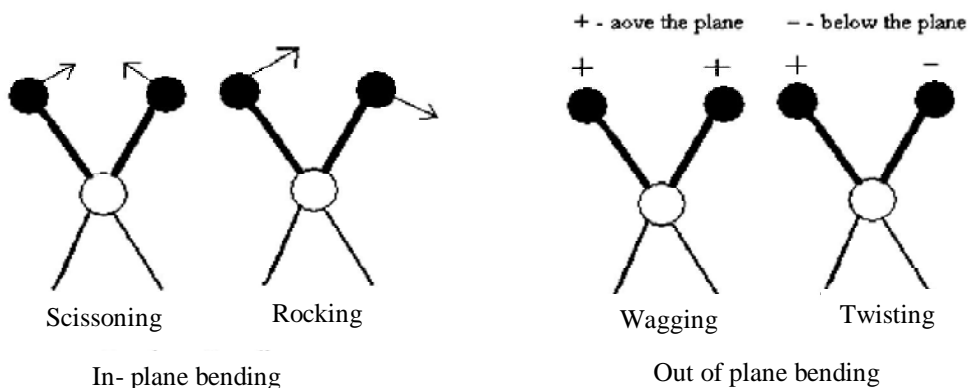
Vibrating bonds are joined to a single, central atom. Vibrational coupling is influenced by a number of factors;

Vibrational coupling

- In addition to the vibrations mentioned above, interaction between vibrations can occur (*coupling*) if the Strong coupling of stretching vibrations occurs when there is a common atom between the two vibrating bonds
- Coupling of bending vibrations occurs when there is a common bond between vibrating groups
- Coupling between a stretching vibration and a bending vibration occurs if the stretching bond is one side of an angle varied by bending vibration
- Coupling is greatest when the coupled groups have approximately equal energies
- No coupling is seen between groups separated by two or more bonds.

Stretching Vibrations

The stretching frequency of a bond can be approximated by Hooke's Law. In this approximation, two atoms and the connecting bond are treated as a simple harmonic oscillator composed of 2 masses (atoms) joined by a spring:

Fig.3.2 Oscillator.

According to Hooke's law, the frequency of the vibration of the spring is related to the mass and the force constant of the spring k, by the following formula:

$\nu = \dfrac{1}{2p} \sqrt{\dfrac{k}{m}}$ where, k is the force constant, m is the mass and ν is the frequency of the vibration.

However, in the case of the asymmetric stretch a dipole moment will be periodically produced and destroyed resulting in a changing dipole moment and therefore infrared active. Combination and blending of all the factors thus create a unique IR spectrum for each compound. Infrared radiation is absorbed and the associated energy is converted into these types of motions. The

absorption involves discrete, quantized energy levels. However, the individual vibrational motion is usually accompanied by other rotational motions.

3.3.3 Sample Preparation

There are a variety of techniques for sample preparation dependent on the physical form of the sample to be analyzed.

i. Solids

There are two main methods for sample preparation involving the use of Nujol mull or potassium bromide disks. However there is also a third option of preparing a solution in a suitable solvent (not infrared active in the region of interest).

ii. Nujol Mull

The sample is ground using an agate mortar and pestle to give a very fine powder. A small amount is then mixed with nujol to give a paste and several drops of this paste are then applied between two sodium chloride plates (these do not absorb infrared in the region of interest). The plates are then placed in the instrument sample holder ready for scanning.

iii. Potassium Bromide disk

A very small amount of the solid (approximately 1-2 mg) is added to pure potassium bromide (KBr) powder (approximately 200 mg) and ground up as fine as possible. This is then placed in a small die and put under pressure mechanically. The pressure is maintained for several minutes before removing the die and the KBr disk formed. The disk is then placed in a sample holder ready for scanning. The success of this technique is dependent on the powder being ground as fine as possible to minimize infrared light scattering off the surface of the particles. It is also important that the sample be dry before preparation. KBr has no infrared absorption in the region 4000-650 cm^{-1}.

iv. Thin Films

The infrared spectrum of a thin film can be easily obtained by placing a sample in a suitable holder, such as a card with a slot cut for the sample window. This method is often used for checking the calibration of an instrument with a polystyrene sample as the bands produced by this material are accurately known.

v. Liquids

This is possibly the simplest and most common method of sample preparation. A drop of the sample is placed between two potassium bromide or sodium chloride circular plates to produce a thin capillary film. The plates are then placed in a holder ready for analysis.

3.4 Thermal Analysis

3.4.1 Differential thermal analysis

Thermal analysis is the analysis of a change in a property of a sample, which is related to an imposed change in the temperature. The sample is usually in the solid state and the changes that occur on heating include melting, phase transition, sublimation, and decomposition. DTA may be defined formally as a technique for recording the difference in temperature between a substance and a reference material against either time or temperature as the two specimens are subjected to identical temperature regimes in an environment heated or cooled at a controlled rate. i) Sample holder comprising thermocouples, sample containers and a ceramic or metallic block. ii) Furnace. Iii) Temperature programmer iv) Recording system.

Vacuum

Ref.   Sample

Heating Coil

Ni block
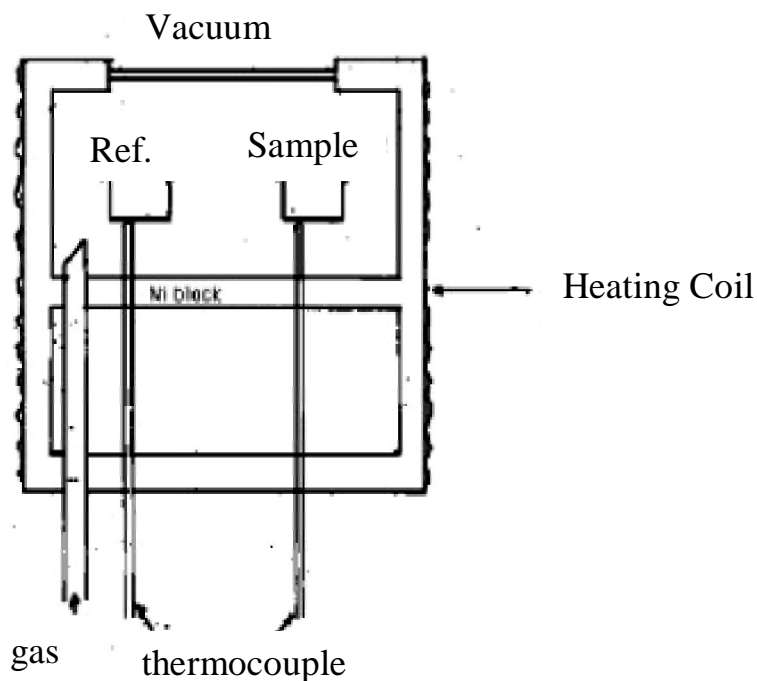
gas   thermocouple

Fig.3.3 A schematic diagram showing different parts of a DTA apparatus.

i) Sample holder comprising thermocouples, sample containers and a ceramic or metallic block.

ii) Furnace. Iii) Temperature programmer. iv) Recording system.

DTA involves heating or cooling a test sample and an inert reference under identical conditions, while recording any temperature difference between the sample and reference. The most widely used thermal method of analysis is Differential thermal analysis (DTA). In DTA, the temperature of a sample is compared with that of an inert reference material during a programmed change of temperature. The temperature should be the same until thermal event occurs, such as melting, decomposition or change in the crystal structure. DTA can therefore be used to study thermal properties and phase changes which do not lead to a change in enthalpy. The baseline of the DTA curve should then exhibit discontinuities at the transition temperatures and the slope of the curve at any point will depend on the micro structural constitution at that temperature.

3.4.2 Thermogravimetric analysis

Thermogravimetric analysis or thermal gravim analysis (TGA) is a method of thermal analysis in which changes in physical and chemical properties of materials are measured as a function of increasing temperature (with constant heating rate), or as a function of time (with constant temperature and/or constant mass loss). Thermogravimetric Analysis is a technique in which the mass of a substance is monitored as a function of temperature or time as the sample specimen is subjected to a controlled temperature program in a controlled atmosphere. TGA is a technique in which, upon heating a material, its weight increases or decreases. TGA measures a sample's weight as it is heated or cooled in a furnace.

3.4.3 TGA technique

TGA measures the amount of weight change of a material, either as a function of increasing temperature, or isothermally as a function of time, in an atmosphere of nitrogen, helium, air, other gas, or in vacuum. TGA can be interfaced with a mass spectrometer RGA to identify and measure the vapors generated, though there is greater sensitivity in two separate measurements. Inorganic materials, metals, polymers and plastics, ceramics, glasses, and composite materials can be analyzed.

Temperature range from 25°C to 900°C routinely. The maximum temperature is 1000°C. Sample weight can range from 1 mg to 150 mg. Sample weights of more than 25 mg are preferred, but excellent results are sometimes obtainable on 1 mg of material. Weight change sensitivity of 0.01 mg. Samples can be analyzed in the form of powder or small pieces so the interior sample temperature remains close to the measured gas temperature.

3.5 Ultraviolet Visible Optical Absorption Spectroscopy

3.5.1 Introduction

For plasma polymerized thin films, Ultraviolet and visible spectroscopic methods is being widely used by many investigators to determine the presence, nature and extent of conjugation in materials, optical energy gaps, direct and indirect transitions and extinction coefficients, etc [1-12].

Most materials absorb some light, and the degree to which they absorb light as a function of the wavelength of the light. Because optical absorption in the visible and near-UV portions of the spectrum is generally the result of absorption of light by electrons in atoms, ions or molecules, the absorption characteristics can yield a considerable amount of information regarding their electronic structure.

Higher Frequency   Visible Spectrum   Lower Frequency

UV   IR

400   500   600   700   800
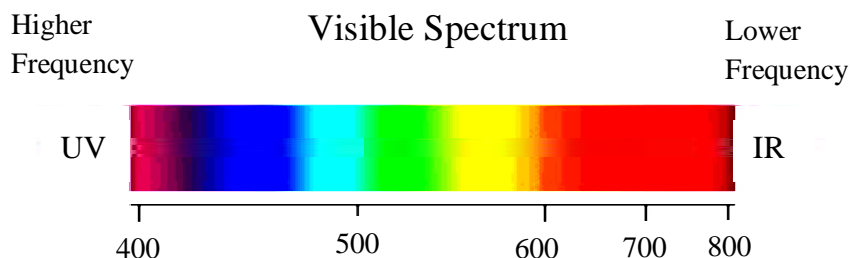
Fig.3.4 Wavelength in nanometers.

The visible region of the spectrum comprises photon energies of 36 to 72 kcal/mole, and the near ultraviolet region, out to 200 nm, extends this energy range to 143 kcal/mole. In the most important region where most investigations are carried out, namely between 200 and 600 nm, there are electronic transitions of double bonds. Whereas, nonaromatic polymers show no specific absorption in the near UV and usually none in the visible region either. The energies

noted above are sufficient to promote or excite a molecular electron to a higher energy orbital. Consequently, absorption spectroscopy carried out in this region is sometimes called "electronic spectroscopy". An incident photon can also be absorbed by a molecule and then the photon energy is converted into an excitation of that molecule's electron cloud. This type of interaction is sensitive to the internal structure of the molecule, since the laws of quantum mechanics only allow for the existence of a limited number of excited states of the electron cloud of any given chemical species. Each of these excited states has a defined energy; the absorption of the photon has to bridge the energy gap between the ground state (lowest energy state) and an allowed excited state of the electron cloud. Molecules can therefore be identified by their absorption spectrum [12].

In addition to absorbance or optical density is a dimensionless quantity defined as the negative of the base-10 logarithm of the transmission, T:

$$A = log_{10}(1/T) \qquad \text{...} \qquad (3.1)$$

An absorbance of 1 corresponds to a transmission of 0.1; an absorbance of 2 corresponds to a transmission of 0.01, and so on. Most spectrometers, after measuring T, use internal circuitry or, common nowadays, operating software to obtain the absorbance. Absorbance units are useful when working with Beer's Law, which states that the absorbance of a solution is proportional to the concentration, C, of the absorber in that solution:

$$A = kC \qquad \text{...} \qquad (3.2)$$

Most simple molecules obey Beer's Law, particularly at low concentration. Others, such as organic dyes, often exhibit a significant departure from Beer's Law at high concentration. This occurs because at higher concentrations, the molecules begin to interact with each other, and can no longer be treated as independent absorbers.

Another quantity that can be measured is the absorption coefficient. The absorption coefficient is a useful quantity when comparing samples of varying thickness. The absorption coefficient is typically the only value reported when discussing the absorption characteristics of absorbing media. To determine the absorption coefficient let us first start with Bouger's Law which relates I to I_0 via the equation

$$I = I_o \, e^{-\alpha d} \qquad \text{...} \qquad (3.3)$$

In this expression "d" is the thickness of the sample in units of centimeters (cm) and, consequently, the absorption coefficient α is to be reported in units of cm^{-1}.

3.5.2 The Beer-Lambert law

The Beer-Lambert law can be derived from an approximation for the absorption coefficient for a molecule by approximating the molecule by an opaque disk whose cross-sectional area, σ represents the effective area seen by a photon of frequency ν. If the frequency of the light is far from resonance, the area is approximately 0, and if ν is close to resonance the area is a maximum. Taking an infinitesimal slab, dz of sample:

I_o is the intensity entering the sample at $z=0$, I_z is the intensity entering the infinitesimal slab at z, dI is the intensity absorbed in the slab, and I is the intensity of light leaving the sample. Then, the total opaque area on the slab due to the absorbers is $\sigma NA\ dz$. Then, the fraction of photons absorbed will be $\sigma NA\ dz\ /\ A$ so,

$$\frac{dl}{l} = -sNdz$$ ………………………………………………. (3.4)

Integrating this equation from $z = 0$ to $z = b$ gives and $I = I_0$ to $I = I$

$$ln\ (I) - ln(I_0) = -\ \sigma Nb$$ ……………………………………………… (3.5)

Or

$$-\ ln\left(\frac{I_0}{I}\right) = -\ \sigma Nb$$ ……………………………………………… (3.6)

Since N (molecules/cm^3) (1 mole / 6.023x10^{23} molecules) 1000 cm^3 / liter = c (moles/liter) i.e. concentration, and 2.303 log(x) = ln(x), the

$$-\ log\left(\frac{I_0}{I}\right) = -\ \sigma\left(\frac{6.023\times10^{20}}{2.303}\right)cb$$ …………………………...……………...……….(3.7)

Or

$$log\left(\frac{I_0}{I}\right) = A = \epsilon cb$$
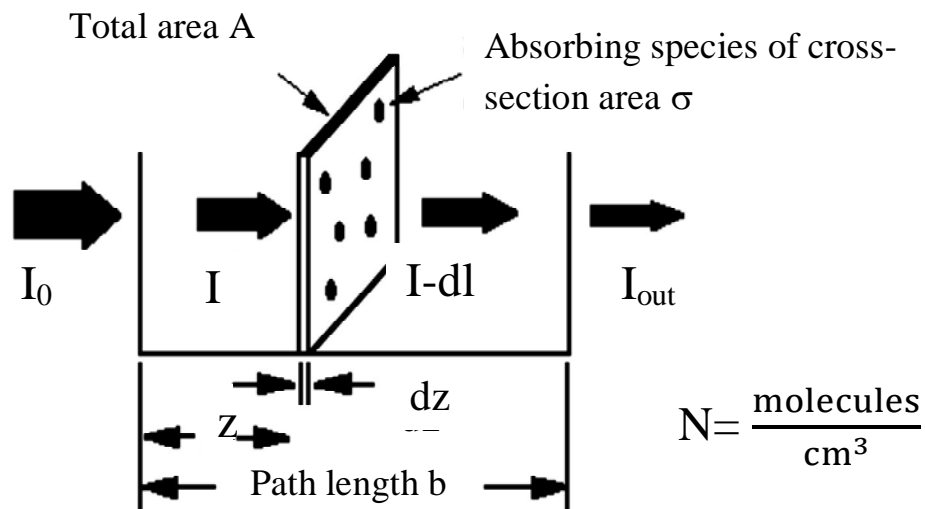
Where, $\varepsilon = \sigma \, (6.023 \times 10^{20} / 2.303) = \sigma \, (2.61 \times 10^{20})$, and ε is a constant of proportionality, called the absorbtivity.

This equation can be written as

$$a = \frac{2.303A}{d} \qquad \dots\dots\dots\dots\dots\dots\dots\dots\dots\dots\dots\dots\dots\dots\dots\dots\dots\dots \quad (3.8)$$

where α is the absorption co-efficient, A is the absorbance, and d is the thickness of the material.

Thus the Beer Lambert law states that, "When a beam of monochromatic radiation passes through a homogeneous absorbing medium; the rate of decrease in intensity of electromagnetic radiation in UV-vis region with thickness of the absorbing medium is proportional to the intensity of the incident radiation".

The relation of extinction co-efficient k with α is

$$a = \frac{4pk}{\lambda} \quad \text{where,} \;\; \lambda \text{ is the wavelength.} \;\dots\dots\dots\dots\dots\dots\dots\dots\dots\dots\dots \quad (3.9)$$

3.5.3 Absorbing species containing π, σ, and n electrons

Absorption of ultraviolet and visible radiation in organic molecules is restricted to certain functional groups (*chromophores*) that contain valence electrons of low excitation energy.
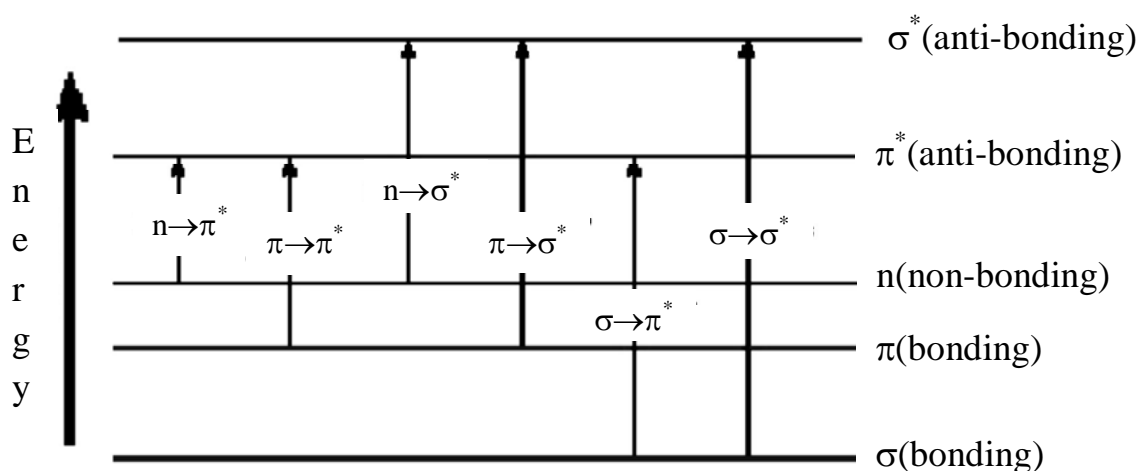
Fig.3.5 Electronic transitions in different energy levels.

The spectrum of a molecule containing these chromophores is complex. This is because the superposition of rotational and vibrational transitions on the electronic transitions gives a combination of overlapping lines. This appears as a continuous absorption band. Possible electronic transitions of π, σ, and *n* electrons are;

$\sigma \to \sigma^*$ Transitions

An electron in a bonding σ orbital is excited to the corresponding antibonding orbital. The energy required is large. For example, methane (which has only C-H bonds, and can only undergo $\sigma \to \sigma_*$ transitions) shows an absorbance maximum at 125 nm. Absorption maxima due to $\sigma \to \sigma_*$ transitions are not seen in typical UV-Vis. spectra (200 - 700 nm)

$n \to \sigma_*$ Transitions

Saturated compounds containing atoms with lone pairs (non-bonding electrons) are capable of $n \to \sigma_*$ transitions. These transitions usually need less energy than $\sigma \to \sigma_{\square *}$ transitions. They can be initiated by light whose wavelength is in the range 150 - 250 nm. The number of organic functional groups with $n \to \sigma_*$ peaks in the UV region is small.

$n \to \pi_*$ and $\pi \to \pi_*$ Transitions

Most absorption spectroscopy of organic compounds is based on transitions of *n* or π electrons to the π_* excited state. This is because the absorption peaks for these transitions fall in an

experimentally convenient region of the spectrum (200 - 700 nm). These transitions need an unsaturated group in the molecule to provide the π electrons.
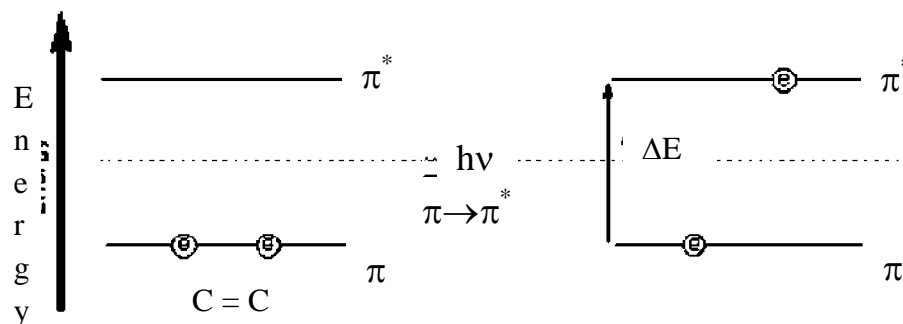
Fig.3.6 Examples of $\pi \rightarrow \pi^*$ Excitation.

Molar absorptivities from n→π^* transitions are relatively low, and range from 10 to100 L mol[1] cm^{-1}. $\pi\rightarrow \pi^*$ transitions normally give molar absorptivities between 1000 and 10,000 L mol^{-1} cm[1].

3.5.4 Direct and indirect optical transitions

For a direct gap material if it absorbs light and the light source is then removed, the optically generated electrons and holes recombine. Since the minimum in the conduction band has the same k value as the maximum in the valance band (Fig.3.7). The electron can drop back easily into the hole in the valance band and the energy lost in the process is emitted as radiation of wavelength $\lambda_c = hc/E_g$, where E_g is the band gap. i.e. the total energy and the momentum of the electron photon system must be conserved.

Direct bandgap　　　　　　　Indirect bandgap
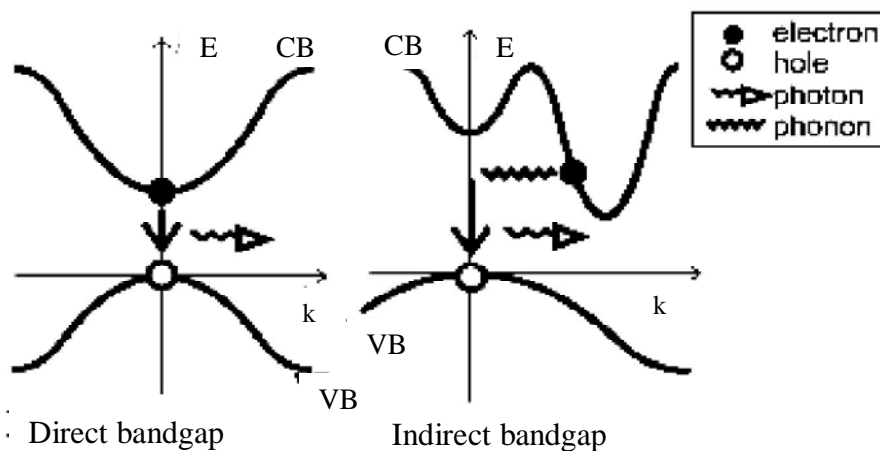
Fig.3.7 Direct and indirect optical transitions diagram.

For the indirect gap material the momentum has to be adjusted by a cooperative process involving a phonon (quantized lattice vibration). Such a process does not emit radiation at the band gap wavelength and the energy lost during a recombination process is effectively dissipated as heat i.e. indirect transition involves the absorption or emission of a phonon to converse momentum. Thus in this case the top of the valence band and the bottom of the conduction band take place at different wave vectors in the Brillouin zone (Fig.3.7). In this respect it is unfortunate therefore that **k** is not effectively a good quantum number in amorphous noncrystalline materials and such materials are usually regarded as indirect gap materials. To estimate the nature of absorption a random phase model is used where the **k** momentum selection rate is completely relaxed. The integrated density of states $N(E)$ has been used and defined by

$$N(E) = \int_{-\infty}^{+\infty} g(E)\, dE \qquad \ldots\ldots\ldots\ldots\ldots\ldots\ldots\ldots\ldots (3.10)$$

The density of states per unit energy interval may be represented by

$$g(E) = \frac{1}{V} \sum \delta(E - E_n) \qquad \ldots\ldots\ldots\ldots\ldots\ldots\ldots\ldots\ldots\ldots\ldots (3.11)$$

Where V is the volume, E is the energy at which g(E) is to be evaluated and E_n is the energy of the nth state.

If $g_v \propto E_p$ and $g_c \propto (E-E_{opt})$, where energies are measured from the valance band mobility edge in the conduction band (mobility gap), and substituting these values into an expression for the random phase approximation, the relationship obtained $V^2 I_2(v) \propto (hv-E_0)^{p+q+1}$, where I_2 (v) is the imaginary part of the complex permittivity. If the density of states of both band edges is parabolic, then the photon energy dependence of the absorption becomes

$$\alpha v \propto v^2 I_2(v)\ (hv - E_{opt})^n \qquad \ldots\ldots\ldots\ldots\ldots\ldots\ldots\ldots. (3.12)$$

So for higher photon energies the simplified general equation, known as Tauc relation is,

$$\alpha hv = B(hv - E_{opt})^n \qquad \ldots\ldots\ldots\ldots\ldots\ldots\ldots\ldots. (3.13)$$

where, $h\nu$ is the energy of absorbed light, n is the parameter connected with distribution of the density of states and B, a constant or Tauc parameter and here *n = 1/2* for direct and *n = 2* for indirect transitions.

3.6 DC Electrical Conduction Mechanism

Conduction may very often be contributed by impurities that provide a small concentration of charge carriers in the form of electrons or ions. At high fields, the electrodes may inject new carriers (holes and electrons) into polymers. At very high fields, these and other processes will lead to complete breakdown of polymers as insulating materials. The imposition of an electrical field upon a polymer will cause a redistribution of any charges in the polymer, provided they are mobile enough to respond in the time scale in the applied field. If some of the mobile charges are able to diffuse throughout the specimen and charge migration through the electrode sample interface is possible, then the charges will support a dc conductance. It should be mentioned that the vacuum-deposited thin film insulators can contain a large density of both impurity and trapping centers. A well judged study of electrical conduction in vacuum deposited thin films cannot be accomplished without consideration of these possibilities [10]. A power law can express the variation of current density with voltage in a material generally:

$$J \propto V^n \qquad \text{..} \quad (3.14)$$

where, n is a power factor. When n is unity, the conduction is ohmic.

If the value of n is less or more than unity, then the conduction process is other than ohmic. Many scientists have investigated three worth-mentioning electrical conduction mechanisms which are operative in the thin films of various organic compounds: [11-22]

The injection of carriers from the electrode by means of thermal or field assisted emission usually referred to as Schottky emission.

The other process in which carriers are produced by the dissociation of donor-accept or centers in the bulk of the material, is called Poole-Frenkel generation. If the generation process is slower than transport by the carriers through the material, the conduction is controlled by generation, specifically by either the Schottky, or Poole-Frenkel (PF) mechanism. Conversely, when the transport is slower than generation, it constitutes the rate-determining step, and the conduction is described by the theory of space-charge-limited current (SCLC). The phenomenon is, if a charge is injected at the electrode PF mechanism. Conversely, when the transport is slower than

generation, it constitutes the rate-determining step, and the conduction is described by the theory of SCLC. The phenomenon is, if a charge is injected at the electrode polymer interface, a large excess carrier density at the injecting electrode will exist and a space-charge-limited current will flow [10, 11].

A brief explanation of these conduction mechanisms is stated below.

3.6.1 Schottky mechanism

Charge injected from a metal to an insulator or semiconductor at medium fields may take place by field-assisted thermionic emission, a process known as Richardson-Schottky effect or simply Schottky emission. This is a procedure of image force induced lowering potential energy for charge carrier emission when an electric field is applied. The potential step changes smoothly at the metal insulator interface as a result of the image force. This happens when the metal surface become polarized (positively charged) by an escaping electron, which in turn exerts an attractive

force, $F_{m} = -\dfrac{e^2}{16 p \epsilon_0 \epsilon x}$ on the electron. The potential energy of the electron due to the image force is thus

$$\phi_m = \frac{e2}{16 p \epsilon_0 \epsilon x} \qquad \qquad \text{……………………………..} \quad (3.15)$$

where, x is the distance of electron from the electrode surface.

The potential step at a neutral barrier with attendant image potential as a function of the distance x from the interface is given by,

$$\phi(x) = \phi_0 + \phi_m = \phi_0 - \frac{e^2}{16 p \epsilon_0 \epsilon x} \qquad \text{…………………………………........} \quad (3.16)$$

Where ϕ_o = Coulombic barrier height of the electrode-polymer interface in Schottky conduction. The barrier potential ϕ (x) in the presence of image forces is illustrated by the line AB in Fig .3.8 Schottky assumed that the image force holds only for x greater than some critical distance x_0 For $x < x_0$, he assumes a constant image force, i.e. the potential energy is a linear function of x, and such that it matches the bottom of the electrode conduction band at the surface.
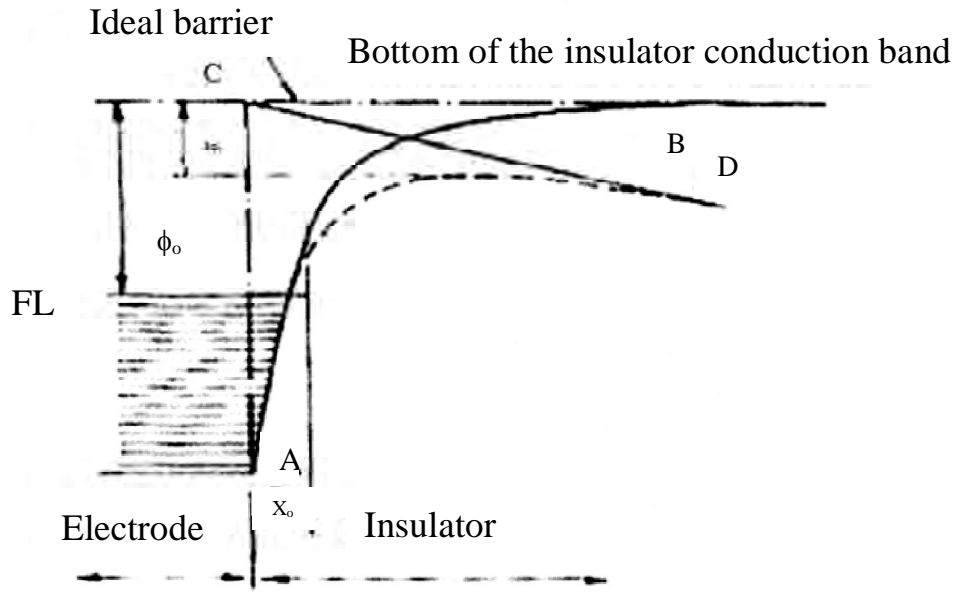
Fig.3.8 Schottky effect at a neutral contact.

When an electric field exists at a metal-insulator interface, it interacts with the image force and lowers the potential barrier. The line CD represents the potential due to a uniform applied field. The dotted line represents the potential $\Delta\phi_s$, when the potential due to a uniform electric field is added to the barrier potential ϕ (x) and thus it is lower than that of without the electric field. Under the influence of the field the potential energy of the barrier with respect to Fermi level of the electrode can be given by

$$\phi(x) = \phi_0 = -\frac{e^2}{16p e^2 e_0 x} - eFx \qquad\qquad (3.17)$$

The equation has a maximum at $\quad x_m = \left(\frac{e}{16 p e^2 e_0 F}\right)^{\frac{1}{2}}$

Therefore, the change $\Delta \phi_s = \phi_0 - \phi (x_m)$ in the barrier height due to the interaction of the applied field with the image potential can be given by

$$\Delta\phi_s = \left(\frac{e^3}{4p e^2 e_0}\right)^{1/2} F^{1/2} = \beta_s F^{1/2} \qquad\qquad (3.18)$$

Because of image force lowering of the barrier, the electrode limited current does not saturate according to the Richardson law

$$J = AT^2 \exp\left(-\frac{f_0}{KT}\right) \qquad\qquad (3.19)$$

but rather obeys the Richardson – Schottky law

$$J = AT^2 \exp\left(-\frac{f_0 - Df_s}{kT}\right)$$ ……………………………………………. (3.20)

$$J = AT^2 \exp\left(\frac{b_s F^{1/2} - f_0}{kT}\right)$$ …………………………………………… (3.21)

where, $A = 4\pi em(kT)^2/h^2$ is the Richardson constant, F = static electric field and is equal to V/d, V = applied voltage, d = film thickness, T = Temperature in Kelvin, k = Boltzmann constant and β_s is the Schottky coefficient which is given by,

$$\beta_s = \left(\frac{e^3}{4p e' e_0}\right)^{1/2}$$ ……………………………………………….. (3.22)

where, e = elementary charge of the electron and ε' is the high frequency dielectric constant of the material

The electrode limited Richardson-Schottky effect in insulators appears to have been first observed by Emptage and Tantraporn, who reported a log I vs. $F^{1/2}$ relationship in their samples. It was suggested that the plot should have to be linear in nature for Schottky type conduction mechanism.

3.6.2 Poole-Frenkel mechanism

The Poole- Frenkel (PF) conduction mechanism is a field assisted thermal ionization process and is the bulk analogue of the Schottky effect at an interfacial barrier. This effect is lowering of a Coulombic potential barrier when it interacts with an electric field, as shown in fig 3.9. The PF lowering of a Coulombic barrier $\Delta\phi$ PF in a uniform electric field is twice that due to the Schottky effect at a neutral barrier, because the potential energy of an electron in a Coulombic field $-\frac{e^2}{4p e_0 \, ex}$ is four times that due to image force effects in Schottky mechanism; i.e.

$$\Delta\phi_{PF} = 2\Delta\phi_s = 2\left(\frac{e^3}{4p e' e_0}\right)$$ …..………………………………….(3.23)

where, β_{PF} is PF coefficient.
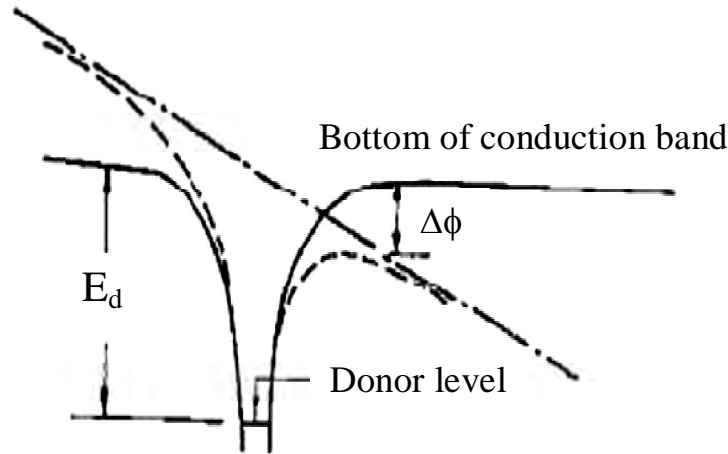
Fig.3.9 Poole-Frenkel effect at a donor center.

From this we can conclude that,

$$\beta_{PF} = 2\left(\frac{e^3}{4p\epsilon\epsilon_0}\right)^{1/2}$$ …………………………………………….. (3.24)

In the bulk limited PF mechanism, the thermal emission of trapped carriers from the bulk material gives rise to conductivity,

$$J = \sigma_0\, F\, exp\left(\frac{b_{PF}F^{1/2} - f_c}{kT}\right)$$ ……………………………………………… (3.25)

where, ϕ_c is the ionization potential of the PF centers.

Consequently, a general expression of the form

$$J = J_0\, exp\left(\frac{b\, F^{\frac{1}{2}} - f}{kT}\right)$$ ……………………………………………… (3.26)

holds equally well for both Schottky and PF mechanisms. Where, J is the current density at a biased voltage.

By taking natural logarithms of Eqn. 3.26 we can write,

$$\beta_{exp} = skTd^{1/2}$$ …………………………………………… (3.27)

where, β_{exp} denotes the value of β obtained experimentally and $s\left(= \frac{DlnJ}{DV^{1/2}}\right)$ is the slope of graph plotted between lnJ and $V^{\frac{1}{2}}$.

3.6.3 Space charge limited conduction mechanism

When an Ohmic contact is made to the insulator, the space charge injected into the conduction band of the insulator is capable of carrying current and when the transport is slower than generation, it constitutes the rate-determining step, and the conduction is described by the theory of space-charge-limited current (SCLC) [10].
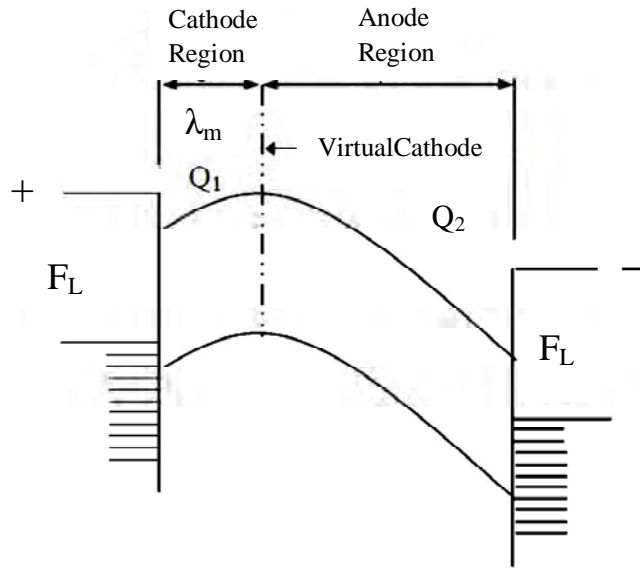
Fig. 3.10 Energy diagram for different regions under space charge limited conduction mechanism.

When a voltage bias is applied to the metal electrodes, this results an addition of positive charge to the anode and negative charge to the cathode. If now the voltage bias increases, the net positive charge on the anode increases and that on the cathode decreases (Fig.3.10). Assuming that the anode region extends throughout the insulator and neglecting the diffusion effect the current can be interpreted by the Mott and Gurney relation.

$$ J = \frac{9\mu \varepsilon \varepsilon_0 V^2}{8d^3} \qquad \text{...} \quad (3.28) $$

Where, μ is the mobility of charge carriers, ε is dielectric constant, ε_0 is the permittivity of free space, V is the applied voltage and d is the thickness. If the insulator contains N_t shallow traps positioned an energy E_t below the conduction band then the free component of the space charge

$$ \rho_f = e \, N_e \, exp\left(-\frac{E_F}{kT}\right) \qquad \text{...} \quad (3.29) $$

and trapped component of space charge

$$\rho_{t = e\,N\,exp\left(-\frac{E_t}{kT}\right)} \qquad\qquad \text{..} \qquad (3.30)$$

thus $\qquad\qquad \theta \equiv \frac{\rho_f}{\rho_t} = \frac{N_c}{N_t} exp\left(-\frac{E_t}{kT}\right) \qquad \text{...} \qquad (3.31)$

where N_c is the effective density of states in the conduction band, and N_t the density of trapping levels situated at an energy E_t below the conduction band edge.

The current density with traps is defined by,

$$J = \frac{9\mu\epsilon\epsilon_0 V^{1/2}}{8d^3}q \qquad \text{...} \qquad (3.32)$$

For a shallow trap SCLC and trap-free SCLC, $\theta = 1$. According to eqn. 3.28, J varies as d^{-1} in the Ohmic region and as d^{-3} in the SCLC region for the trap-filled SCLC part. For a fixed V, the dependence of ln J on ln d should be linear with slope $l \geq -3$.

Lampert calculated the voltage at which the transition from the Ohmic to shallow trap SCLC region ($V_{tr)}$ occurs is given by,

$$V_{tr} = \frac{8}{9}n_0\frac{ed^2}{e} \qquad\qquad \text{..} \qquad (3.33)$$

Where, n_0 volume generated free carrier density, n_0 s independent of both μ and J.

According to Fig. 3.11 it was found that the second linear region would extend up to a certain voltage, called as the crossover voltage, and beyond which the current would vary with the voltage as a power law:

$$J \propto V^2 \qquad\qquad \text{...} \qquad (3.34)$$

Which would continue until the current is close to the saturation current, i.e. the maximum current that the electrode could supply. However in real samples which contain several trap sites to capture the electrons that had been injected inside the sample. There are two types of traps;

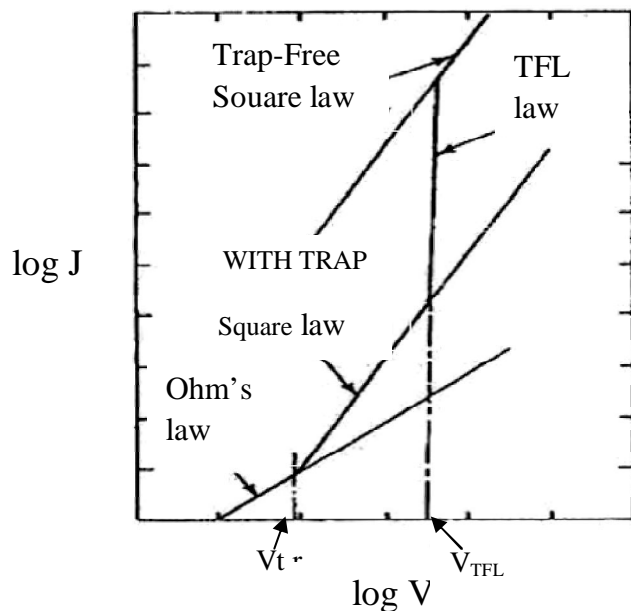Chapter-3   Theoretical Background

Fig.3.11 Space charge limited conduction characteristic for an insulator containing shallow traps.

the ones above the Fermi level are the shallow traps, and the others below the Fermi level being the deep traps. During trapping both shallow and deep traps would get filled. The voltage at which all the traps would get completely filled is called the trap filled limit (TFL). Beyond V_{TFL} all the excess charges would be i $_{With-Trap}$ he conduction band and the current would approach the trap free square law as described in Eqn.3.33 [22, 23].

3.6.4 Thermally activated conduction processes

Electronic conduction in organic, molecular compounds differs in several important ways from the more familiar kind in metals and semiconductors. An important feature of the band system is that electrons are delocalized and spread over the lattice. Some delocalization are naturally expected when an atomic orbital of any atom overlaps appreciably with those of more than one of its neighbors, but delocalization reaches an extreme form in the case of a regular 3dimensional lattice. The band theory assumes that the electrons are delocalized and can extend over the lattice. When electronic conduction is considered in polymers, band theory is not totally suitable because the atoms are covalently bonded to one another, forming polymeric chains that experience weak intermolecular interactions. But macroscopic conduction will require electron movement, not only along the chain but also from one chain to another. If two solids are put in contact, the Fermi levels equalize at the interface, the other energy levels moving to

accommodate this. In pure insulator the Fermi level bisects the forbidden band. Impurities may introduce allowed levels into the forbidden band, and this moves the Fermi level up and down.

As the temperature is increased the charge carrier concentration increases strongly with temperature. This dominates the temperature dependence of the conductivity, giving it an Arrhenius - like character. It is difficult to generalize about the temperature dependence of dc conduction whether it is ionic or electronic since so many processes are possible. Ohmic (low field) conduction whether ionic or electronic, gives exponential temperature dependence, given by,

$$J = J_o \, exp \left(\frac{-DE}{kT} \right)$$ …………………………………… (3.35)

where , J_o is a constant and ΔE is the activation energy for carrier generation.

Now, $$J = Ne\mu$$ ………………………………………..... … (3.36)

Where, N is the number of charge carriers, e their charge, and μ their mobility.

With extrinsic ionic conduction, it is the mobility i.e. the activated process, ΔE being the energy for the ion to hop. With extrinsic electronic conduction, the electrons may move by hopping. However, if the electronic conduction is by excitation into the conduction band, the production of free electrons, n not their mobility, μ is activated. Whatever the Ohmic mechanism, a log J vs. 1/T plot (Arrhenius plot) will usually exhibit increasing linear slopes (activation energies) as T is raised [23].

In bulk material ionic conduction occurs due to the drift of defect under the influence of an applied electric field. The degrees of ionic impurities that may be totally ignored in the context of other properties may have a significant effect on conductivity. A theoretical expression may be derived for the current density,

$$J = sin \, h \, (eaE/2kT)$$ ………………………………………….. (3.37)

where E is the electric field, a is the distance between neighboring potential wells, e = electronic charge.

Reference

[1]. Hogarth C. A., "The optical properties of amorphous semiconductors", Conden Mater Phys., 1, (1996).

[2]. Yakuphanoglu F., Arslan M., Kucukislamoglu M., Zengin M., 'Temperature dependence of the optical band gap and refrective index of poly (ethylene terepthalate) oligomer- DDQ complex thin film', Sol. Energy, 79, 96-100, (2005).

[3]. Kim J., Jung D., Park Y., Kim Y., Moon D. W., Lee T. G., "Quantitative analysis of surface amine groups on plasma-polymerized ethylenediamine films using UV-visible spectroscopy compared to chemical derivatization with FT-IR spectroscopy, XPS and TOF-SIMS', Appl. Surf. Sci, 253, 4112 - 4118, (2007).

[4]. Al-Mamun, Islam A.B.M.O, Bhuiyan A.H. 'Structural, electrical and optical properties of copper selenide thin films deposited by chemical bath deposition technique'. J. Mater. Sci. 16,263-268, (2005).

[5]. Akther H., Bhuiyan A. H., 'Electrical and optical properties of plasma polymerized N, N, 3, 5,-tetramethylaniline thin films', New J. Phys. 7, 173, (2005).

[6]. Yakuphanoglu F., Cukuoali A., Yilmaz I., 'Refrectie index and optical absorption properties of the complexes of a cyclobutane containing thiazoyl hydrazone lignad', Optical Materials, 27, 1363-1368, (2005).

[7]. Yakuphanoglu F., Cukuoali A., Yilmaz I., 'Determination and analysis of the dispersive optical constants of some organic films', Physica B, 351, 53-58, (2004).

[8]. Zaman M., Bhuiyan A. H., ' Optical properties of plasma polymerized tetraethylorthosilicate thin films', Bangladesh J. Phys, 2(1), 107-113, (2006).

[9]. Hu Xiao, Zhao Xiongyan, Uddin A., Lee C. B. 'Preparation characterization and electronic and optical properties of plasma polymerized nitriles', Thin Solid Films, 477, 81-87, (2005).

[10].Chen C. Ku , Raimond Liepins, 'Electrical Properties of Polymers'; Hanser Publishers, Munich - Vienna – New York (1987).

[11]. Mathai C. J., Saravanan S., Jayalekshmi S., Venkatachalam S., Anantharaman M. R., 'Conduction mechanism in plasma polymerized aniline thin films' Mater. 57, 2253 - 2257, (2003).

[12]. Nagaraj N., Subba Reddy Ch. V., Sharma A. K., Narasimha Rao V. V. R.. J., 'DC conduction mechanism in polyvinyl alcohol films doped with potassium thiocyanate', Power Sources, 112, 326-330, (2002).

[13]. Sayed W. M. Salem. T. A., 'Preparation of polyaniline and studying its electrical conductivity', J. Appl. Polym. Sci., 77, 1658 - 1665, (2000).

[14]. Chowdhury F-U-Z, Bhuiyan A. H., 'The dc electrical conduction mechanism of heat-treated

plasma- polymerized diphenyl (PPDP) thin films', Indi. J. Phys., 76, 239-244, (2002).

[15]. Akther H., Bhuiyan A. H. 'Space charge limited conduction in plasma polymerized N, N, 3, 5 tetramethylaniline thin films' New J. Phys. 7, 173, (2005).

[16]. Shah Jalal A.B.M., S. Ahmed, A.H. Bhuiyan and M. Ibrahim, 'On the conduction mechanism in plasma-polymerized m-Xylene thin films', Thin Solid Films, 288, 108-111, (1996).

[17]. Silverstein M. S., Visoy-Fisher I., 'Plasma polymerized thiophene: molecular structure and electrical properties', Polym. 43, 11-20, (2002).

[18]. John R. K., Kumar D. K.,'Structural, Electrical and Optical studies of plasma polymerized and iodine doped polypyrrole', J. Appl. Polym. Sci., 83, 1856 - 1859, (2002).

[19]. El-Nahass M. M., Abd-El-Rahman K. F., Darwish A. A. A., 'Electrical conductivity of 4-tricyanovinyl- N, N-diethylaniline', Physica B ,403, 219-223, (2008).

[20]. Bae I.-S., Jung C.-K., Cho S.-J., Song Y.-H., Boo J.-H., 'A comprehensive study of plasma polymerized organic thin films on their electrical and optical properties', J. Alloys and Compounds, 449, 393-396, (2008).

[21].Gould R.D., Lopez M.G., "Poole-Frenkel conductivity prior to electroforming in evaporated Au-SiOx-Au-sandwich structures", Thin Solid Films, 342-344, 94-97, (1999).

[22]. Bhattacharyya S., Laha A., Krupanidhi S. B. 'Analysis of leakage current conduction phenomenon in thin S_r Bl $2T_a$2O9 films grown by excimer laser ablation.' J. Appl. Phys. ,91, 4543-4548, (2002).

[23]. Maisel Leon I, Glang R., 'Hand Book of Thin Film Technol.' McGraw Hill Book Company, NY, (1970).

Chapter-4

Materials and Experimental Details

4.1 Introduction

This chapter deals with the plasma polymerization scheme of Quinoline which includes the details of monomer, substrate, capacitively coupled glow discharge plasma polymerization set up for polymer formation, the thickness measurement method, FTIR, UV-vis spectroscopy, DTA TGA and contact electrode deposition technique for electrical measurement of PPQ thin film. Measurement of current as a function of voltage is also described here.

4.2 The Monomer

Quinoline (The British Drug House Ltd. B. D.H. Laboratory Chemistry Division. Poole England.) used in the preparation of thin film was collected from local market. The chemical structure of the monomer is shown in Fig 1 and its typical properties are stated in Table 4.1.

Table 4.1 General properties of Quinoline.

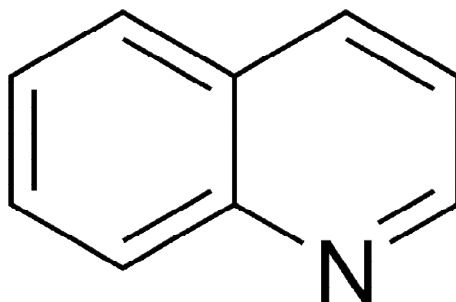| Chemical formula	C_9H_7N
Molar mass	129.16 g/mol
Appearance	Yellowish oily liquid
Density	1.093 g/mL
Melting point	-15 °C (5 °F, 258K)
Boiling point	510 K /760 mm Hg

Fig.4.1 Chemical structure of Quinoline (C_9H_7N).

Quinoline is a heterocyclic aromatic organic compound with the chemical formula C_9H_7N. It is a colorless hygroscopic liquid with a strong odor. Aged samples, especially if exposed to light, become yellow and later brown. Quinoline is only slightly soluble in cold water but dissolves readily in hot water and most organic solvents. Quinoline itself has few

applications, but many of its derivatives are useful in diverse applications. Quinoline is used mainly as an intermediate in the manufacture of other products. Quinoline is a colorless liquid with a peculiar odor. Slightly denser than water.

Quinoline, any of a class of organic compounds of the aromatic heterocyclic series characterized by a double-ring structure composed of a benzene and a pyridine ring fused at two adjacent carbon atoms. The benzene ring contains six carbon atoms, while the pyridine ring contains five carbon atoms and a nitrogen atom. The simplest member of the quinoline family is quinoline itself, a compound with molecular structure C_9H_7N.

4.3 Substrate Material and Its Cleaning Process

The substrates used were pre cleaned glass slides (25.4 mm X 76.2 mm X 1.2 mm) of Sail Brand, China, purchased from local market. The samples were prepared by depositing the PPQ thin film and electrodes on to them. To get a homogeneous, smooth and flawless thin polymer film, which is a common property of plasma polymers, it is essential to make the substrate as clean as possible. The substrates were chemically cleaned by acetone and thoroughly rinsed with distilled water then dried in hot air.

4.4 Capacitively Coupled Plasma Polymerization Set-up

A glow discharge is a kind of plasma and the plasma polymerization setup has been use denormously in recent years to form various kinds of plasma polymers. Different configuration of polymerization set up varies the properties of plasma polymers i.e. the geometry of the reaction chamber, position of the electrodes, nature of input power etc. A schematic diagram of the capacitively coupled Plasma polymerization system used in the present study is shown in Fig 4.2.
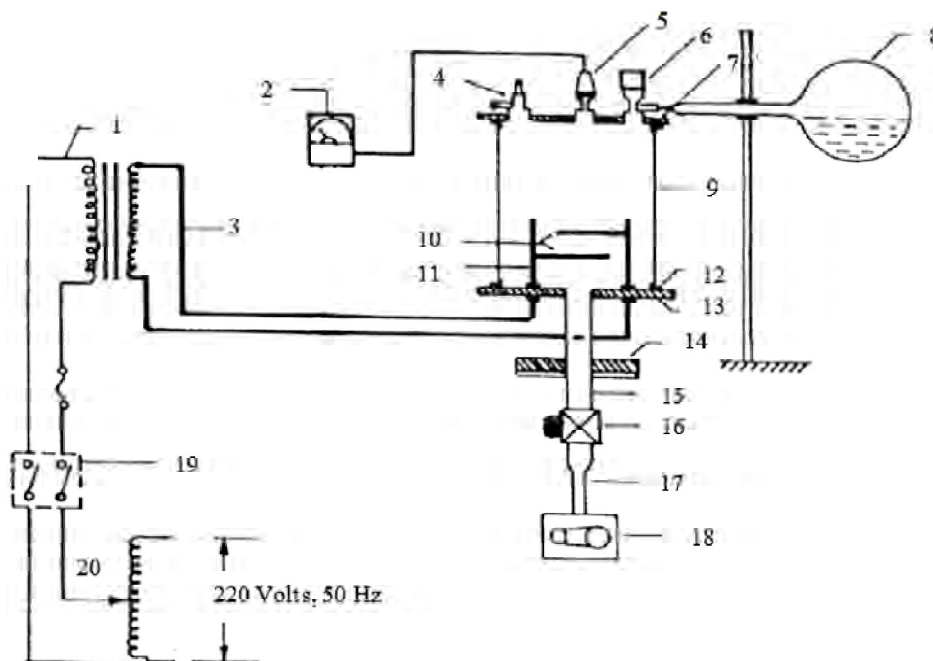
Fig.4.2 Schematic diagram of the plasma polymerization set-up.

1 high voltage power supply, 2 pirani gage, 3s high tension leads, 4 gas inlet valve, 5 guage head, 6 monomer injection valve, 7 flow meter, 8 monomer container, 9 Pyrex glass dome, 10 metal electrodes, 11 electrode stands, 12 gasket, 13, lower flange, 14 bottom flange, 15 brass tube, 16 valve, 17 liquid nitrogen trap, 18 rotary pump, 19 switch and 20 variac.

i. Plasma reaction chamber

The glow discharge reactor is made up of a cylindrical Pyrex glass bell-jar having 0.15 m in inner diameter and 0.18 m in length. The top and bottom edges of the glass bell-jar are covered with two rubber L -shaped (height and base 0.015m, thickness, 0.001 m) gaskets. The cylindrical glass bell jar was placed on the lower flange. The lower flange is well fitted with the diffusion pump by an I joint. The upper flange is placed on the top edge of the bell-jar.

The flange is made up of brass having 0.01 m in thickness and 0.25 m in diameter. On the upper flange a laybold pressure gauge head, Edwards high vacuum gas inlet valve and a monomer injection valve are fitted. In the lower flange two highly insulated high voltage feed-through are attached housing screwed copper connectors of 0.01m high and 0.004 m in diameter via Teflon^{TM} insulation.

ii. Electrode system

iii. Pumping unit

iv. Vacuum pressure gauge

vi. Monomer injecting system

vii. Supporting frame

viii. Flow meter

ix. Liquid nitrogen trap

4.5 Generation of Glow Discharge Plasma

Glow discharges are produced by an applied static or oscillating electric field where energy is transferred to free electrons in vacuum. Inelastic collisions of the energetic free electrons with the gas molecules generate free radicals, ions, and species in electronically excited states. This process also generates more free electrons, which is necessary for a self-sustaining glow. The excited species produced are very active and can react with the surfaces of the reactors as well as themselves in the gas phase. The chamber of the glow discharge reactor is evacuated to about 10^2 Torr. A high-tension transformer along with a variac is connected to the feed-through attached to the lower flange. While increasing the applied voltage, the plasma is produced across the electrodes at around 10^{-1} Torr chamber pressure.

4.6 Deposition of Plasma Polymerized Thin Film

The important feature of glow discharge plasma is the non-equilibrium state of the overall system. In the plasmas considered for the purpose of plasma polymerization, most of the negative charges are electrons and most of the positive charges are ions. Due to large mass difference between electrons and ions, the electrons are very mobile as compared to the nearly stationary positive ions and carry most of the current. Energetic electrons as well as ions, free radicals, and vacuum ultraviolet light can possess energies well in excess of the energy sufficient to break the bonds of typical organic monomer molecules which range from approximately 3 to 10 eV. Some typical energy of plasma species available in glow discharge as well as bond energies encountered at pressure of approximately 10^{-2} Torr.

Fig.4.3 Glow discharge plasma during deposition.

After finding the desired plasma glow in the reactor the monomer vapor is injected downstream to the primary air glow plasma for some time. Incorporation of monomer vapor changed the usual color of   plasma into a light bluish color. Fig 4.3 is the photograph of light bluish color monomer plasma in the plasma reactor. The deposition time was varied from 40-90 minute to get the PPQ thin films of different thicknesses. The optimized conditions of thin film formation for the present study are:

Separation between two electrodes	4 cm
Position of the substrate	Lower electrode
Deposition Power	40 W
Pressure in the reactor	10^{-2} Torr
Deposition time	40 to 90 minutes

4.7 Contact Electrodes for Electrical Measurements

i) Electrode material

Aluminium (Al) (purity of 4N British Chemical Standard) was used for electrode deposition. Al has been reported to have good adhesion with glass slides. Al film has advantage of easy self-healing burn out of flaws in sandwich structure.

Fig.4.4 The Vacuum Coating unit.

ii) Electrode deposition

Electrodes were deposited using a Vacuum Coating Unit (High Hind Vacuum co. Ltd., India) (Fig.4.4). The system was evacuated by an oil diffusion pump backed by an oil rotary pump. The chamber could be evacuated to a pressure less than 10^{-5}. The glass substrates with mask were supported by a metal rod 0.1 m above the tungsten filament. For the electrode deposition Al was kept on the tungsten filament. The filament was heated by low-tension power supply of the coating unit. The low-tension power supply was able to produce 100 A current at a potential drop of 10 V. During evacuation of the chamber by diffusion pump, the diffusion unit was cooled by the flow of chilled water and its outlet temperature was not allowed to rise above 305 K. When the penning gauge reads about 10^{-5} Torr, the Al on tungsten filament was heated by low-tension power supply until it as melted.
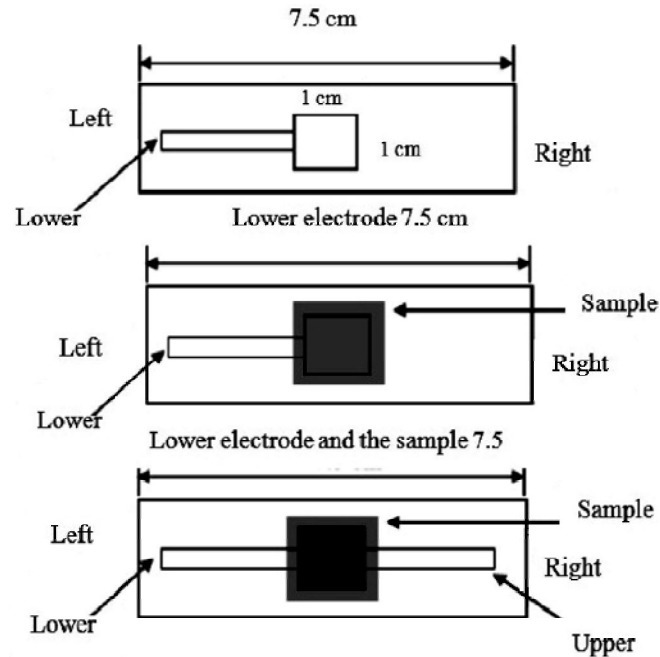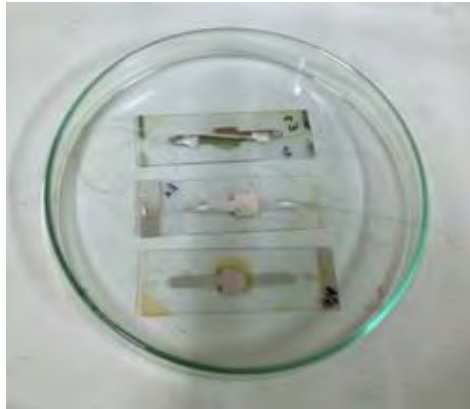
Fig.4.5 Electrode sample assembly.

Fig.4.6 Sample for electrical measurements.

4.8 Multiple-Beam Interferometry

This method utilizes the resulting interference effects when two silvered surfaces are brought close together and are subjected to optical radiation. This interference technique, which is of great value in studying surface topology in general, may be applied simply and directly to film thickness determination. When a wedge of small angle is formed between unsilvered glassplates, which are illuminated by monochromatic light, broad fringes are seen arising from interference between the light beams reflected from the glass on the two sides of the air wedge.At points along the wedge where the path difference is an integral and odd number of wavelengths, bright and dark fringes occur respectively. If the glass surfaces of the plates are

coated with highly reflecting layers, one of which is partially transparent, then the reflected fringe system consists of very fine dark lines against a bright background. A schematic diagram of the multiple-beam interferometer along with a typical pattern of Fizeau fringes from a film step is shown in Fig.4.7.

Fig.4.7 Multiple Beam Interferometric set-up in the laboratory.

a silver layer As shown in this figure, the film whose thickness is to be measured is over coated with to give a good reflecting surface and a half-silvered microscope slide is laid on top of the film whose thickness is to be determined. A wedge is formed by the two microscope slides, and light multiply reflected between the two silvered surfaces forms an interference pattern with a discontinuity at the film edge as shown in Fig.4.8.

Fig.4.8 Sample holders for thickness measurement.
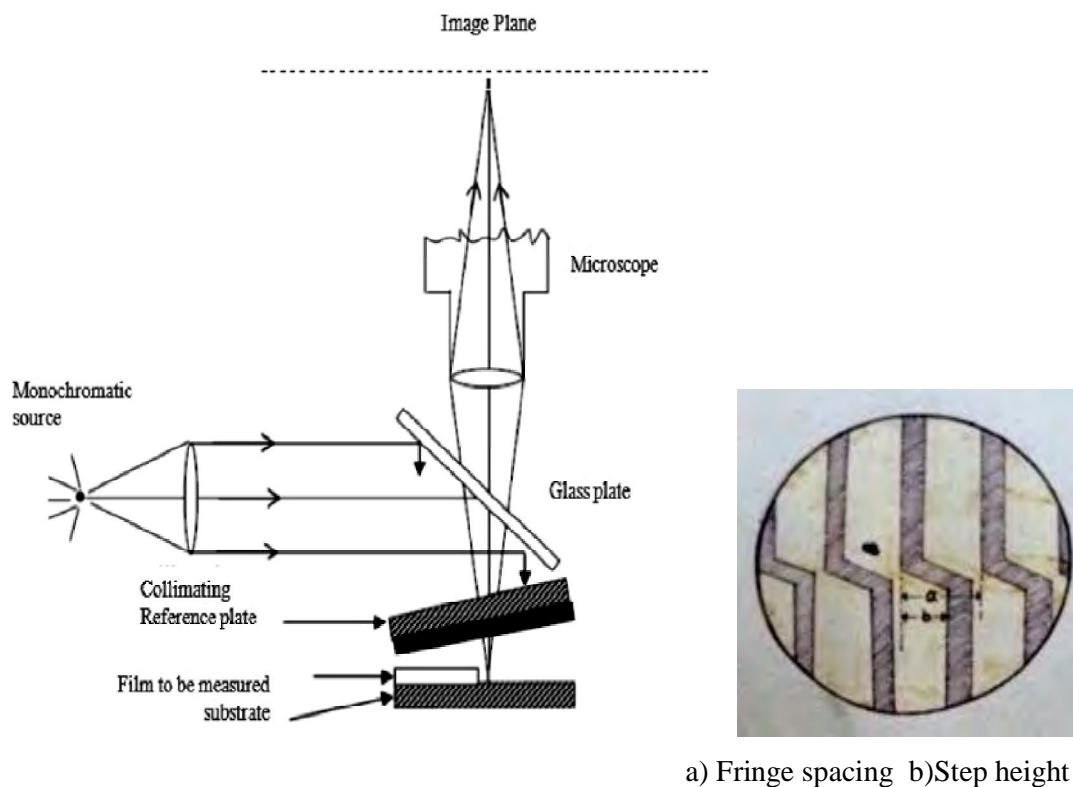
a) Fringe spacing b)Step height

Fig. 4.9 Interferometer arrangement for producing reflection Fizeau fringes of equal thickness.

Thickness of the film d can then be determined by the relation, $d = \dfrac{\lambda}{2} \dfrac{b}{a}$. Where is the wavelength and b/a is the fractional discontinuity identified in the figure. In general, the sodium light is used, for which λ = 5893 Å. In measurement one half silvered glass slide is selected for maximum resolution. A resolution of about 20 A may be obtained in a careful measurement. In conclusion, it might be mentioned that the Tolansky method of film thickness measurement [1] is the most widely used and in many respects also the most accurate and satisfactory one.

4.9 Experimental Procedure for FTIR Spectroscopy

The FTIR sepectroscopic analysis was carried out by a double beam SHMADZU FTIR-8900 sepectrophotometer. The sample for FTIR measurement was prepared by above mentioned KBr technique. All the spectra were recorded in transmittance mode and the wave number range was from 4000 to 500 cm^{-1}. The FTIR spectrum of quinoline liquid monomer was also recorded by placing the liquid between two thin KBr pellets. The strength of an FTIR absorption spectrum is dependent on the number of molecules in the beam. With a KBr disk

the strength will be dependent on the amount and homogeneity of the sample dispersed in the KBr powder. The spectrometer is repeatability of the transmittance, 0.5%, except the wave number range, where the absorption bands of the water vapor exist.

Fig.4.10 FTIR Spectroscopy set-up.

4.10 Experimental Procedure for Scanning Electron Microscopy

The PPQ thin films were deposited onto small pieces of chemically cleaned glass substrates by plasma polymerization technique. The surface morphology of the PPQ thin films have been investigated by the scanning electron microscopy (SEM) [JEOL JSM-7600F]. The Energy-dispersive Analysis of X-rays (EDAX) which is connected to the Microscope also performed for the elemental analysis of the samples.

Fig.4.11 Scanning electron microscopy set-up in the laboratory.

4.11 Experimental Procedure for DTA/TGA

The PPQ films were scarped off from the substrate to use as the sample for the DTA/TGA investigation. The DTA/TGA scans of PPQ thin films were taken using a computer controlled TG/DTA 6900 system connected to an EXSTAR 6000 station, Seiko Instruments Inc., Japan. TG/DTA module uses a horizontal system balance mechanism.

Fig.4.12 TGA/DTA system.

4.12 Experimental Procedure for UV-vis Spectroscopy

The PPQ thin films of different thickness for UV-vis spectroscopy were prepared in a glow discharge reactor onto chemically cleaned glass substrates. The optical absorption measurements were made in the wavelength range 190-1100 nm by using a dual beam Shimadzu UV-1601 (UV-visibe spectrophotometer) at room temperature. The spectrum of quinoline monomer was also recorded with the same spectrophotometer. An identical, uncoated glass substrate in the reference beam made a substrate absorption correction.

Fig.4.13 UV-vis Spectroscopy set-up.

4.13 Experimental Procedure for Electrical Measurements

For electrical measurements, the Al/ PPQ/ Al sandwich configuration were formed by using an Edward vacuum coating unit E-306A (Edward, UK).The system was evacuated by an oil diffusion pump backed by an oil rotary pump at a pressure of about 10^{-5} Torr. The J-V characteristics of thin films of different thicknesses were studied in the voltage range of 0.1 - 50.0 V at room temperature. The current across the thin films was measured by a high impedance Keithley 6517B electrometer (Keithley Instruments, Inc., USA) and the DC voltage was applied by an Agilent 614A stabilized DC power supply (Agilent Technologies Japan Ltd, Tokyo, Japan). For these measurements the samples were heated by a heating coil which was wrapped around the specimen chamber. The measurements were carried out under dynamic vacuum of about 1.33 Pa and the temperature was measured by a chromel-alumel (Cr-Al) thermocouple placed very close connected to the sample which was to a197 A digital microvolt (DMV) meter.
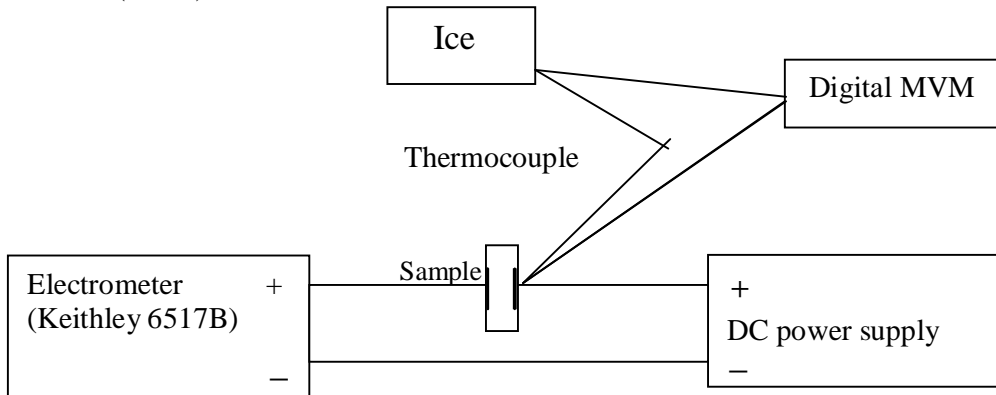

Fig.4.14 A schematic circuit diagram for DC measurements.

(a) DC power supply

(b) Keithley 6517B electrometer

Fig.4.15 DC electrical measurement set-up.

Reference

[1]. Tolansky S., "Multiple Beam Interferometry of Surfaces and Films", Clarendon Press, Oxford (1948)

Chapter-5

## Results and Discussion

5.1 Introduction

Plasma polymerization is a unique and rather unconventional thin film technology which yields polymers having properties different from those of conventional polymers. Sometimes plasma polymers have cross- linked structure and have good chemical and physical stability. So these are used in the areas where mechanical, thermal, and electrical strengths are necessary. In view to this, thermal, structural, optical and electrical properties of the PPQ thin films were studied by FESEM, EDX, DTA, TGA, FTIR, UV-vis spectroscopic analysis and DC electrical properties are discussed in this chapter.

5.2 Scanning Electron Microscopy and EDX Analysis

The FESEM micrographs of PPQ thin films were taken in two magnifications ($\times$50k and $\times$ 100k) are shown in Fig. 5.1. From the micrographs it can be visualized that the surface of the plasma polymerized PPQ thin films is uniform, flawless and fracture free. So smooth plasma polymerized PPQ thin films are produced. No significant change is observed in PPQ thin films even in higher magnifications.
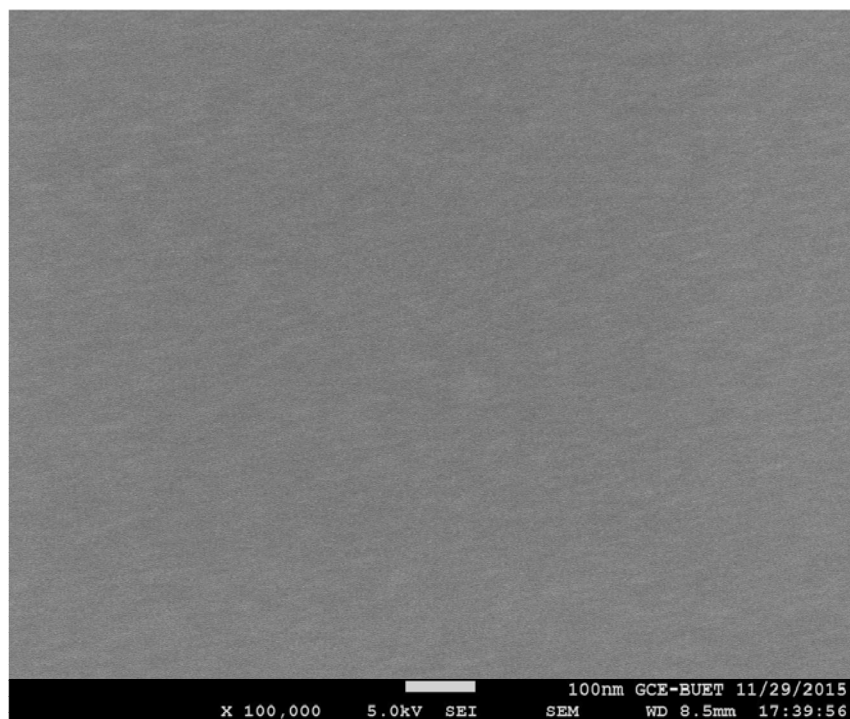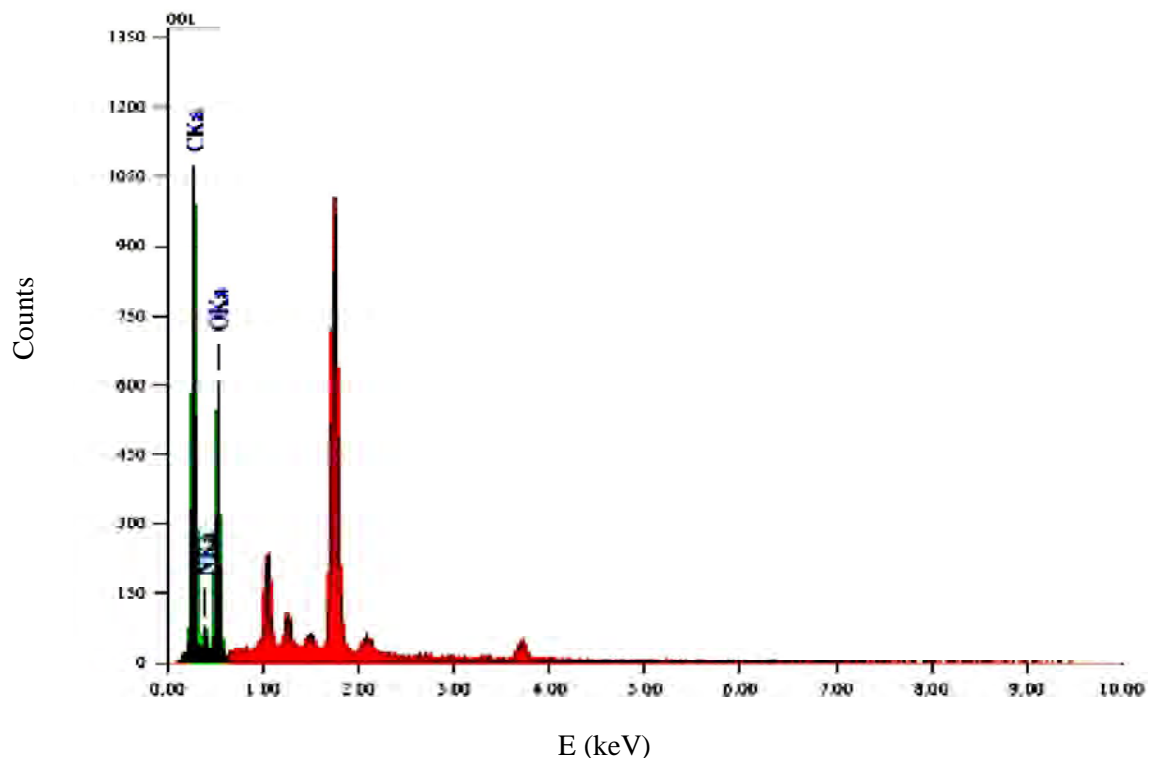

(a)
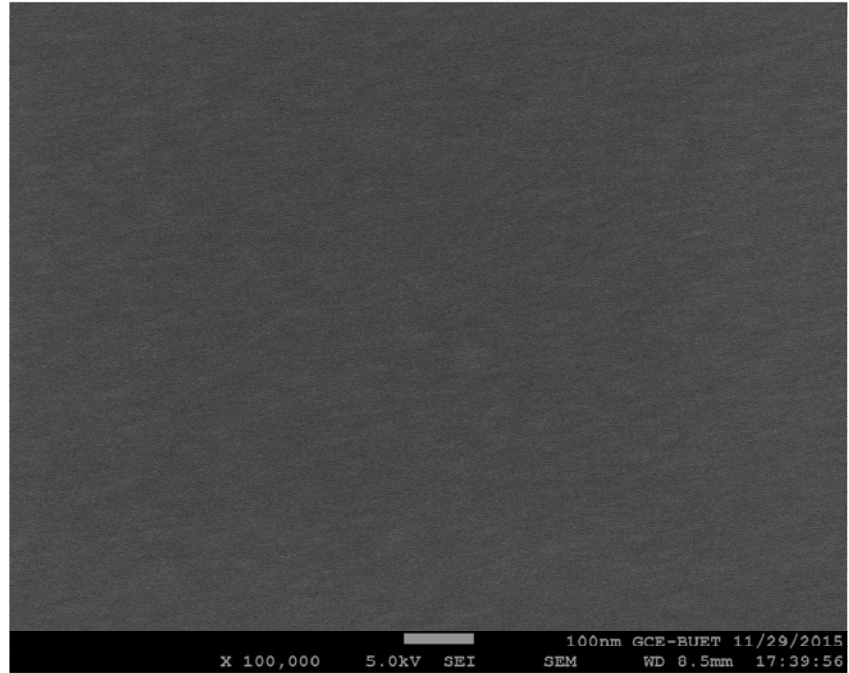
(b)

Fig.5.1 FESEM Micrographs of PPQ thin film (a) ×50k and (b) ×100k.

E (keV)

Fig.5.2 EDX Spectrum of PPQ thin film.

EDX spectrum of PPQ was recoreded by the EDX setup connected with the FESEM and is presented in Fig 5.2. The observation indicates the presence of Carbon(C), Nitrogen(N) and Oxyzen(O) in the PPQ thin films which is shown in table 5.1.

Table 5.1 Mass% and atom% of elements in PPQ.

Element	Mass%	Atom%
C	46.30	52.40
N	16.27	15.79
O	37.44	31.81

From the results it is clear that C has the highest percentage. The main obstacle of EDX is that it can not detect the presence of H. The presence of O in PPQ implies incorporation of carbonyl and/or hydroxyl groups through the reaction of the free radicals or from the chamber during plasma polymerization and these two phenomena are common in plasma polymer. It is also predicated that the PPQ films are deficient in carbon and nitrogen with respect to the monomer, which may be due to the breakdown of bonds owing to the complex reaction during plasma polymerization.

5.3 Thermal Analysis

DTA and TGA traces of the PPQ taken in the temperature range 303 – 1150 K at a scan rate of 20 K/min in nitrogen atmosphere are shown in Fig.5.3. DTA run of PPQ samples shows an exotherm, which reaches a maximum at around 673 K. On the other hand, TGA curve exhibits wt loss of PPQ with increasing temperature. The wt decrease starts from 370 K and 6% wt loss occurs up to 370 K due to loss of adsorbed water. The mass loss of about12% takes place between of 370 and 600 K. Molecular mass hydrocarbon gases may be due too loss of non constitutional water and low molecular mass hydrocarbon gases. Above 673 K major degradation occurs. From TGA trace, PPQ is observed to be stable up to about 600K.
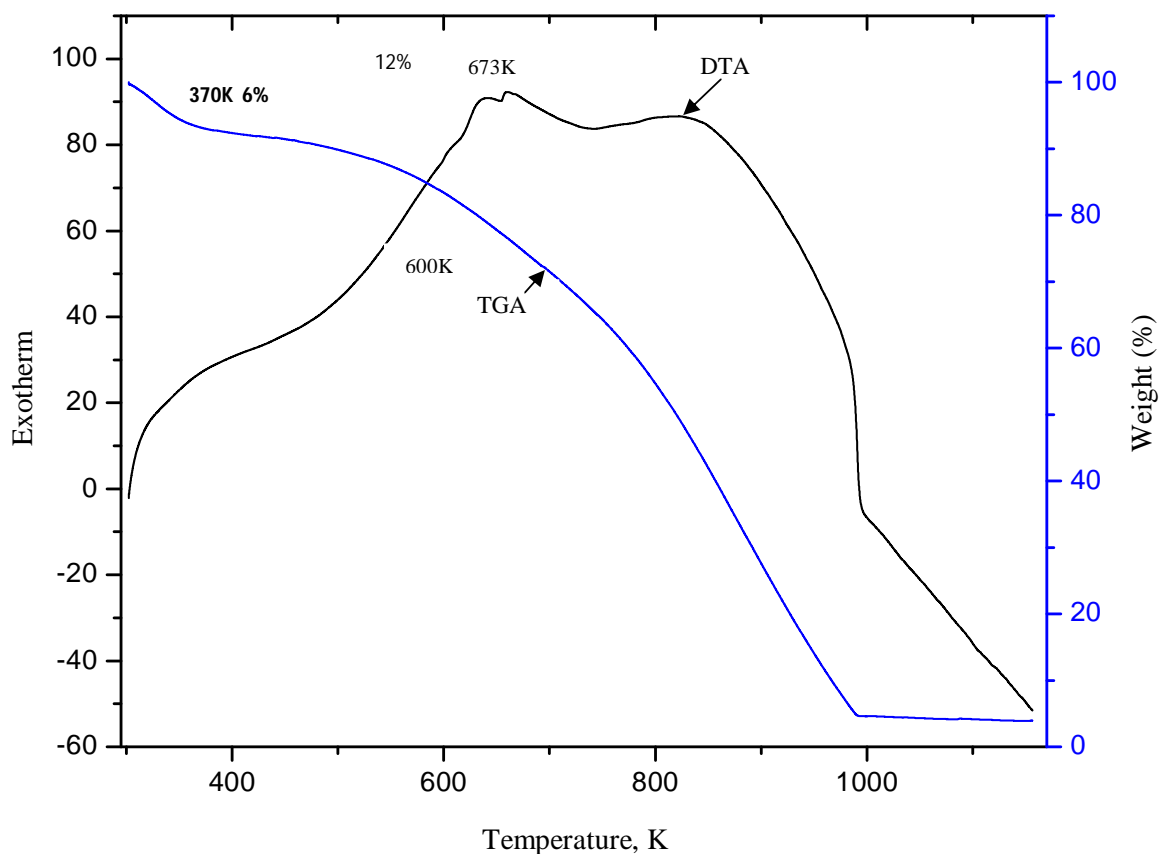
Fig.5.3 DTA and TGA traces of PPQ.

5.3.1 FTIR Analysis

In general the FTIR spectrum of the plasma polymer in comparison with the conventional polymer of the monomer may contain most major peaks characteristic of the conventional polymer, but not always nor in a quantitative manner. Sharp peaks in the spectrum of the conventional polymer generally become less resolved broader bands and so significantly reduce in plasma polymers. The FTIR spectra of Quinoline monomer and deposited thin film are represented as curves Q and PPQ respectively in Fig.5.4.
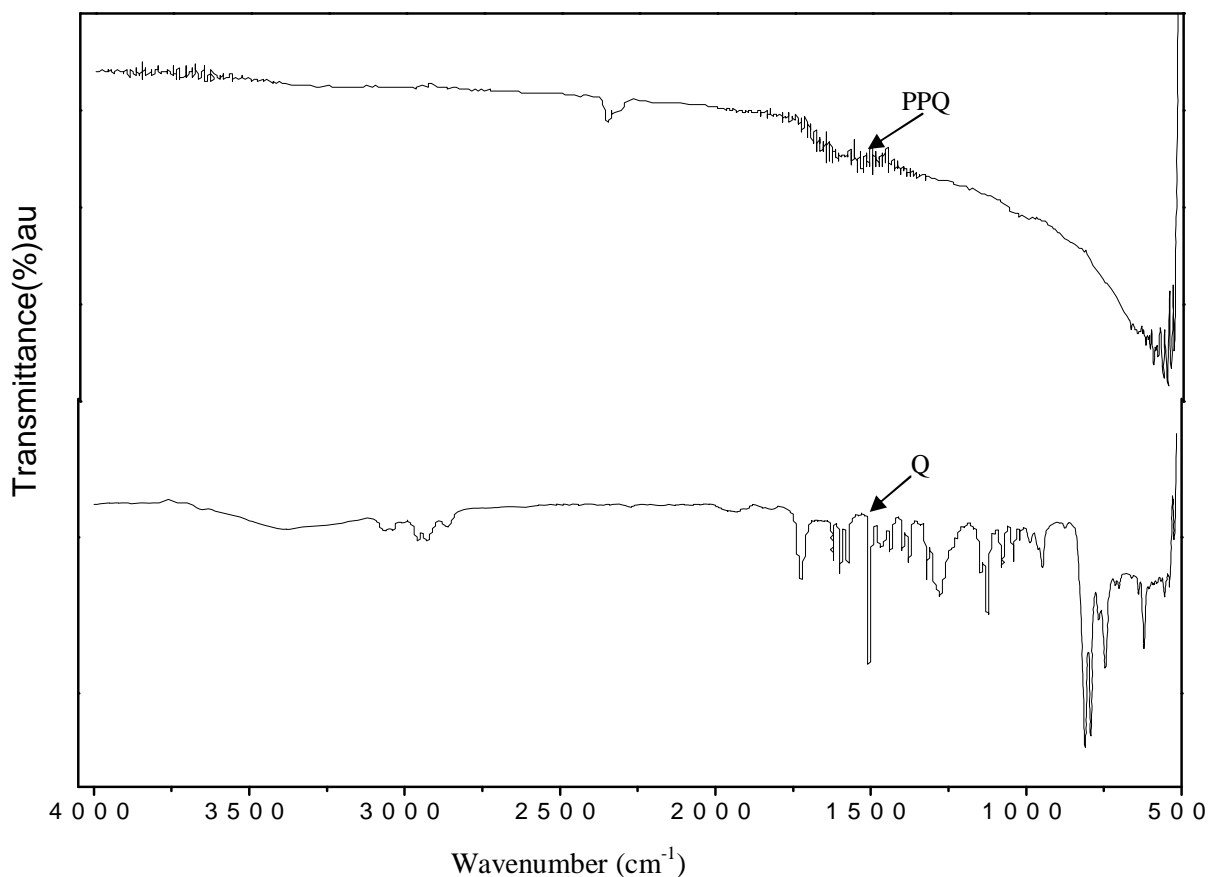
Fig.5.4 FTIR spectra of quinoline and PPQ.

The vibrational assignments of fundamental frequencies of quinoline are reported in Fig 5.4.The aromatic and hetero aromatic structure show the presence of C-H stretching vibrations in the region 2900 – 3100 cm^{-1} C-H in-plane bending in the region 1050 -1100 cm^{-1} and C-H out-of-plane bending in the region 600 - 750 cm^{-1}, in this region the bands are not appreciably affected by the nature of the substituent. The frequencies observed between 3100 – 2800 cm^{-1} in FTIR. On the other hand, based on the normal co-ordinate analysis and potential energy distribution calculation the strong and medium FTIR bands found at 1550 and 1500 cm^{-1} are assigned to C-N stretching vibrations. The in-plane and out-of-plane bending vibrations of C-N bonds area found in their characteristic regions and they are listed in table 1. The FTIR bands observed between 1500 and 1124 cm^{-1} are assigned to C-C stretching vibrations. The in-plane and out-of-plane b ending of carbon vibrations are found in their characteristic regions. The C-N stretching vibration at 550 cm^{-1} is observed in Q.

In the spectrum PPQ the absorption band at 2800 cm^{-1} may arise due to C-H stretching vibration, which is similar to that in Q. The observed absorption band at 1600-1500 cm^{-1} for C-N stretching is found as that of Q. The C-N stretching vibration at 550 cm^{-1} is also observed in the PPQ spectrum. It is found that the chemical nature of the PPQ thin films deposited by plasma polymerization technique departed from that of the monomer Q. Now these observations show that the sharpness of the absorption bands in the spectrum of PPQ decreases significantly compared to that of Q because of hydrogen loss. This is an indication of monomer fragmentation during plasma polymerization.

Table 5.2 Assignments of FTIR absorption bands for Q and PPQ.

Assignments	Wavenumber (cm^{-1})	
	Q	PPQ
C-H stretching	3100,3000,2900	2800
C – N stretching	1550,1500	1600-1500
C – H in- plane bending	1100,1050	1200-1100
C – H out- of plane bending	750,700,650,600	550

5.4 UV-vis Spectroscopic Analysis

The UV-vis absorption spectra of PPQ thin films of different thicknesses recorded at room temperature are presented in Fig 5.5. It is seen that the absorption peak intensity increases with the increase of PPQ thin film thickness and peaks are also broadened with the increase of thickness. It is observed that the wavelength at the maximum absorption of PPQ thin films is about 178 nm. Due to the plasma polymerization the aromatic rings of monomers may be dissociated and fragmented, forming more non conjugated bond in the plasma polymerized thin films. The absorption coefficient, α at various wavelengths were also calculated using the Eqn (3.8) Plots of α, against photon energy, hν, for PPQ thin films for various thickness are shown in Fig 5.6. It is seen that α falls exponentially with the decrease of hν. This exponential fall may be due to the amorphousity or due to the defects present in PPQ thin films. The optical band gap E_g of PPQ thin film can be obtained by using Tauc relation (Chapter-3) for different regions of α

- hv curves. As discussed in Chapter -3, the plot of $(\alpha h\nu)^{1/2}$ vs hv for indirect transition and plot of $(\alpha h\nu)^2$ against hv for direct transition for PPQ thin films of various thicknesses are shown in Fig.5.7 and Fig.5.8, respectively. The E_g obtained from the intercept of the linear portion of the α-hv curve in the hv axis and the E_g values for direct and indirect transitions are recored in Table 5.3.

Table 5.3 $E_{g(d)}$ and $E_{g(i)}$ of thin films of PPQ.

Film thickness, d(nm)	Direct transition energy gap, $E_{g(d)}$ (eV)	Indirect transition energy gap, $E_{g(i)}$ (eV)
475	3.49	2.20
350	3.40	2.00
254	3.30	2.05
178	3.50	2.00

It is observed that the allowed direct transition energy gap, $E_{g(d)}$ and allowed indirect transition energy gap, $E_{g(i)}$ values are varied from 3.50 to 3.30 eV and from 2.20 to 2.00 eV respectively with thickness of the PPQ thin films. This change in E_g may be due to the difference in chemical structure of PPQ thin films of different thicknesses.
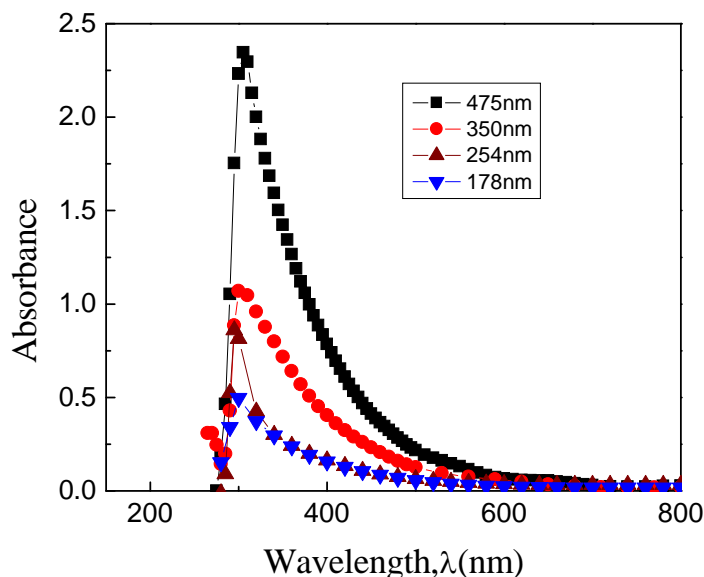
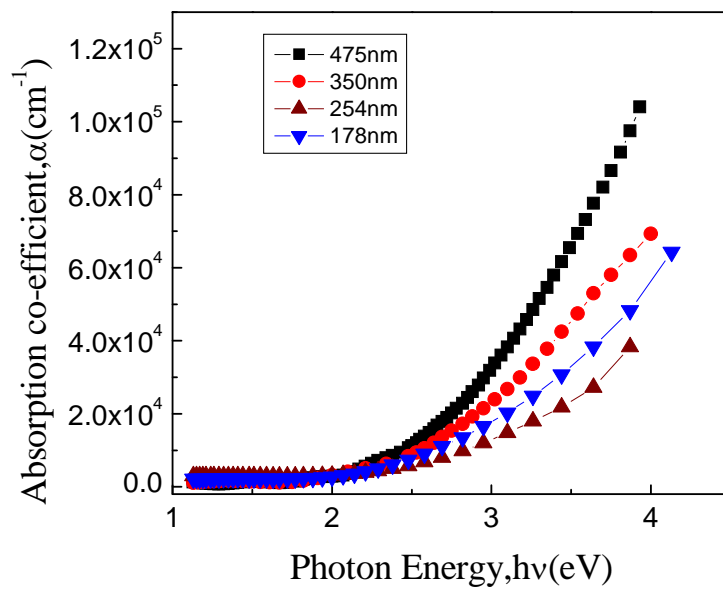Fig.5.5 Absorbance vs wavelength plots for PPQ thin films of different thicknesses.

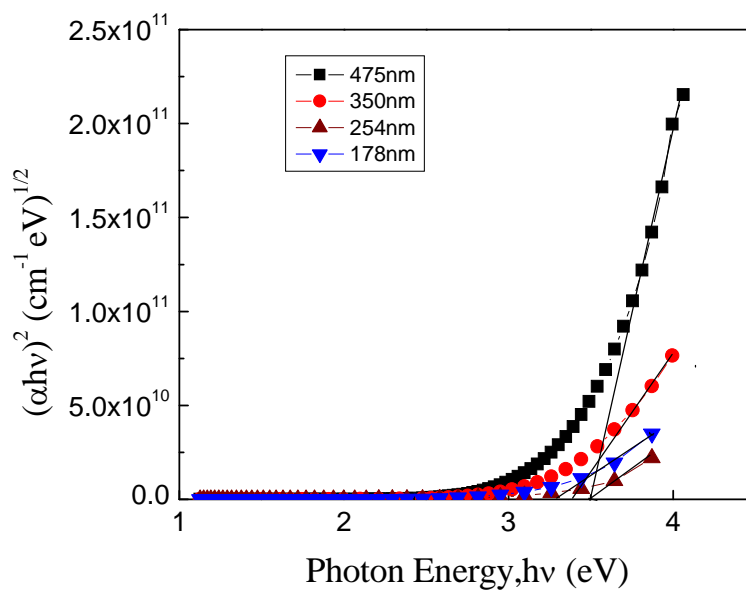Fig.5.6 Absorption Coefficient vs photon energy plots for PPQ thin films of different thicknesses.

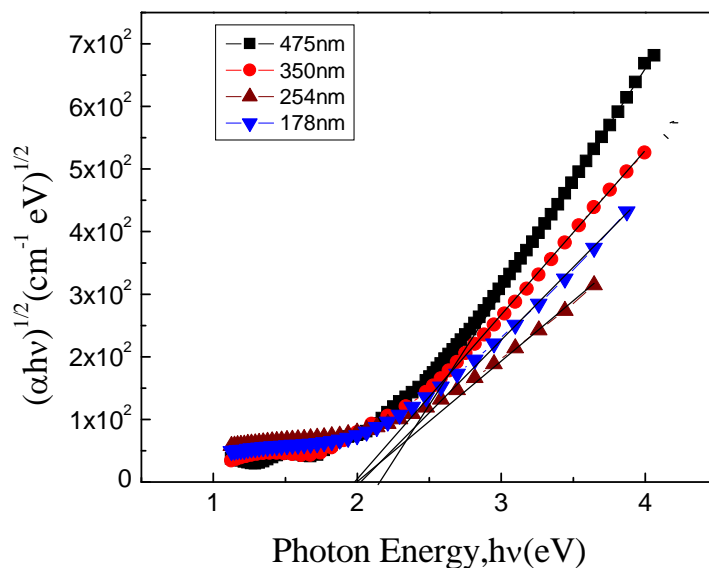Fig.5.7 $(\alpha h\nu)^2$ vs $h\nu$ plots for PPQ thin films of different thicknesses.

Fig.5.8 $(\alpha h\nu)^{1/2}$ vs $h\nu$ plots for PPQ thin films of different thicknesses.

5.5 Current Density – Voltage Characteristics

Current density – Voltage (J-V) characteristics of PPQ thin films of different thicknesses (210, 260, 350, and 440 nm) were studied in Al/PPQ/Al sandwich configuration, in the voltage range of 0.1 - 50V at the temperatures of 298, 323, 348 and 373 K. The observed J-V characteristics of the thin films are presented in Fig. 5.9 to Fig. 5.13. Each of the J-V curve shows two different slopes in the lower and higher voltage regions, following the power law of the form $J \propto V^n$ (Chapter-3) where n is a power index. The slopes of the J-V curves in the two voltage regions are recorded in Table 5.4. It is seen that at lower voltages the slopes are $0.41 \leq n \leq 1.04$ which indicate approximate Ohmic region while at higher voltages the slopes of $1.54 \leq n \leq 5.07$ represents the non-Ohmic region. J-V plots at the higher voltage region suggests that the current in this voltage region may be due to Schottky, PF or SCLC mechanism in PPQ thin films. From the theories of conduction mechanisms discussed in Chapter-4, it can be understood that the relation $J \propto d^{-l}$, where l is a parameter depending upon the trap distribution can give an idea of conduction mechanism. A slope $l < 3$ at a higher voltage region suggests the possibility of Schottky or PF mechanism and $l \geq 3$ indicates the possibility of SCLC mechanism.

Table 5.4 Slopes of J-V curves.

Sample Thickness d (nm)	Measurement Temperature (K)	Value of slopes	
		Low Voltage (ohmic)	High Voltage (Nonohmic)
210	298	0.57	3.28
	323	0.75	2.39
	348	0.50	1.91
	373	1.04	2.25
260	298	0.52	1.6
	323	0.57	1.64
	348	0.52	2.89
	373	0.58	5.05
350	298	0.55	1.57
	323	0.41	2.68
	348	0.50	1.95
	373	0.51	1.65
440	298	0.57	1.54
	323	0.51	1.67
	348	0.59	2.45
	373	0.53	1.73

Fig.5.14 represents PPQ film thickness vs current density curve for 40 V. The plot has yielded a negative slope with a value of 1.5 and 3.5 for low and high thicknesses, respectively. It is seen that in the low thickness films slope is smaller than that for SCLC mechanism. In the higher thickness films, there is a trend of changing the slope towards higher value. These observations ruled out the possibility of SCLC mechanism in the limit of lower thickness and it could be predicted that the conduction mechanism in these films is most probably either Schottky or PF. According to Eqn. 3.26, for Schottky or PF mechanism the expression for the current should give rise to a linear graph if ln J is plotted vs. $V^{1/2}$. From the plots of lnJ vs $V^{1/2}$ for PPQ films at different temperatures in Figs. 5.15 – 5.18 for a PPQ thin film of different thicknesses, which indicate lnJ is proportional to $V^{1/2}$ and gives a straight line in the higher voltage region. Thus, the conduction mechanism in these films is of Schottky or PF type.
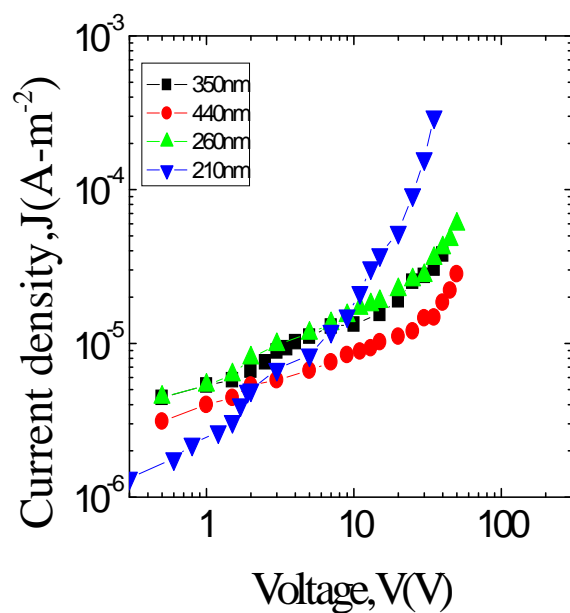
Fig 5.9 Plots of current density against applied voltage at room temperature for PPQ thin films of different thicknesses.
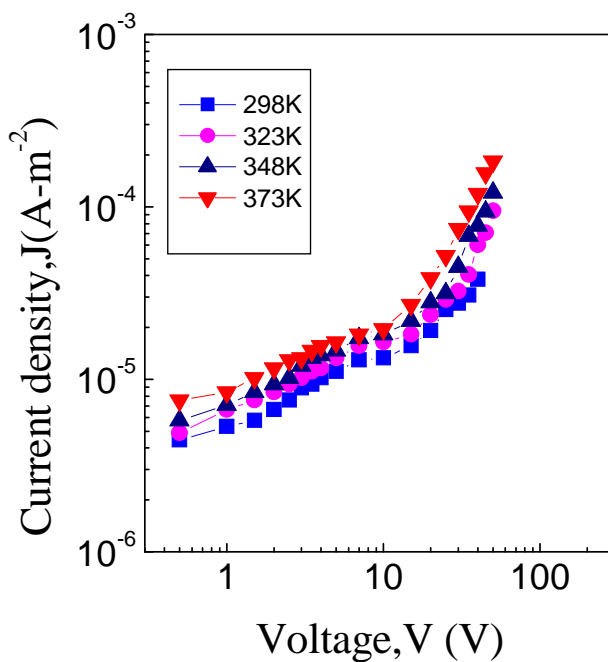

Fig.5.10 Plots of current density against applied voltage at different temperatures for a PPQ thin film (d=440nm).
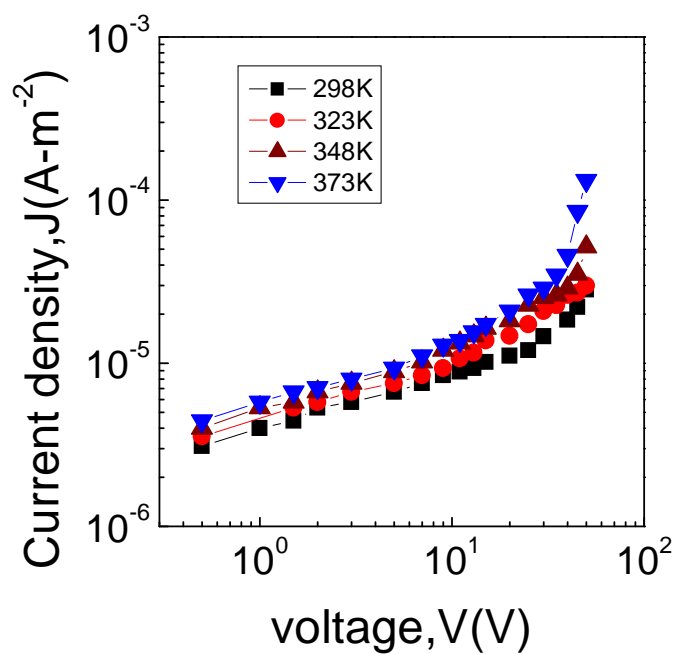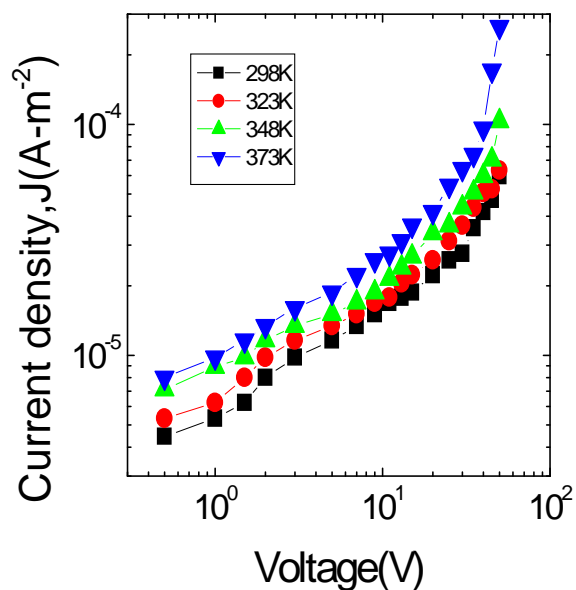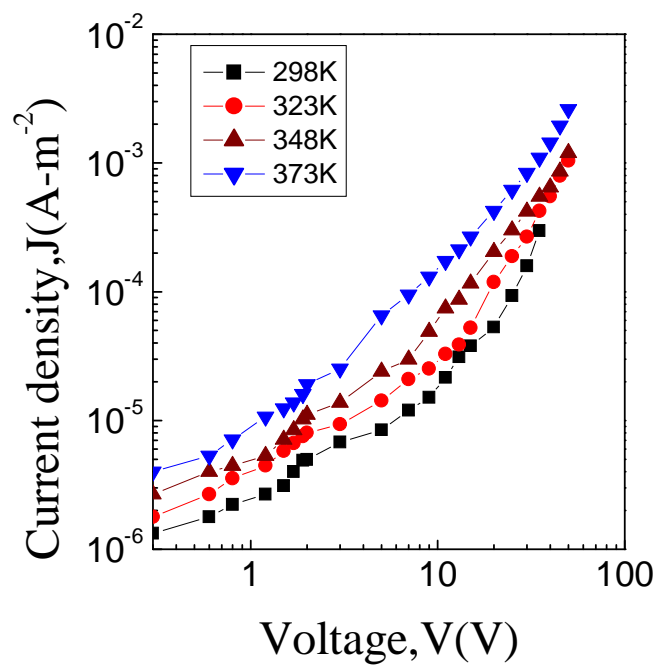
Fig.5.11 Plots of current density against applied voltage at different temperatures for a PPQ thin film (d = 350nm)

Fig.5.12 Plots of current density against applied voltage at different temperatures for a PPQ thin film (d=260nm).

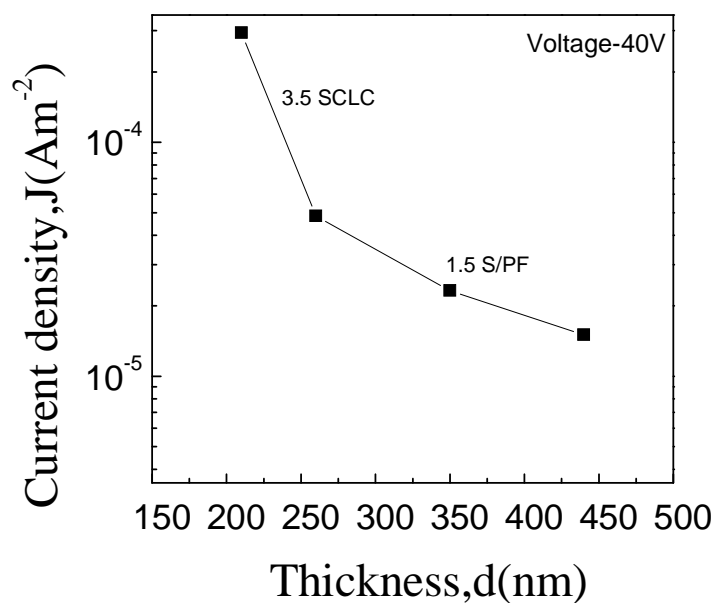Fig.5.13 Plots of current density against applied voltage at different temperatures for PPQ thin film (d=210nm).

Fig.5.14 Plots of room temperature current density against thickness of the different thicknesses of PPQ thin film in the non – ohmic region.
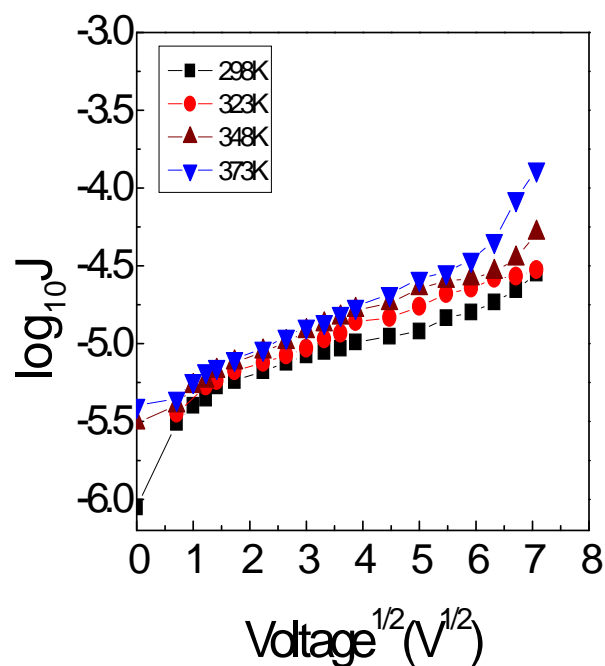
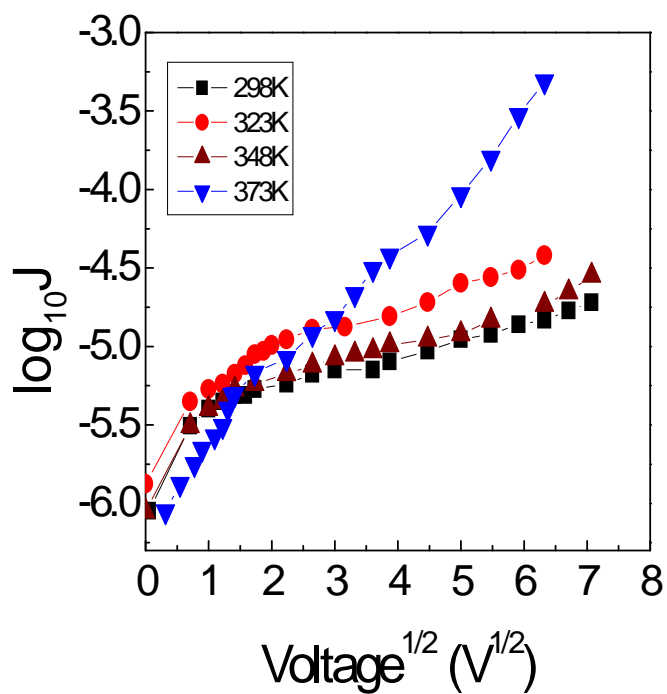Fig.5.15 Plots of lnJ vs. $V^{1/2}$ at different temperatures for a PPQ thin film (d= 440nm) (J in Am^{-2}).

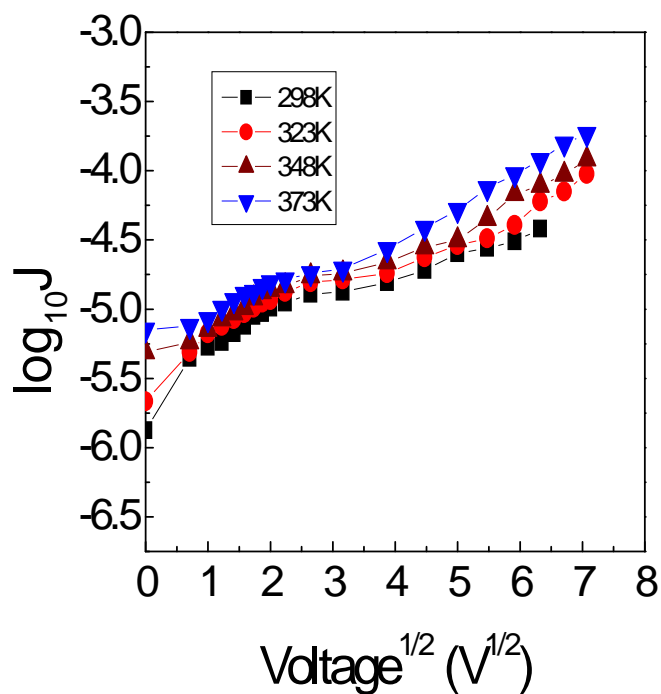Fig.5.16 Plots of lnJ vs. $V^{1/2}$ at different temperatures for a PPQ thin film (d = 350 nm) (J in Am^{-2}).

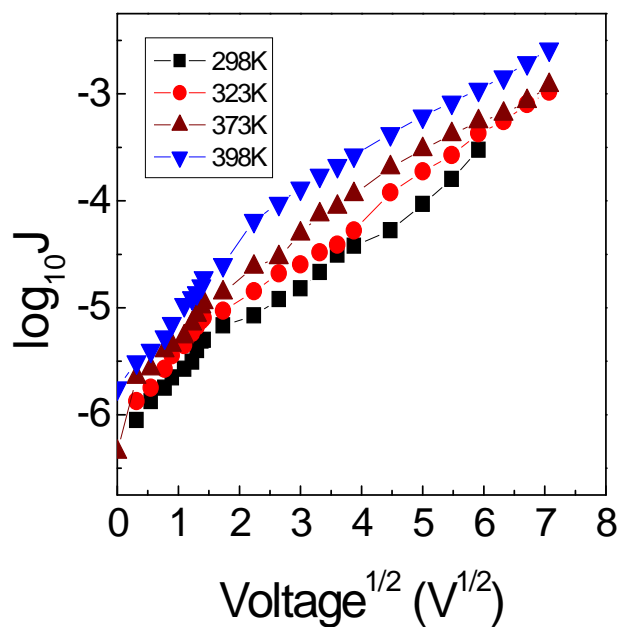Fig.5.17 Plots of ln J vs. $V^{1/2}$ at different temperatures for a PPQ thin film (d= 260nm) (J in Am^{-2})

Fig.5.18 Plots of lnJ vs. $V^{1/2}$ at different temperatures for a PPQ thin film (d= 210nm) (J in Am^{-2})

5.6 Temperature Dependence of Current Density

Fig.5.19 to 5.22 shows the dependence of current density, J on inverse absolute temperature, 1/T, for PPQ thin films of different thicknesses. There are two curves, one in the ohmic region with an applied voltage, 10V, and the other in the Schottky region with an applied voltage, 30V. Each of the curves has two different slopes in the low temperature and in the higher temperature regions. The activation energies calculated from the slopes of plots of Fig.5.19 to 5.22 for all samples are reported in table 5.5.

Table 5.5 Values of activation energy ΔE (eV) for PPQ thin films of different thicknesses.

Thickness	Activation energies, ΔE (eV)			
	30V		10V	
	Temperature		Temperature	
	high	low	high	low
440	0.76	0.14	0.78	0.16
350	0.84	0.19	0.75	0.09
260	0.95	0.20	0.79	0.11
210	0.89	0.19	0.69	0.27

From Table.5.5, for applied voltage 10V (Ohmic), the low activation energy in the lower temperature carriers cannot take part in the conduction throughout the bulk of the material. As the hopping behavior, which has an activation energy of few meV, the lower temperature activation energy can be explained as hopping behavior. The higher value of activation energies in the lower and higher voltage regions in the higher temperature side may due to the band conduction of the carrier through the bulk of the PPQ thin films. For applied voltage 10V (Ohmic), the activation energy is observed to be around 0.15 ± 0.07eV at the low temperature region and that at the higher temperature region is 0.75 ± 0.02 eV. While for applied voltage 30V (Schottky), the activation energies are observed to be around 0.18 ± 0.02 eV at the low temperature region and 0.86 ± 0.07 eV at the higher temperature region. The low temperature activation energy can be explained as hopping behavior but the increase of activation energy with increasing temperature can be explained as gradual transition from the hopping regime and conduction may be due to movement of carrier between distinct energy level in the high temperature region.
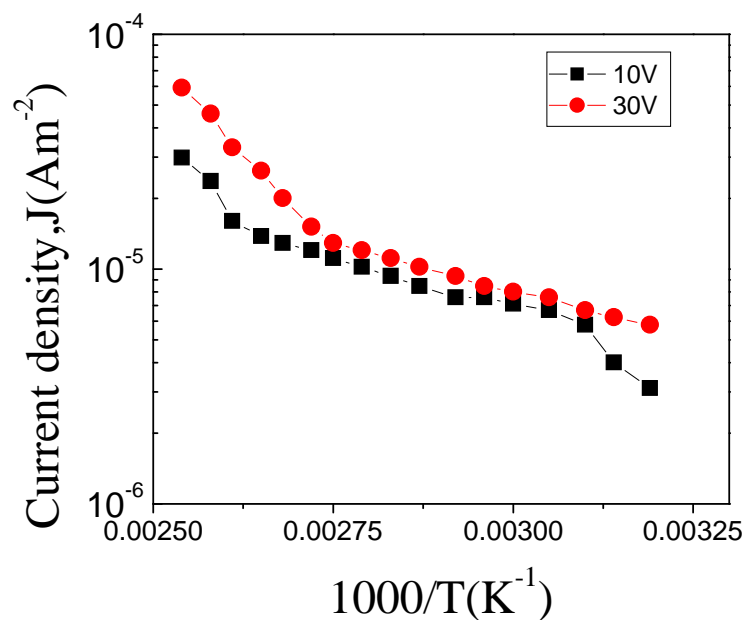
Fig.5.19 Plots of current density vs inverse of absolute temperature for PPQ thin film in ohmic and non-ohmic regions (d=440nm).

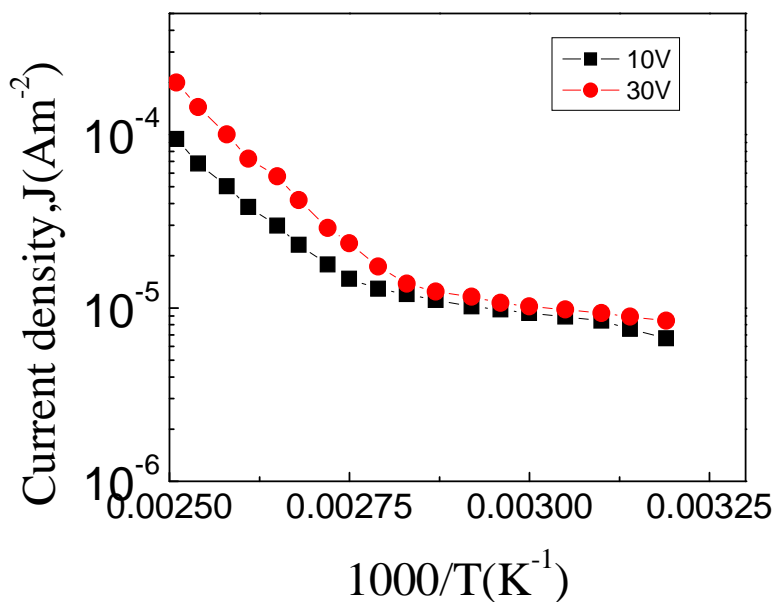Fig.5.20 Plots of current density vs inverse of absolute temperature for PPQ thin film in ohmic and non-ohmic regions (d=350nm).
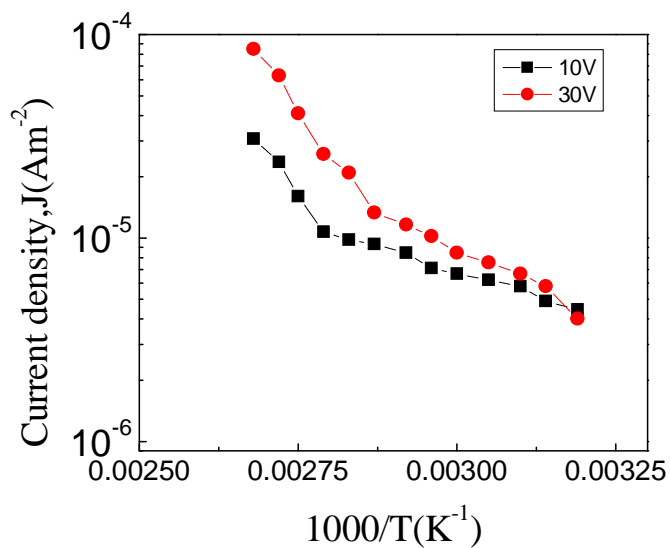
Fig.5.21 Plots of current density vs inverse of absolute temperature for PPQ thin film in ohmic and non-ohmic regions (d=260nm).

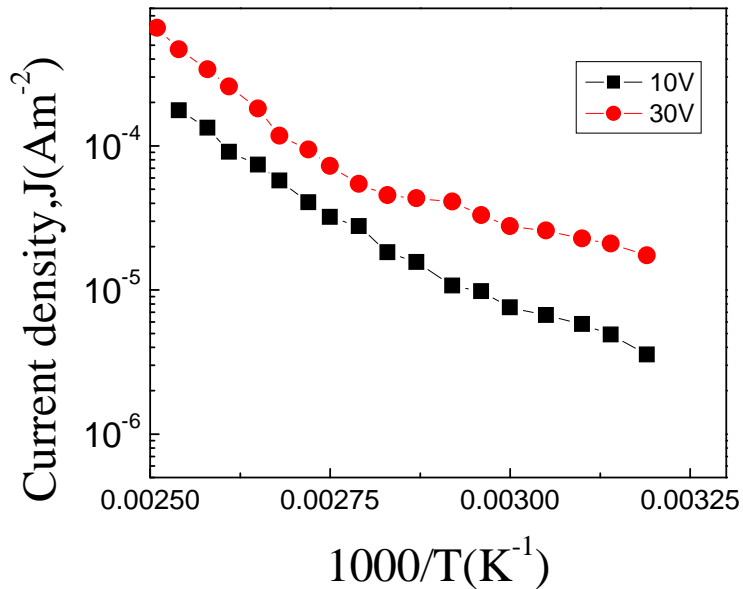Fig.5.22 Plots of current density vs inverse of absolute temperature for PPQ thin film in ohmic and non-ohmic regions (d=210nm).

Reference

[1]. Conley R. T., 'Infrared Spectroscopy', Allyn and Bacon, Inc., Boston, (1972).

[2]. Matin R., Bhuiyan A. H., 'Infrared and ultraviolet-visible spectroscopic analyses of plasma polymerized 2, 6 diethylaniline thin films', Thin Solid Films, 534, 100-106, (2013).

[3]. Kamal M. M., Bhuiyan A. H., 'Direct durrent electrical characterization of plasma polymerized pyrrole-N, N, 3, 5 tetramethylaniline bilayer thin films,' J. Appl. Polym. Sci., 125, 1033–1040, (2012).

[4]. Majumder, S., Bhuiyan A. H., 'DC conduction mechanism in plasma polymerized vinylene carbonate thin films prepared by glow discharge technique', Polym. Sci., Ser. A, 53, 85-91, (2011).

[5]. Akther H. and Bhuiyan, 'Electrical and optical properties of plasma polymerized N, N,3,5,-tetramethylaniline thin films', New J. Phys. 7,173, (2005).

[6]. Kamal M. M., Bhuiyan A. H., 'Structural and optical characterization of plasma polymerized pyrrole monolayer thin films,' J. Appl. Polym. Sci., 1, (2013).

[7]. Chowdhury F –U-Z, Bhuiyan A. H.,'An investigation of the optical properties of plasma polymerized diphenyl thin films,' Thin Solid Films, 360 , 69-74, (2000).

Chapter-6

Conclusions

6.1 Conclusions

The PPQ thin films of different thicknesses were prepared from quinoline by using a capacitively coupled plasma polymerization technique. Conclusion of the results of structural, optical and dc electrical properties of PPQ produced from quinoline are included below:

The surface morphology and chemical composition of PPQ are analyzed by FESEM and EDX respectively. The FESEM micrographs of thin films of PPQ taken in various magnifications show that PPQ thin films are smooth, flawless and fracture free. No significant difference is observed in micrographs of various magnifications. EDX analysis indicates the presence of C, N and O in the samples. The presence of O in PPQ implies incorporation of carbonyl and hydroxyl groups through the reaction of the free radicals. It is also predicted that the PPQ films are deficient in carbon and nitrogen with respect to the monomer, which may be due to the breakdown of bonds owing to the complex reaction during plasma polymerization.

DTA run of PPQ samples shows an exotherm, which reaches a maximum at around 673 K indicating a gradual change of its properties. TGA curve exhibits the mass loss of PPQ with increasing temperature. PPQ is observed to be stable up to about 673 K. The uniform mass loss up to whole temperature range in the TGA trace is a cause of thermal breakdown of PPQ structure.

From the FTIR spectra it is observed that the absorption peaks in the PPQ are not sharp when compared with those for quinoline and some of the FTIR absorption features of quinoline are noticeable in the spectrum of PPQ. Plasma technique has affected the chemical structure of the deposited films. This is an indication of monomer quinoline fragmentation during plasma polymerization.

The average values of both allowed direct transition, $Eg_{(d)}$, and allowed indirect transition, $Eq_{(i)}$ energy gaps are identified in PPQ thin films. The values of $Eg_{(d)}$ and $Eg_{(i)}$ do not change appreciably with thickness. The average value of $Eg_{(d)}$ is, 3.50 eV and that of $Eg(i)$ is 2.20eV. The J-V characteristics of PPQ revealed that the dependence of J on V is Ohmic in the lower voltage region and non Ohmic at higher voltage levels. The thickness dependence of current density in the higher voltage region has predicted Schottky/PF type conduction mechanism in PPQ. Thus it is concluded that the conduction mechanism in PPQ thin films is most probably a Schottky/PF type mechanism.

For applied voltage 10V (Ohmic), the activation energy is observed to be around 0.15 ± 0.07eV at the lower temperature region and that at the higher temperature region is 0.75 ± 0.02 eV. While for applied voltage 30V (Schottky/PF), the activation energies are observed to be around 0.18 ± 0.02 eV at the low temperature region and 0.86 ± 0.07 eV at the higher temperature region. The low temperature activation energy can be explained as hopping behavior but the increase of activation energy with increasing temperature can be explained as gradual transition from the hopping regime and so in the higher temperature region conduction may be due to movement of carrier between distinct energy levels.

6.2 Suggestions for Further Research

In this work an attempt was made to investigate the structural, optical and the dc electrical behavior of PPQ. But, more characteristics of PPQ thin films can be investigated, which will help finding suitable applications of these materials. The following investigations on PPQ thin films may be carried out. The surface morphology and chemical investigation can be done by the thermal analysis DTA and TGA at different heating rates which will be helpful to ascertain the reaction kinetics in the PPQ films.

PPQ can be modified to change electrical properties by heat treatment and doping. Doping of these films can be carried out while preparing those films in the plasma chamber or by exposing them in dopant gases. It can be also deposited as a coating on other polymers. The PPQ can be prepared in an asymmetric electrode configuration or inductively coupled, plasma polymerization set-up with rf power and can be characterized by the above mentioned techniques.